European Journal of Taxonomy 1056: 1–75
https://doi.org/10.5852/ejt.2026.1056.3280
europeanjournaloftaxonomy.eu
ISSN 2118-9773
2026 · Gaspard D.

Received: 1 September 2025 • *Accepted: 24 February 2026* • *Published: 19 May 2026*

Topic editor: Magalie Castelin • *Desk editor: Kristiaan Hoedemakers*

Monograph

urn:lsid:zoobank.org:pub:FAACB47C-22CE-4478-9377-958039DF1039

Overlooked brachiopods from the Karubenthos & Madibenthos expeditions (French Caribbean) – biodiversity and ecology

Danièle GASPARD

Centre de recherche en Paléontologie-Paris (CR2P), Sorbonne-Université, Muséum national d'Histoire naturelle, CNRS, CP 38, 8 Rue Buffon, F-75005 Paris, France.
Email: daniele.gaspard@mnhn.fr

Abstract. Several marine expeditions by the Muséum national d'Histoire naturelle (Karubenthos and Madibenthos) with the RV "*L'Antea*" around the French Caribbean Islands, allow for the first time to highlight, among benthic faunas, the presence and diversity of representatives of the phylum Brachiopoda. Thirty species, including two new ones: *Tichosina madininensis* sp. nov. and *Argyrotheca beaumalei* sp. nov., and one never recorded before from the Caribbean Sea (*Amphithyris* aff. *buckmanni* Thomson, 1918) were recognised, belonging to the three subphyla composing the phylum. The diversity of the fauna, its morphological and microstructural characteristics, geographical distribution, and ecology are taken into consideration when comparing it with similar fauna from elsewhere in the Caribbean Sea and all over the world when available. Among genera, *Gryphus* Megerle von Mühlfeldt, 1871, *Tichosina* Cooper, 1977 with several species, and *Erymnia* Cooper, 1977 are the largest forms, while some of the smallest collected were *Cryptopora* Jeffreys, 1869, and *Argyrotheca* Dall, 1890. The latter genus has representatives with bright colours that should be considered as jewels of the benthos there. The pigments involved in their colouration deserve attention (analyses using Raman Spectroscopy are in progress). The commonest species collected, *Terebratulina cailleti* Crosse, 1865, is found attached to various substrates. All these brachiopods, as attached benthic organisms but overlooked for such a long time, are reliable archives of the local environment. Some of these brachiopods are living attached to or beneath corals, and to sponges, and are now considered to be in danger as a consequence of coral bleaching due to climate change and also to pollution.

Keywords. Brachiopoda, biodiversity, Caribbean, ecology.

Gaspard D. 2026. Overlooked brachiopods from the Karubenthos & Madibenthos expeditions (French Caribbean) – biodiversity and ecology. *European Journal of Taxonomy* 1056: 1–75. https://doi.org/10.5852/ejt.2026.1056.3280

Introduction

As part of the program "Tropical Deep-Sea Benthos" and "Our Planet Revisited", several research cruises and expeditions were organised by the Muséum national d'Histoire naturelle, Paris (MNHN) in 2012, 2015 and 2016, using the oceanographic vessel *L'Antea* (expeditions leader: Prof. Ph. Bouchet) as well as an additional expedition to French Guiana (2014) aboard the RV *Hermano Gines*. These expeditions aimed to document the diversity of the marine flora and fauna of the French Caribbean islands, specifically

Guadeloupe and Martinique. Despite previous efforts, the benthic fauna of this region remains insufficiently known, particularly around Martinique where sampling had previously been largely restricted to littoral environments, in contrast to Guadeloupe and its islets. The expedition name Karubenthos derived from the indigenous Arawak term "Karukera", the historical name for Guadeloupe meaning "the Island with beautiful waters" whereas "Madinina" refers to Martinique as "the Island of flowers".

Among the phyla represented in the collected material, this study focuses on brachiopods. Brachiopoda originated in the Early Cambrian and are benthic marine lophophorates characterised by a bivalved shell composed of a dorsal and ventral valve arranged in a bilateral symmetry. Although brachiopods are well documented globally, their distribution and diversity in the Caribbean have received comparatively little attention. They are considered to have little economic importance, being largely unpalatable (Thayer & Allmon 1991) and often of small size (Asgaard & Stentoft 1984), but they play a significant ecological role as filter feeders attached to a variety of substrates, including corals. Importantly, brachiopods function as valuable bioarchives recording environmental conditions during growth (Lethulle *et al*. 2023).

Previous investigations in the wider Caribbean region, including the Gulf of Mexico, yielded important material, notably from the U.S. Coast Survey vessel *Blake* reported by Agassiz (1888), as well as the records of Dall (1871, 1886). Subsequent studies by Crosse (1865), Crosse & Fischer (1866), Fischer & Oehlert (1891), Cooper (1977), and Logan (1990) documented several brachiopod species, including endemic taxa from Guadeloupe, Martinique and offshore French Guiana. It is noted that the exposure of the stations along the Atlantic or the Caribbean side can represent slight environmental differences. More recently, the reports of Rojas *et al*. (2015, 2022) along the Colombian Caribbean coasts allowed comparisons with one of the genera and led to discussion about the occurrence of some species and their interactions with other bottom faunas.

Representatives of all three Brachiopoda Duméril, 1806 subphyla (Linguliformea Williams, Carlson, Brunton, Holmer & Popov, 1996, Craniiformea Williams *et al*., 1996 and Rhynchonelliformea Williams *et al*., 1996) were recovered during the expeditions although Rhynchonelliformea were by far the most abundant.

Additional material from earlier Caribbean expeditions housed at the Smithsonian Institution was examined and previously discussed in an oral presentation (Gaspard 2000). Preliminary reports on the present material have since been published (Gaspard 2018; Gaspard *et.al*. 2018), and geochemical analyses have explored the environmental conditions of the shells (Letulle *et al*. 2021, 2023).

Material and methods

Material (Fig. 1)

Seven stations sampled during Karubenthos 1 exped., 2012; 100 of the 143 stations sampled during Karubenthos 2 exped., 2015 (Fig. 1A) and 17 during Madibenthos exped., 2016 (Fig. 1B) yielded brachiopods, comprising representatives of 16 genera with thirty species. More could probably have been collected but the tiny size of certain shells and their transparency prevented us from observing them, and some, owing to their way of life in cavities, beneath pebbles or boulders, remain invisible. In contrast, coloured shells of other species deserve attention. Very few specimens from French Guiana provide complementary material. All the specimens are curated at the Muséum national d'Histoire naturelle, Paris (MNHN).

- A single species of Linguliformea was found.
- Separated valves of two species of Craniiformea.
- The brachiopod fauna collected consists mainly of Rhynchonelliformea.

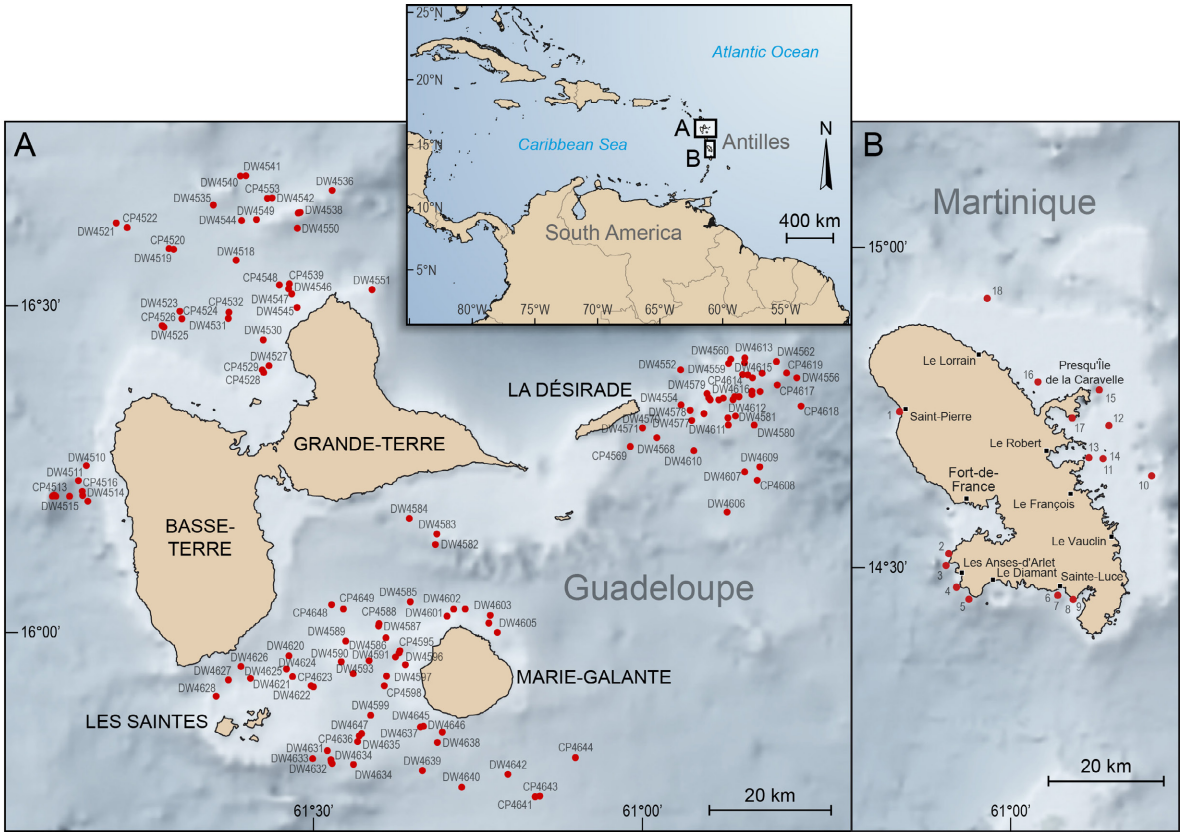

Fig. 1. Sampled stations during the French expeditions in the Caribbean Sea. **A**. Karubenthos 2. **B**. Madibenthos.

Methods

The specimens were imaged at the Muséum national d'Histoire naturelle (CR2P, MNHN, Paris), and observed macroscopically (shape, size and ornamentation: costae, colour) for the external morphology. The internal features were observed on separate valves to recognise, among other characters, the shape of the brachidium (appendix at the origin of the name to the phylum), the presence of spicules on the body wall to protect the soft parts, and/or setae from invaginated follicles along mantle grooves commonly protruded beyond the margins of the shell. Then, the shells were embedded in Epoxy resin, cut to produce polished sections, then observed, after etching (a few seconds in RDC, Laboratoire Moderne ©) and gold/palladium coating, under a scanning electron microscope (SEM) JEOL© and/or Hitachi© to observe the microstructure. When available, polished but non-etched shell sections of some species were observed at a nanoscale using a Bruker© atomic force microscope (AFM).

As mentioned above, brachiopod shells record the characteristics of the environment in which they grow. Hence, geochemical analyses were performed after preparing the shells as recommended in Romanin *et al*. (2018), thus allowing sea water temperatures to be ascertained (Letulle *et al*. 2021, 2023).

The results of multiproxy assessment of the brachiopod calcite shell highlight the role these organisms play as reliable archives of the environment. As recommended by Letulle *et al*. (2023) on modern shells, geochemical analyses were performed on this material along with some temperate, Subantarctic and Antarctic species.

The coloured patterns observed on some tiny shells (cf. *Argyrotheca* Dall, 1900) raised questions about the pigments involved in the colouration. These pigments are sometimes preserved in coloured fossil shells (Gaspard *et al*. 2019).

Results

The classification of the specimens under study follows the supra-ordinal classification presented by Williams *et al*. (1996) and subsequently reported in the *Treatise of Invertebrate Paleontology* by Kaesler (1997–2006) and Selden (2007).

Phylum Brachiopoda Duméril, 1806
Subphylum Linguliformea Williams, Carlson, Brunton, Holmer & Popov, 1996
Order Lingulida Waagen, 1885
Superfamily Discinoidea Gray, 1840
Family Discinidae Gray, 1840
Subfamily Discininae Schuchert & Le Vene, 1929
Genus *Discradisca* Stenzel, 1964

Discradisca antillarum (d'Orbigny, 1845)
Fig. 2A–B

Orbicula antillarum d'Orbigny, 1845: 368, pl. 28 figs 34–36.

Orbicula antillarum – d'Orbigny 1853: 371, pl. 1 fig. 2.
Discinisca antillarum – Dall 1871: 42; 1873: 201; 1920: 278. — Davidson 1888, pt. 3: 204, pl. 26 fig. 31, 31a.
Discradisca antillarum – Cooper 1977: 51, pl. 2 figs 13–24.

Material examined (including figured material)

FRENCH GUIANA • 1 dorsal valve; stn CP 4399; 05°59′6″ N, 52°11′3″ W; depth 66–67 m; 8 Aug. 2014; Convention APA-973-1; MNHN, MNHN-IB-2017-221 (Fig. 2A–B).

Type locality

Cuba.

Description

Shell roughly dorsi-biconvex: no ventral valve was observed in the samples, the dorsal valve is subcircular in outline, with a conical profile. Apex near the third posterior part, obviously smooth while the slopes are ornamented with close growth lines crossed by tiny radial costae.

Pale to brownish colour. Owing to the paucity of the material sampled during these expeditions, the internal features are not described.

Depth range

67 m.

Distribution

The species is known off French Guiana. Fairly wide distribution in the Caribbean (d'Orbigny 1845; Cooper 1977, in Jamaica), Nicaragua as far as Brazil (Dall 1920).

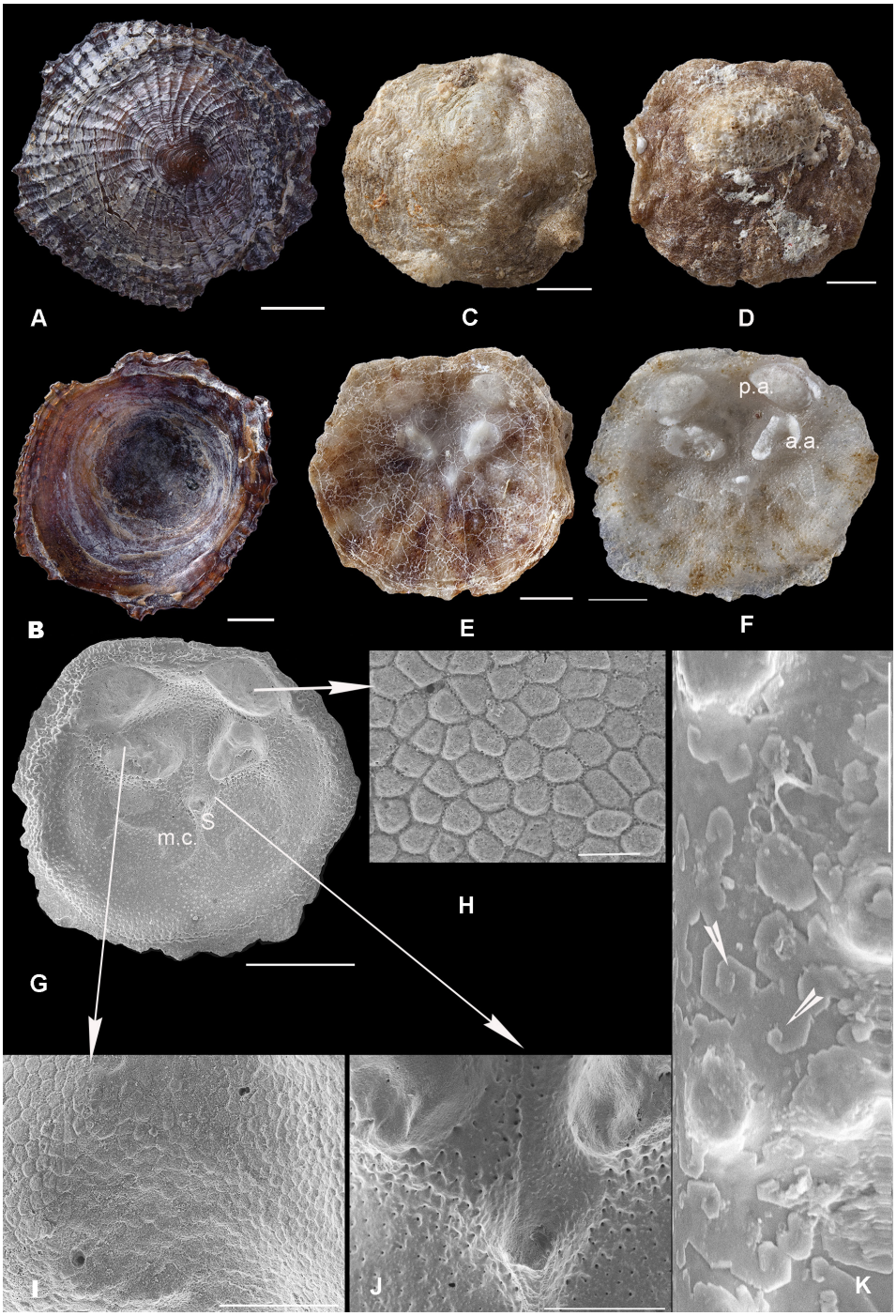

Fig. 2. A–**B**. *Discradisca antillarum* (d'Orbigny, 1845), MNHN-IB-2017-221. **A**. External dorsal valve. **B**. Interior of the same valve. — **C**–**K**. *Novocrania anomala* (Müller, 1776). **C**–**D**. External dorsal valves of MNHN-IB-2022-964 and MNHN-IB-2022-965. **E**. Dorsal valve interior from the same valve as D. **F**. Dorsal valve interior, revealing the anterior adductors (a.a.) and posterior adductors (p.a.), MNHN-IB-2022-966. **G**–**K**. SEM views of MNHN-IB-2022-966. **G**. Interior of the same preceding dorsal valve, revealing the anterior adductors, dorsal mantle canals (mc), posterior adductors, oblique internal scar and septum (S). **H**. Close-up view of the posterior adductor myotest. **I**. Close-up view of the anterior adductor area. **J**. Close-up view of the anterior part of the anterior adductors and the septum. **K**. Spiral growing tablets of the semi-nacreous layer at the valve floor (arrowheads). Scale bars: A–F = 1 mm; G = 1.5 mm; H = 20 µm; I = 100 µm; J = 500 µm; K = 10 µm.

Subphylum Craniiformea Williams *et al*., 1996
Oder Craniida Waagen, 1885
Superfamily Cranioidea Menke, 1828
Family Craniidae Menke, 1828
Genus *Novocrania* Lee & Brunton, 2001

Novocrania anomala (Müller, 1776)
Fig. 2C–K

Patella anomala Müller, 1776.

Material examined (including figured material)

MARTINIQUE – **off Pointe de la Baleine** • 1 valve; stn AS 370; 14°31′1″ N, 61°05′9″ W; depth 20 m; 30 Sep. 2016; Madibenthos exped.; MNHN, MNHN-IB-2022-966 (Fig. 2F–K). – **Robert Bay (E of Islet Madame)** • 1 valve; stn AS 403; 14°40′2″ N, 60°52′5″ W; depth 11 m; 24 Sep. 2016; Madibenthos exped.; MNHN, MNHN-IB-2022-964 (Fig. 2C) • 1 valve; same data as for preceding; MNHN, MNHN-IB-2022-965 (Fig. 2D–E). – **E of Loup Bordelais (Le Robert)** • 1 shell; stn AB 405; 14°32′2″ N, 60°50′6″ W; depth 23 m; 25. Sep. 2016; Madibenthos exped.; MNHN. – **Baie du Galion (Gros Raisin)** • 4 dorsal valves; stn AB 400; 14°43′9″ N, 60°54′1″ W; 17 m; 25 Sep. 2016; Madibenthos exped.; MNHN.

Type locality

Norway.

Description

Morphology. The dorsal valves observed are nearly sub-rounded to approximately sub-quadrate, with an irregular surface marked by growth lines, and an outline reflecting the texture of the substrate. These valves are flatly conical with a brown/yellowish colour either uniform or radial, visible also at the valve interior indicating a thin shell (Fig. 2C–E). The valve interior reveals wide posterior adductor scars that are round to sub-oval (Fig. 2F–G), arched to U-shaped anterior adductors, small anterior muscle scars on each side of the median septum or at the lateral posterior part of the latter (Fig. 2E–G).

Microstructure. The SEM allows observation of the distribution of punctae, at the internal valve surface, as well as details of the myotest (Fig. 2H–J), pustules mainly at the posterior part (Fig. 2G) and mosaic of calcite elements from the margins including the spiral growth of the tablets that form the "semi-nacreous" layer (Checa *et al*. 2009) (Fig. 2K).

Depth range

11–23 m.

Distribution

The species is known from the Caribbean Sea off Cuba (cf. Dall 1920), Jamaica (Jackson *et al*. 1971), off Central America (Cohen *et al*. 2014) to the North Atlantic Ocean (Gaspard 2003), the Mediterranean Sea (Fischer & Oehlert 1891), Red Sea (Zuschin & Mayrhofer 2009), the Indian and eastern and central Pacific oceans.

Ecology

This species spends its life cemented by the ventral valve to hard substrates (e.g., pebbles or small blocks, corals) and rarely in muddy locations.

Remarks

This species first mentioned by Dall (1871), from the Caribbean, as a variety of *Crania anomala* then as a separate species (1886), was reported by Cooper (1977) as *Crania* aff. *pourtalesi* as it was under *Neocrania pourtalesi* (Lee & Brunton 1986) before renaming the species as *Novocrania pourtalesi*, 2001. A recent review of the genus prompted Robinson (2017) to highlight the correct species spelling of *N. pourtalesii* and discuss the possible synonymy between *N. pourtalesii* and *N. anomala.*

See for complete synonymy and discussion in Robinson (2017: 507).

Novocrania aff. ***turbinata*** (Poli, 1795)
Fig. 3

Material examined (including figured material)

GUADELOUPE – **N of Grande Terre** • 1 shell; stn CP 4529; 16°24′ N, 61°35′ W; depth 176–183 m; 11 Jun. 2015; Karubenthos 2 exped.; MNHN, MNHN-IB-2022-967 (Fig. 3A) • 1 shell; stn DW 4542; 16°40′ N, 61°34′ W; depth 394–400 m; 13 Jun. 2015; Karubenthos 2 exped.; MNHN, MNHN-IB-2022-968 (Fig. 3B–C).

Type locality

Reported as probably off the coast of Sicily (cf. Robinson 2017).

Description

Morphology. A different shell, thicker than that of *N. anomala* (formerly considered as *N. pourtalesii*), flatly conical, with a more regular surface and a subquadrate outline (Fig. 3A), and an apex located between the valve centre and the posterior margin. Sometimes wide radial zones, orange coloured, are observed at the posterior part. Concentric major growth marks ornament the shell surface with subtle tiny spines arranged in rows (Fig. 3B).

Ventral valve. This valve is nearly flat to concave like a cup, the interior reveals: sub-round or sub-oval posterior adductor muscle scars lightly convex in some cases, small oblique internal muscle scars latero-anterior to the posterior adductors and, sometimes a small median process, i.e., the rostellum with a curved tip. Large mantle canals are somewhere engraved in the surface (Fig. 3C). The convex marginal rim is pustulous.

Microstructure. SEM observations highlight the spiral growth of the semi-nacreous tablets as for the preceding species.

Depth range

176–400 m, Karubenthos 2 exped.; 7–400 m reported by Robinson (2017).

Distribution

The species is known from the Caribbean Sea to the North Atlantic Ocean and the Mediterranean Sea. See also the Indian, eastern and central Pacific oceans (Robinson 2017).

Ecology

The shell of this species is pro parte cemented to hard substrate by its ventral valve.

Remarks

Comparisons with the reports of Dall (1871, 1886), Jeffreys (1878), Davidson (1886), Fischer & Oehlert (1891), the report of Logan & Long (2001), then the work of Cohen *et al*. (2014), as well as the material examined by Robinson (2017: 513–517) and his subsequent discussion about synonymy have led to the inclusion of this material in the species *Novocrania turbinata*.

See synonymy in Robinson (2017: 513).

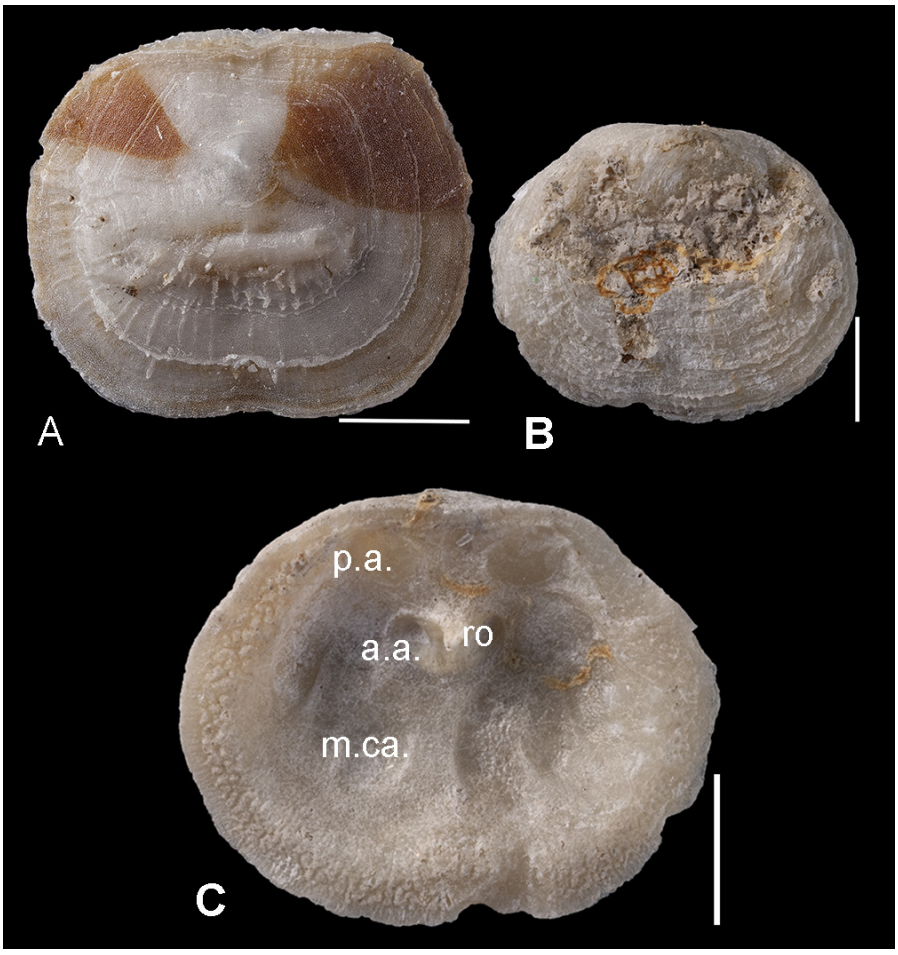

Fig. 3. *Novocrania turbinata* (Poli, 1795). **A**. External dorsal valve, with coloured patterns and marked growth lines, MNHN-IB-2022-967. **B**. External ventral valve, revealing a worn area (surface of cementation), MNHN-IB-2022-968. **C**. Interior of the same valve. The anterior (a.a.) and posterior (p.a.) adductors, mantle canals (m.ca) and rostellum (ro) are identified. Scale bars = 2 mm.

Subphylum Rhynchonelliformea Williams *et al*., 1996
Order Rhynchonellida Kuhn, 1949
Superfamily Dimerelloidea Buckman, 1918
Family Cryptoporidae Muir-Wood, 1955
Genus *Cryptopora* Jeffreys, 1869

Cryptopora rectimarginata Cooper, 1959
Figs 4–5

Cryptopora rectimarginata Cooper, 1959: 20, pl. 1 figs 15–19, pl. 2 figs 1–11.

Cryptopora gnomon – Cooper 1954 (not Jeffreys): 364.
Cryptopora rectimarginata – Cooper 1977: 55, pl. 2 figs 1–4, pl. 5 figs 1–8, pl. 27 figs 7–14.

Material examined (including figured material)

GUADELOUPE – **N of Grande Terre** • 1 shell; stn DW 4518; 16°34′ N, 61°37′ W; depth 426–441 m; 9 Jun. 2015; Karubenthos 2 exped.; MNHN • 2 shells; stn DW 5444; 16°38′ N, 61°37′ W; depth 413–423 m; 13 Jun. 2015; Karubenthos 2 exped.; MNHN • 27 shells; stn DW 4546; 16°31′ N, 61°32′ W; depth 268–306 m; 14 Jun. 2015; Karubenthos 2 exped.; MNHN • 1 shell; same data as for preceding; MNHN, MNHN-IB-2022-973 (Fig. 4D) • 1 shell; same data as for preceding; MNHN, MNHN-IB-2022-974 (Fig. 4E) • 1 shell; same data as for preceding; MNHN, MNHN-IB-2022-975 (Fig. 4F) • 4 shells; stn DW 4549; 16°38′ N, 61°35′ W; depth. 343–402 m; 14 Jun. 2015; Karubenthos 2 exped.; MNHN • 6 shells; stn DW 4550; 16°37′ N, 61°31′ W; depth 432–482 m; 14 Jun. 2015; Karubenthos 2 exped.; MNHN. – **W of Basse Terre** • stn DW 4514; 16°12′ N, 61°51′ W; depth 792–800 m; 8 Jun. 2015; Karubenthos 2 exped.; MNHN, MNHN-IB-2022-977 (Fig. 5A–E) • 1 valve; same data as for preceding; MNHN, MNHN-IB-2022-1082. – **E of La Désirade** • 2 shells; stn DW 4556; 16°24′ N, 60°49′ W; depth 367–428 m; 15 Jun. 2015; Karubenthos 2 exped.; MNHN • 2 shells + 1 juv.; stn DW 4558; 16°22′ N, 60°50′ W; depth 312–385 m; 16 Jun. 2015; Karubenthos 2 exped.; MNHN, MNHN-IB-2022-976 (Fig. 4I) • 1 shell; same data as for preceding; MNHN, MNHN-IB-2022-978 (Fig. 5F–H) • 12 shells; stn DW 4560; 16°25′ N, 60°52′ W; depth 185–250 m; 16 Jun. 2015; Karubenthos 2 exped.; MNHN • 2 shells; stn DW 4568; 16°17′ N, 61°01′ W; depth 208–362 m; 17 Jun. 2015; Karubenthos 2 exped.; MNHN • 1 shell; stn DW 4569; 16°17′ N, 61°01′ W; depth 250–359 m; 17 Jun. 2015; Karubenthos 2 exped.; MNHN • 3 shells; stn DW 4570; 16°19′ N, 61°00′ W; depth 286–343 m; 17 Jun. 2015; Karubenthos 2 exped.; MNHN • 1 shell; same data as for preceding; MNHN, MNHN-IB-2022-971 (Fig. 4B) • 4 shells; stn DW 4572; 16°19′ N, 60°55′ W; depth 396–399 m; 17 Jun. 2015; Karubenthos 2 exped.; MNHN • 1 shell; same data as for preceding; MNHN, MNHN-IB-2022-970 (Fig. 4A). – **W of La Désirade** • 2 shells; stn DW 4582; 16°08′ N, 61°19′ W; depth 400–420 m; 19 Jun. 2015; Karubenthos 2 exped.; MNHN • 1 shell; stn CP 4608; 16°14′ N, 60°49′ W; depth 618–632 m; 24 Jun. 2015; Karubenthos 2 exped.; MNHN, MNHN-IB-2022-972 (Fig. 4C). – **N of Marie-Galante** • 8 shells; stn DW 4586; 16°00′ N, 61°23′ W; depth 204–251 m; 21 Jun. 2015; Karubenthos 2 exped.; MNHN. – **W of Marie-Galante** • 1 shell; stn DW 4632; 15°49′ N, 61°28′ W; depth 376–393 m; 27 Jun. 2015; Karubenthos 2 exped.; MNHN • 7 shells; stn DW 4634; 15°48′ N, 61°26′ W; depth 304–310 m; 27 Jun. 2015; Karubenthos 2 exped.; MNHN.

Type locality

Off NW Ireland.

Description

Morphology. The tiny dimensions of the representatives of this species means they are often overlooked. Smooth translucent thin-shell, biconvex, rarely exceeding 2 mm in length among sampled specimens, triangular with round angles anteriorly, rather rectimarginate. The foramen is wide open, elongate

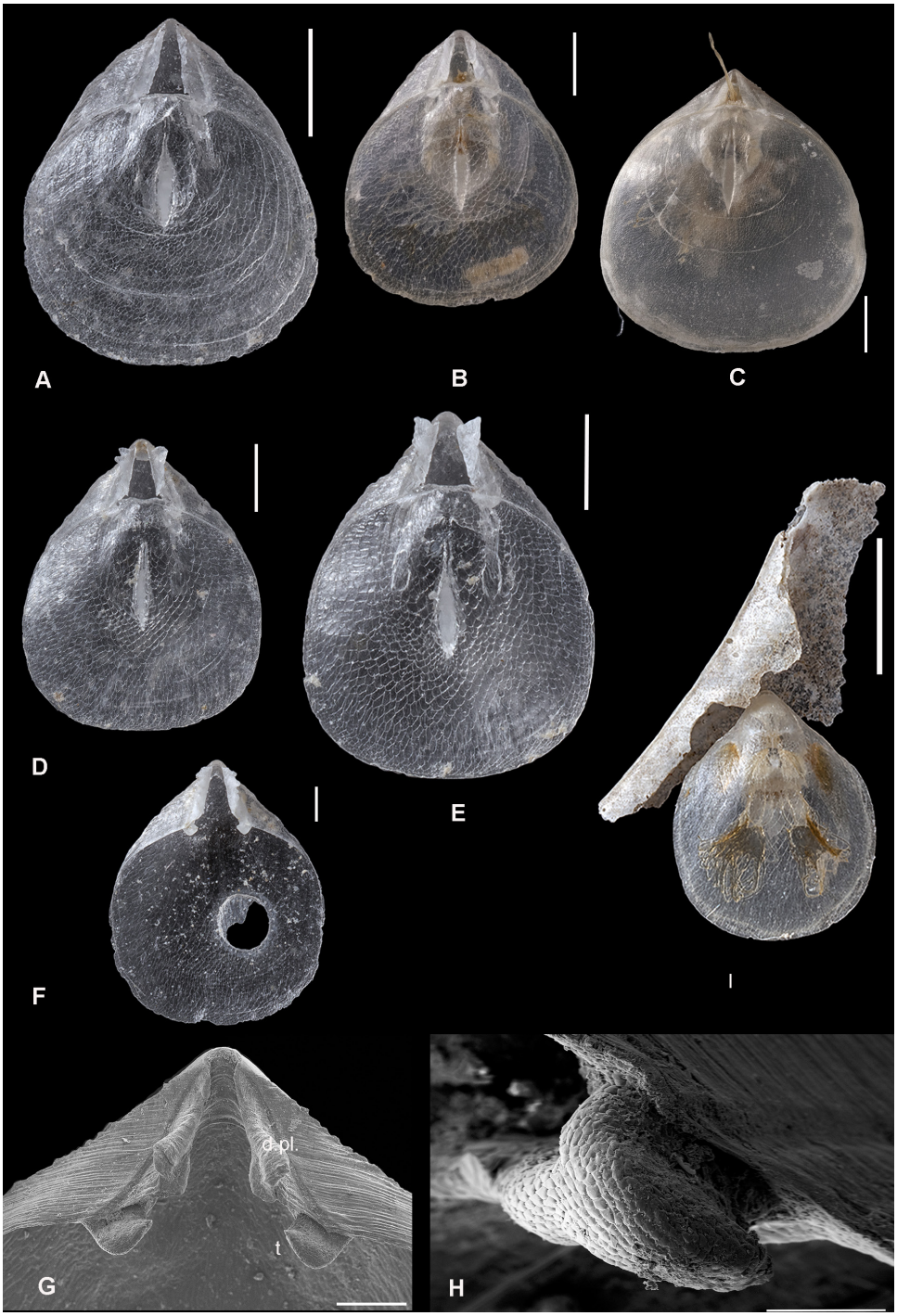

Fig. 4. *Cryptopora rectimarginata* Cooper, 1959. **A**. Dorsal view of an adult specimen, MNHN-IB-2022-970. **B**. Smaller specimen, MNHN-IB-2022-971. **C**. Specimen with a slender pedicle, MNHN-IB-2022-972. **D**. Specimen beginning to develop deltidial plates, MNHN-IB-2022-973. **E**. Specimen from the same station as specimen C, with more developed winged deltidial plates, MNHN-IB2022-974. **F**. Ventral valve widely bored by a gastropod, revealing the teeth, MNHN-IB-2022-975. **G**. Posterior part of ventral valve of an obviously juvenile specimen, revealing the pedicle collar, deltidial plates (d.pl.) and teeth (t), MNHN-IB-2022-1082. **H**. Close-up view of a tooth showing a well-arranged mosaic of fibre ends, MNHN-IB-2022-1082. **I**. Juvenile specimen attached in living position to an organic substrate, MNHN-IB-2022-976. Scale bars: A, I = 1 mm; B = 500 µm; C–F = 1 mm; G = 200 µm; H = 100 µm.

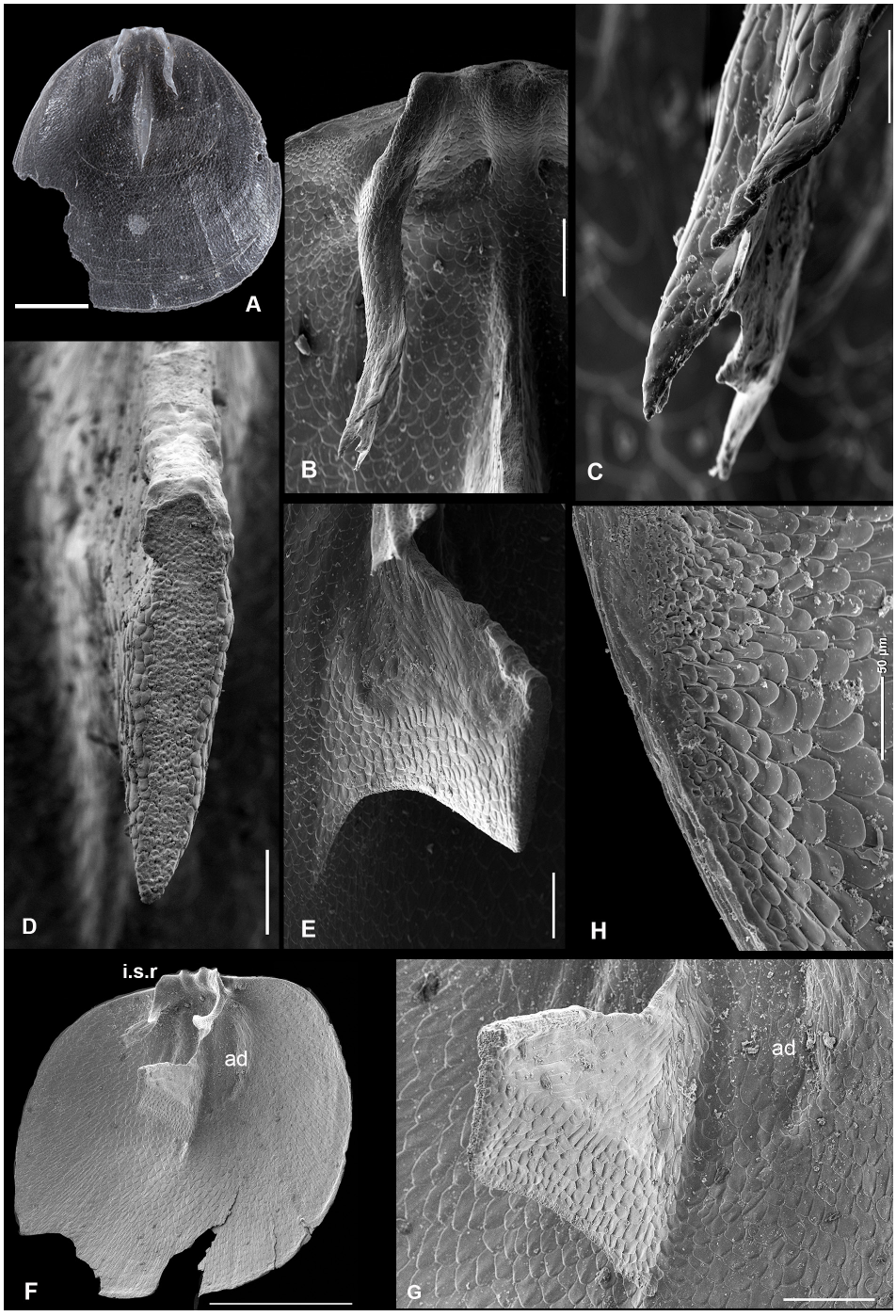

Fig. 5. *Cryptopora rectimarginata* Cooper, 1959. **A–E**. Dorsal valve interior revealing the cardinal process, crura and median septum, MNHN-IB-2022-977. **B–H**. SEM views. **B**. Half dorsal valve, showing the cardinal process, the crural plates ending in hand-like crura. **C**. Close-up view of the hand-like crura. **D**. Upper part of the septum with its microstructure. **E**. Lateral view of the high median septum, with its partly fibrous mosaic. **F**. Interior of a dorsal valve partly tilted laterally to reveal: the high inner socket ridges (i.s.r), the crural plates, high septum separating the adductors (ad) and the fibrous mosaic at the valve floor, MNHN-IB-2022-778. **G**. Close-up view of the septum illustrating the change of fibre orientations ending by a brachiotest at its lateral posterior part, MNHN-IB-2022-778. **H**. Fibrous mosaic from the inner valve margin to the middle valve, MNHN-IB-2022-778. Scale bars: A, F = 1 mm; B, E = 200 µm; C, H = 50 µm; D = 100 µm; G = 400 µm.

triangular, bordered by elevated narrow winged deltidial plates (Fig. 4A–C). Some specimens possess more developed winged expansions of the deltidial plates (Fig. 4D–F) that could be confused with those of the species *C. curiosa* Cooper, 1973, but these expansions are less round than in the latter species from the Indian Ocean (Cooper 1973). In some cases, the pedicle can be longer than the shell. It terminates via short rootlets at the point of attachment to the substrate (Fig. 4I).

Ventral valve. The ventral valve interior reveals relatively strong dental plates (Fig. 4G–H).

Dorsal valve. The dorsal valve interior shows a small cardinal process, erect inner dental socket ridges, wide open dental sockets, typical long crural branches ending in hand-like crura (Fig. 5A–C), blade-like median septum ending by a high plateau antero-ventrally (Fig. 5D–G) and faint muscle scars (Fig. 5G).

Microstructure. In addition to the fibrous mosaic viewed through transparent shells (Fig. 4B, D–E), observations using the SEM reveal the fibrous mosaic of the valve floor, teeth, arms and crura, sides and plateau of the median septum (Fig. 5B, E, G–H), as well as the brachiotest (Fig. 5G). Their orientation and size modifications are highlighted (Figs 4E, 5D–H).

Depth range

185–800 m, Karubenthos expedition; elsewhere: 136–850 m.

Distribution

The species is known in the Gulf of Mexico, in the Straits of Florida, Florida Keys, S of Grand Bahama Island, S–SW of Panama City; Barbados (Cooper 1959, 1977; Asgaard & Stentoft 1984; Logan 1990).

Ecology

The thin and long slender pedicle allow easy movements and orientation of the thin shell in the sea water. This species has a relative wide depth tolerance.

Remarks

Rhynchonellid brachiopods are uncommon in the Gulf of Mexico and in the Caribbean Sea. *Cryptopora* is the only genus currently known there.

Order Terebratulida Waagen, 1883
Suborder Terebratulidina Waagen, 1883
Superfamily Terebratuloidea Gray, 1840
Family Terebratulidae Gray, 1840
Subfamily Gryphinae Sahni, 1929
Genus *Gryphu*s Megerle von Mühlfeldt, 1871

Gryphus bartletti (Dall, 1882)
Fig. 6

Terebratula bartletti Dall, 1882: 885.

Terebratula bartletti – Dall 1886: 200, pl. 6 figs 4a–c. — Davidson 1886: 14, pl. 1 figs 20–21.
Gryphus bartletti – Dall 1920: 314. — Logan 2007: 3092.
?*Tichosina bartletti* – Cooper 1977: 64, pl. 3 figs 27–28, pl. 10 figs 11–17.
Eurysina? *bartletti* – Cooper 1983: 259, pl. 9 figs 18–22, pl. 65 figs 15–16.

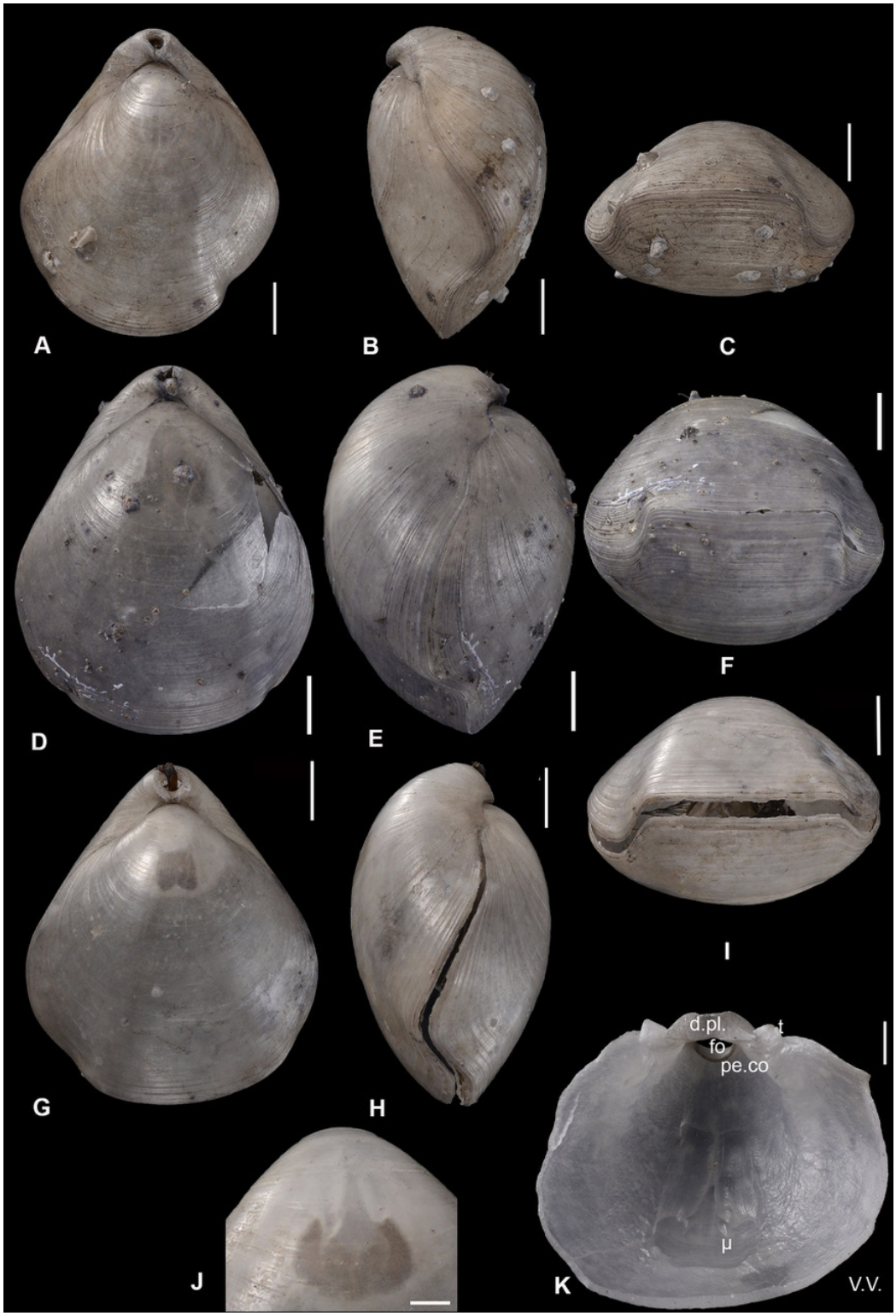

Fig. 6. *Gryphus bartletti* (Dall, 1882). **A**–**C**. Dorsal, right lateral and anterior views of an adult, MNHN-IB-2022-979. **D**–**F**. Dorsal, left lateral and anterior views of a gibbous specimen, MNHN-IB-2022-980. **G**–**I**. Three views of a relatively wide specimen, MNHN-IB-2022-981. **J**. Set of muscle imprints viewed by transparency at the external ventral valve (V.V.). **K**. Same set of muscle imprints (μ) viewed inside, foramen (fo), deltidial plates (d.pl), pedicle collar (pe.co), MNHN-IB-2022-1081. Scale bars: A–J = 5 mm; K = 2 mm.

Material examined (including figured material)

GUADELOUPE – **E of La Désirade** • 1 shell; stn DW 4574; 16°22′ N, 60°54′ W; depth 140–340 m; 18 Jun. 2015; Karubenthos 2 exped; MNHN, MNHN-IB-2022-979 (Fig. 6A–C) • 1 shell; same data as for preceding; MNHN, MNHN-IB-2022-981 (Fig. 6G–J) • 1 fragmented valve; same data as for preceding; MNHN, MNHN-IB-2022-1081. – **W of Marie-Galante** • 1 shell; stn CP 4595; 15°58′ N, 61°22′ W; depth 208–211 m; 22 Jun. 2015; Karubenthos 2 exped.; MNHN, MNHN-IB-2022-980 (Fig. 6D–F).

Type locality

Barbados.

Description

Morphology. Adult shells of this species can reach 30 mm. The shape is elongate, ventri-biconvex, with a lightly curved umbo truncated obliquely by a wide foramen with a strong tendency to be labiate. The maximum width is anterior to the mid length (Fig. 6A, D, G). The lateral margins are inclined ventrally to the anterior part, then suddenly change orientation to highlight the high folding of the broad anterior margin (Fig. 6B–C, E–F, H–I). The shell surface is marked by growth lines and laterally by capillae that cross the main growth lines.

Dorsal valve. The valve interior reveals the cardinal process and wide inclined outer hinge plates, high crural bases, posterior dental sockets blunt and anterior ones wide open. The descending branches (or lamellae) are large and slightly oblique, and the transverse band presents a relatively high median fold. When broken, the brachidium lets the elongate adductor prints to be visible at the shell floor.

Ventral valve. The ventral valve reveals muscle imprints inside and by transparency (Fig. 6J–K).

Microstructure. Three-layered shell under the organic periostracum: acicular primary layer, fibrous secondary layer and prismatic/columnar tertiary layer, both entirely crossed by endopunctae.

Depth range

140–340 m, Karubenthos 2 exped.; 115–915 m in Cooper (1977).

Distribution

The species is recorded S of Martinique, W of Montserrat, NE of La Isabela (Cuba), off French Guiana, Virgin Islands (Cooper 1977), Barbados, West Florida, off Grenada.

Ecology

Owing to the shape of the foramen, the shell is attached by a short pedicle to hard substrates, generally with the dorsal valve lying next to them. The species has a wide depth tolerance.

Subfamily Tichosininae Cooper, 1983
Genus *Tichosina* Cooper, 1977

Tichosina bullisi Cooper, 1977
Figs 7–8

Tichosina bullisi Cooper, 1977: 66–67, pl. 6 figs 1–8.

non *Tichosina bullisi* – Rojas *et al*. 2015: 57, fig. 2a–d.

Material examined (including figured material)

GUADELOUPE – **W of Marie Galante** • 1 shell; stn CP 4595; 15°58′ N, 61°22′ W; depth 208–211 m; 22 Jun. 2015; Karubenthos 2 exped.; MNHN. – **S of Marie Galante** • 1 shell; stn DW 4638; 15°50′ N, 61°19′ W; depth 305–312 m; 28 Jun. 2015; Karubenthos 2 exped; MNHN. – **W of Marie Galante** • 1 shell; stn DW 4599; 15°53′ N, 61°25′ W; depth 262–266 m; 22 Jun. 2015; Karubenthos 2 exped.; MNHN, MNHN-IB-2022-982 (Fig. 7A–C) • 2 valves; same data as preceding; MNHN, MNHN-IB-2022-1072 (Fig. 7F, K), MNHN-IB-2022-1073 (Fig. H). – **E of La Désirade** • 1 shell; stn DW 4558; 16°22′ N, 60°50′ W; depth 312–385 m; 15 Jun. 2015; Karubenthos 2 exped.; MNHN • 1 shell; stn DW 4574; 16°22′ N, 60°54′ W; depth 140–340 m; 18 Jun. 2015; Karubenthos 2 exped.; MNHN, MNHN-IB-2022-983 (Fig. 7D–E) • 1 shell; stn CP 4614; 16°23′ N, 60°50′ W; depth 260–270 m; 25 Jun. 2015; Karubenthos 2 exped.; MNHN. – **N of Les Saintes** • 1 shell; stn DW 4626; 15°57′ N, 61°37′ W; depth 210–233; 26 Jun. 2015; Karubenthos 2; MNHN, MNHN-IB-2022-984 (Figs 7G, I–J, 8A–B).

Type locality

Off Nicaragua.

Description

Morphology. Mostly adult large ventri-biconvex shells, rather pentagonal than triangular, widest at nearly mid length. Shells have been found white, pale cream or nearly dark (suspicion of pollution) ornamented by faint capillae on the lateral sides (Fig. 7A–B, D). The foramen is round to slightly labiate, the broad anterior margin rather monoplicate (Fig. 7C) and the ventral umbo suberect. The lateral margins (S-shaped) are incurved ventrally at the anterior part (Fig. 7B). Growth marks are easily seen particularly at the mid anterior shell part with sometimes traces of attachment of congenerics, cf. *Podichnus centrifugalis* Bromley & Surlyk, 1973 (Bromley & Surlyk 1973), here observed on the outer surface (Fig. 7F).

Dorsal valve. The valve interior reveals the semi-elliptical cardinal process, a relatively large variable loop, with high and long crural bases, dental sockets wide open anteriorly, crural processes turned to the median plane, descending branches shaping brackets, folded transverse band wide with two slightly curved anterolateral ends (Fig. 7I–J). When the lophophore is in place or removed from its support (the brachidium), one can observe spicules at its base with a simple shape compared to those of the body wall. When the valve is cleaned from the lophophore, large spicules on the body wall are observed protecting the soft parts. They also exist along the mantle canals with a more elongate form. These mantle canals can be observed by transparency and at the internal surface of the valves: vascula media and vascula lateralis (Fig. 7D–E). The brachidium being broken, the elongate teardrop-shaped adductor scars are observed (Fig. 7K).

Ventral valve. The valve reveals concave deltidial plates and, at the posterior part of the valve interior, the teeth are small and the pedicle collar present. The body wall has wide spicules close each to the other (Fig. 8A), the spicules becoming thinner anteriorly towards the vascula. The observation of internal surface of the body wall fragments reveals the polygonal pattern of the orange gonads (Fig. 8B). Spicules were observed at the basal lophophore arms (Fig. 8C). When the body wall is removed, the complex shape of the muscles, adductors (anterior and posterior) and diductors and/or their imprints, is visible (Fig. 7G–H).

Microstructure. Longitudinal sections of the shells allow observation of a three-layered shell under the organic periostracum: a thin acicular primary layer, a fibrous secondary layer and a thick tertiary layer (Fig. 8D–E), the fibres being in continuity with the prisms (Fig. 8F). At the posterior and anterior regions an alternance of secondary and tertiary layers is observed (Fig. 8D, G) with marks of major growth rhythms. The latter are very close together near the internal surface and near the anterior edge in aged specimens. At the nano level, fibres and prisms reveal elementary growth lines and submicrometric

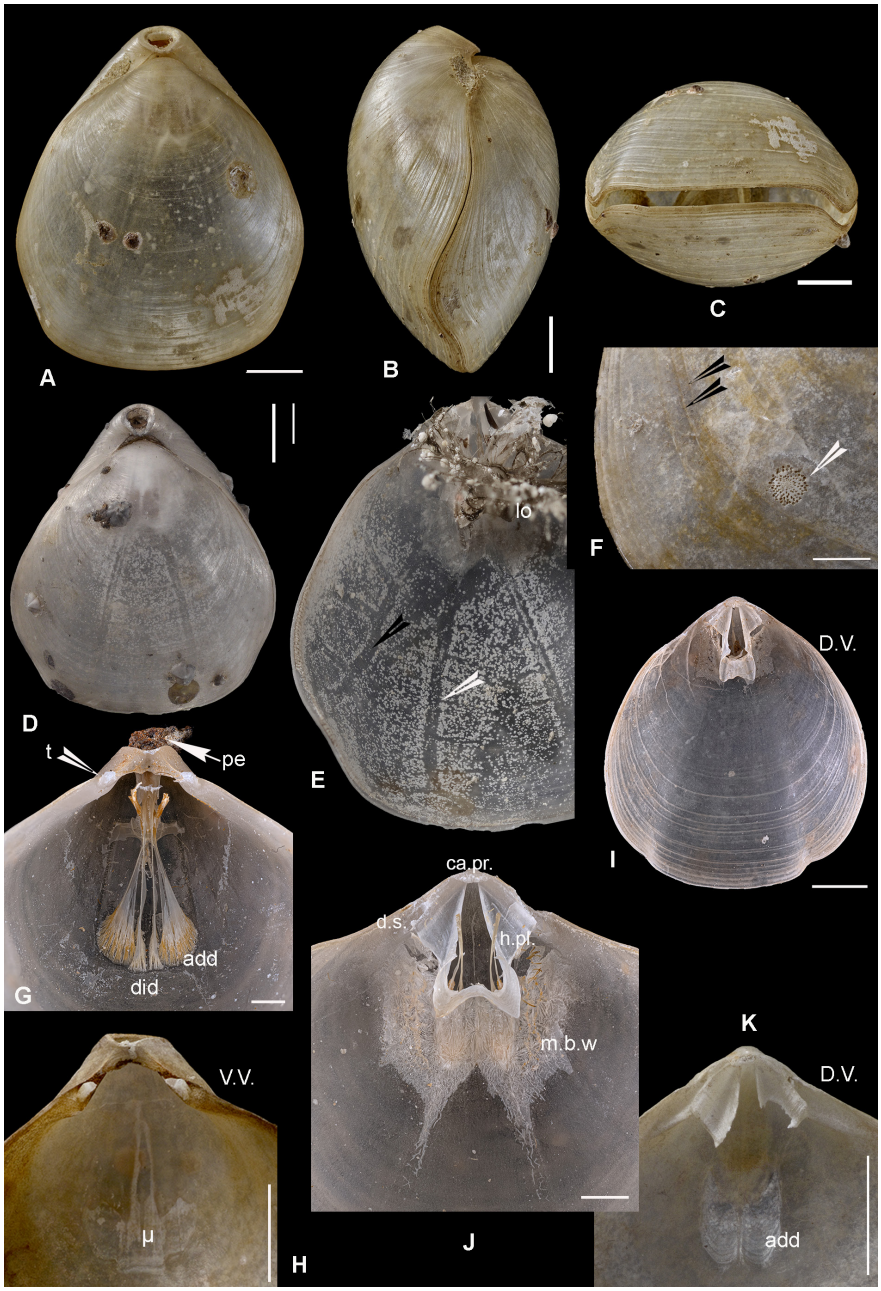

Fig. 7. *Tichosina bullisi* Cooper, 1977. **A–C**. Dorsal, lateral and anterior views of a specimen from Guadeloupe Islet, MNHN-IB-2022-982. **D**. Dorsal view of a specimen revealed by transparency: adductors and vascula, MNHN-IB-2022-983. **E**. Dorsal valve interior with the vascula media (white arrowhead) and vascula lateralis (black arrowhead), lophophore (lo), MNHN-IB-2022-983. **F**. Traces of boring from a brachiopod pedicle attachment: *Podichnus centrifugalis* Bromley & Surlyk (1973) (white arrowhead), and location of major growth lines (black arrowhead), MNHN-IB-2022-1072. **G**. Posterior view of a ventral valve interior with the teeth (t), pedicle (pe), adjustors attached to it, adductors (add) and diductors (did), MNHN-IB-2022-984. **H**. Posterior view of a ventral valve interior with the imprint of a set of adductors and diductors (μ), MNHN-IB-2022-1073. **I**. Dorsal valve interior (same shell as G), with the brachidium. **J**. Same valve sightly tilted posteriorly to expose the cardinal process (ca.pr.), dental sockets (d.s.), hinge plates (h.pl.), and reveal the mantle body wall (m.b.w) heavily spiculate and the departure of mantle canals. **K**. Posterior dorsal valve interior (D.V.) with broken brachidium, revealing the teardrop shape of adductors (add); MNHN-IB-2022-1072. Scale bars: A–D, F, H–I, K = 5 mm; E, G, J = 2 mm.

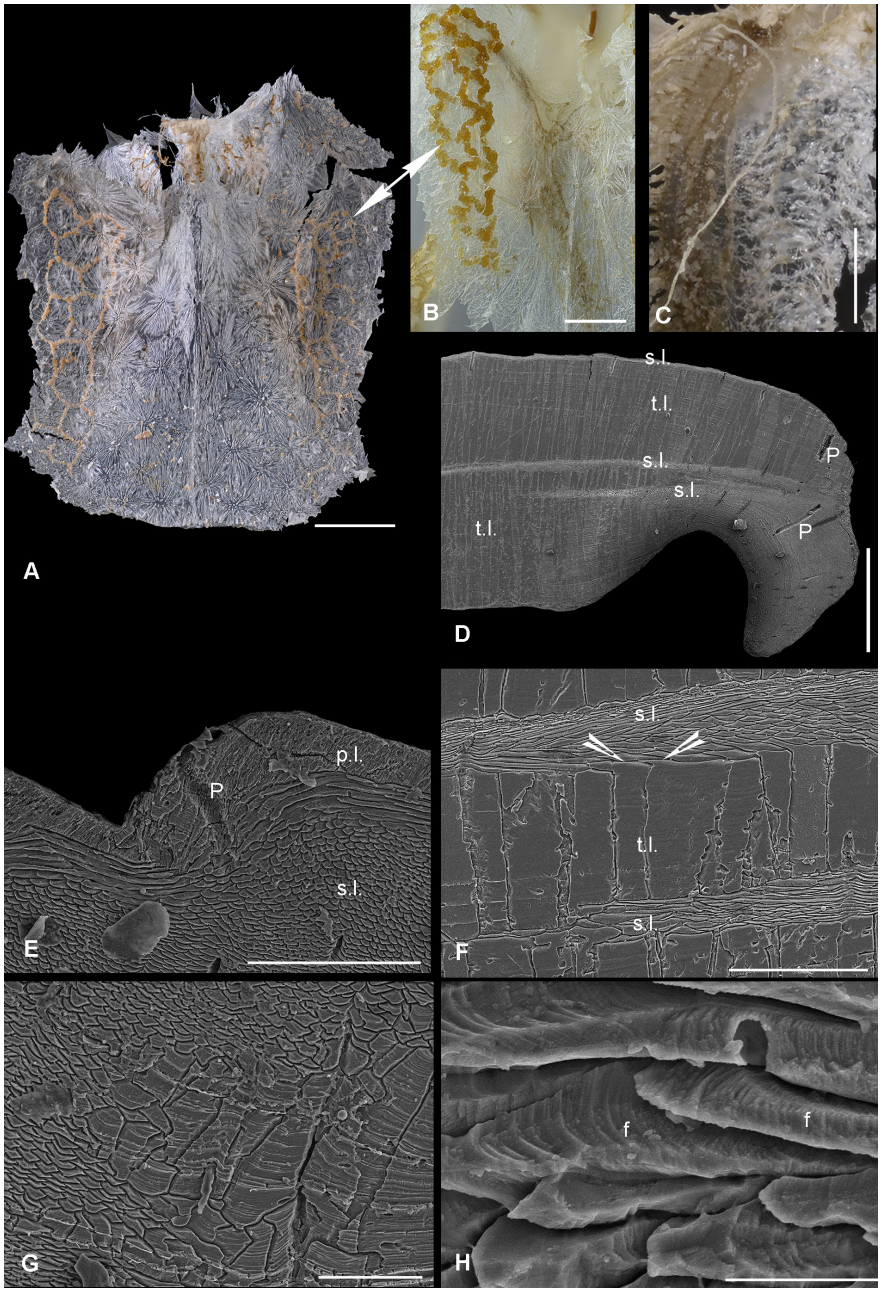

Fig. 8. *Tichosina bullisi* Cooper, 1977. **A**. Ventral mantle body wall heavily spiculate with orange polygonal net of gonads seen by transparency, MNHN-IB-2022-984. **B**. Opposite side of the mantle body wall revealing the gonads, MNHN-IB-2022-984. **C**. Spicules at the basal part of the lophophore arms, MNHN-IB-2022-983. **D**–**H**. SEM views along a median longitudinal section through a shell of *Tichosina* Cooper, 1977; MNHN-IB-2022-985. **D**. Posterior part of a longitudinal section to show the three-layered shell under the organic periostracum: the very thin acicular primary layer, thin secondary layer (s.l.) and thicker tertiary layer (t.l.) with some alternating s.l. and t.l. A few punctae (P) cross the shell there. **E**. Close-up view of the primary layer above the fibrous secondary layer. **F**. Continuity from fibres of the secondary layer to prisms/columns of the tertiary layer (arrowheads). **G**. Several alternating secondary and tertiary layers near the anterior part of the longitudinal section. **H**. Close-up view in the secondary layer to reveal the micro-growth rhythms along the fibres (f) and submicrometric granules between two consecutive elementary growth lines. Scale bars: A = 2 mm; B–C = 1 mm; D = 500 µm; E–F = 100 µm; G = 50 µm; H = 10 µm.

granules (Fig. 8H). Sometimes, a close-up view at the primary layer reveals the presence of microboring organisms (Fig. 8E).

Depth range

140–385 m, Karubenthos 2 exped.; 201–289 m, Cooper (1977).

Distribution

The species was recorded by Cooper (1977) in the Caribbean Sea: off Nicaragua.

Remarks

The high number of species (17 sp. nov. + 1 sp. 1) in the genus *Tichosina* reported by Cooper (1977) led to some comments by Rojas *et al*. (2015) who tentatively synonymised *T. dubia* and *T. bullisi* with *Tichosina plicata* (see also Rojas *et al*. 2022). In the present work, it is not easy to follow the position of these authors for *Tichosina bullisi*, according to the proportions of the different parts of the articulation and brachidium, and because they did not illustrate a wide comparative representation of the brachidium of the different species.

In addition, Cooper (1983: 259) introduced a new genus: *Eurysina* for some of the species of *Tichosina* thereby increasing the confusion.

In the present study, I follow the position of Logan (2007) in the *Treatise* for this species and the others described below. But in other aspects, to give an idea of the real shape of the brachidium for each species, it is necessary, when imaged, to take into consideration the convexity of the valves. More often the dorsal valve can be tilted slightly posteriorly, which completely changes the aspect of the proportions and shape of the brachidium. While Cooper's work is quite pioneering for the Caribbean region pro parte, he rendered species recognition somewhat difficult by ignoring in other aspects the potential variability in a population, even between populations of a same species.

Tichosina cubensis (Pourtalès, 1867)
Fig. 9

Terebratula cubensis Pourtalès, 1867: 109.

Terebratula cubensis – Dall 1871: 3, pl. 1 figs 2, 8–15. — Davidson 1880: 28, pl. 2 figs 10–11.
Lyothyris sphenoidea – Davidson 1886: 12, pl. 2 figs 9a–b, 21–22. (part)
Gryphus cubensis – Dall 1920: 315 – Cooper 1954: 364
Tichosina cubensis – Cooper 1977: 67, pl. 22 figs 1–8, pl. 27 figs 15–22.

non *Terebratula vitrea* var. *sphenoidea* Jeffreys, 1878 – Phillipi 1844: 404, pl. 22 fig. 6.

Material examined (including figured material)

GUADELOUPE – **E of La Désirade** • 1 shell; stn CP 4558; 16°22′ N, 60°50′ W; depth 312–385 m; 15 Jun. 2015; Karubenthos 2 exped.; MNHN, MNHN-IB-2022-986 (Fig. 9) • 1 shell; stn DW 4572; 16°19′ N, 60°55′ W; depth 396–399 m: 17 Jun. 2015; Karubenthos 2 exped.; MNHN.

Type locality

Off Havana, Cuba.

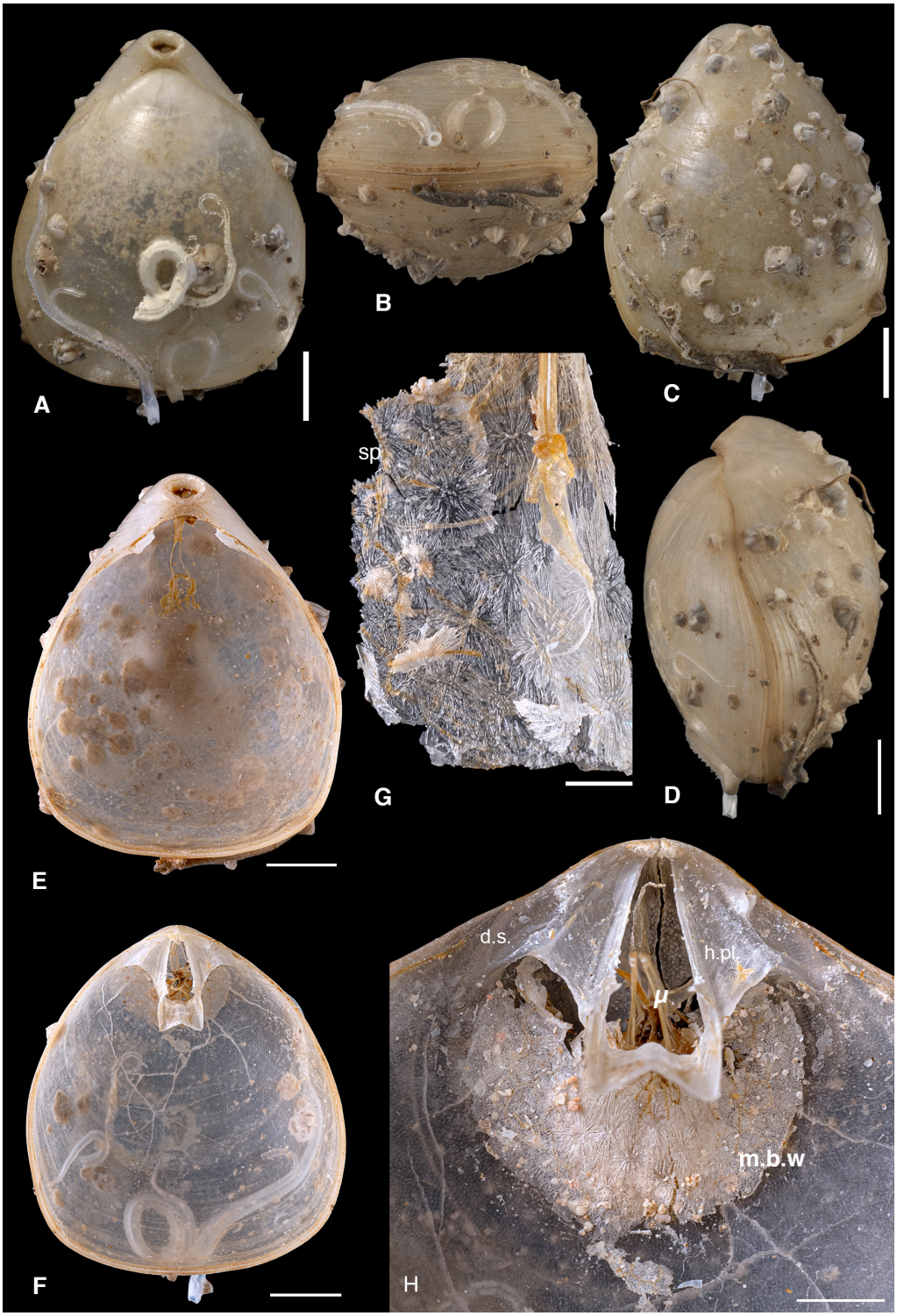

Fig. 9. *Tichosina cubensis* (Pourtalès, 1867), MNHN-IB-2022-986. **A–D**. Dosal, anterior, ventral and lateral views of an adult specimen covered with worm tubes and a crustacean (Thecostraca). **E**. Ventral valve interior with teeth. **F**. Dorsal valve interior with the brachidium. **G**. Wide stellar spicules (sp) of the body wall. **H**. Posterior part of the dorsal valve interior, slightly tilted to reveal the mantle body wall (m.b.w.) with spicules, and muscles (μ) under the transverse band of the brachidium, the wide anteriorly open dental sockets (d.s.), wide inclined hinge plates (h.pl.), and the short but pointed crural processes. Scale bars: A–F = 5 mm; G = 1 mm; H = 2 mm.

Description

Morphology. Large adult ventri-biconvex shell with a rounded triangular outline (Fig. 9A, C), lateral commissures slightly incurved ventrally, then roughly straight (Fig. 9D), anterior margin rectimarginate (Fig. 9B), to broadly and very slightly monoplicate. Ventral umbo barely curved, truncated by a large round foramen; a short pedicle collar is observed inside it (Fig. 9A, E). The symphytium that bounds dorsally the wide foramen is concave and large anteriorly but partly hidden by the bulging dorsal umbo (Fig. 9A, E). The growth marks are best revealed at the anterior part of the shell and laterally (Fig. 9B, D).

Ventral valve. After disarticulation of the valves, the ventral valve interior reveals relatively thin and elongate teeth (Fig. 9E) and the location of the ventral muscles.

Dorsal valve. The valve interior shows the presence of a transverse cardinal process, dental sockets covered posteriorly and widely open anteriorly, a loop relatively short with wide hinge plates limited by narrow elevated crural bases, short crural processes ± oriented to the plane of symmetry of the valve, crural processes arriving at the level of the anterior part of the hinge plates, short arched descending branches and a wide transverse band showing a median fold (Fig. 9F). When the valve is observed slightly tilted posteriorly, the transverse band of the loop reveals an obviously marked fold. Beneath and laterally to this loop the limited mantle body wall is revealed with the classical wide spicules of the genus *Tichosina* (Fig. 9G–H). This body wall is protecting the soft parts including the set of muscles.

Microstructure. The punctate three-layered shell is similar with that of *T. bullisi.*

Depth range

312–385 m, Karubenthos 2 exped.; 146–963 m in Cooper (1977).

Distribution

The species is recorded from the Gulf of Mexico: common in the Straits of Florida, off Key west, Florida and on the Mississippi cone east of Cape Romano Florida, found off Cuba, NE and SW of Sainte Lucie, NE and E of Dominica, W of Anguilla, N of Virgin Islands, S and N of Guadeloupe (Cooper 1977).

Ecology

The shells are often covered with small crustaceans and worms in their tubes that, while suspension feeders, are opportunists (rather than acting by kleptomania) (Fig. 9A–D).

Tichosina madininensis sp. nov.

urn:lsid:zoobank.org:act:BC0EA037-0FF7-4FBD-A53C-FF71E3E7A6DB

Fig. 10A–G

Tichosina sp1 – Cooper 1977: 88, pl. 12 figs 8–12.

Diagnosis

Quasi equally convex medium sized shell, rather bulged at the dorsal posterior part, with a rounded outline, a relative wide foramen and a narrow paraplicate anterior margin. Brachidium narrow, with a marked median fold of the transverse band and spicules of the mantle body wall thin.

Differential diagnosis

The species differs from the other members of the genus, primarily in its smaller size and dorsal convexity. Addtionally, the anterior margin differs in being neither rectimarginate (*T. cubensis*), nor moderately monoplicate (*T. plicata*), nor highly and widely monoplicate (*T. bullisi*). The brachidium does not possess lateral extensions as in *T. solida*. The paraplicate anterior margin has not been observed in any other species of the genus.

Etymology

The species is named after the Amerindian name of the Island of Martinique: Madinina.

Type material

Holotype

GUADELOUPE – **E of La Désirade** • shell; stn DW 4613; 16°25′ N, 60°50′ W; depth 210–240 m; 25 Jun. 2015; Karubenthos 2 exped.; MNHN, MNHN-IB-2022-987a (Fig. 10A–C).

Paratypes

GUADELOUPE – **E of La Désirade** • 1 dorsal valve; stn DW 4613; 16°25′ N, 60°50′ W; depth 210–240 m; 25 Jun. 2015; Karubenthos 2 exped.; MNHN, MNHN-IB-2022-987b (Fig. 10D). – **W of Marie-Galante** • 1 shell; stn CP 4598; 15°56′ N, 61°23′ W; depth 207–211 m; 22 Jun. 2015; Karubenthos 2 exped.; MNHN, MNHN-IB-2022-988 (Fig. 10E–G).

Type locality

Guadeloupe, E of La Désirade, 16°25′ N, 60°50′ W.

Description

Morphology. A white, medium-sized, translucent shell was observed with an anterior margin revealing differences from the other species of the genus *Tichosina*. Maximum width at mid-dorsal valve or slightly anterior to it, moderately curved ventral umbo cut by a slightly labiate to round foramen (Fig. 10A, E). The lateral margins are nearly straight (Fig. 10B, G) and the anterior one is undulating, paraplicate (Fig. 10C, F).

Dorsal valve. Mantle canals and body wall were observed by transparency on the dorsal valve (Fig. 10A). The spicules in the mantle body wall (Fig. 10D) present some differences from those of the other species included in the genus *Tichosina* (but the age of the specimen can be important). The brachidium has a median fold. Traces of close adductors can be observed by transparency at the posterior part of the valve.

Microstructure. The scarcity of this fragile material prevents observation of the microstructural details.

Remarks

Numerous other specimens could help reconsider the status of the genus.

Depth range

207–240 m, Karubenthos 2 exped.; 201–238 m (Cooper 1977).

Distribution

The species was reported from Virgin Islands (Cooper 1977, cf. sp.1).

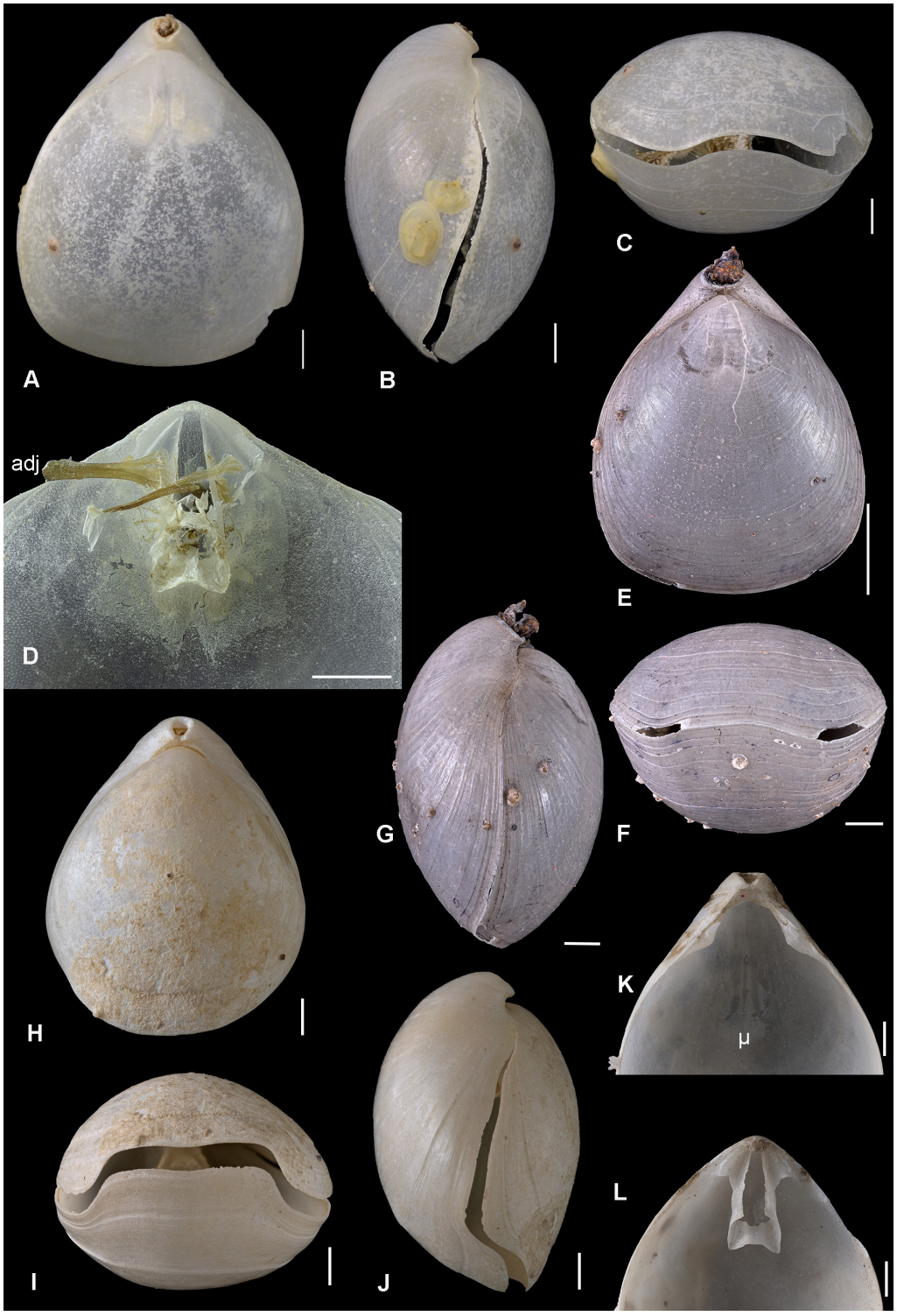

Fig. 10. A–G. ?*Tichosina madininensis* sp. nov. **A–C**. Dorsal, lateral and anterior views of the holotype, MNHN-IB-2022-987a. **D**. Posterior dorsal valve interior, with the adjustor muscles (adj) attached to the hinge plates, and the brachidium, MNHN-IB-2022-987b. **E–G**. Dorsal, anterior and lateral views of a paratype, MNHN-IB-2022-988. — **H–L**. *Tichosina obesa* Cooper, 1977. **H–J**. Elongate specimen, MNHN-IB-2022-989. **K–L**. MNHN-IB-2022-990. **K**. Ventral valve interior of a specimen revealing the teeth and the main muscular cast (adductor, ventral adjustor and diductors (μ). **L**. Posterior dorsal valve interior, with its brachidium. Scale bars: A–C, E–G = 5 mm; D, H–L = 2 mm.

Tichonisa obesa Cooper, 1977
Fig. 10H–L

Material examined (including figured material)

GUADELOUPE – **E of La Désirade** • 9 shells; stn DW 4553; 16°21′ N, 60°54′ W; depth 111–162 m; 15 Jun. 2015; Karubenthos 2 exped.; MNHN • 1 shell; same data as preceding; MNHN, MNHN-IB-2022-989 (Fig. 10H–J) • 1 shell; same data as for preceding; MNHN, MNHN-IB-2022-990 (Fig. 10K–L).

Type locality

Off Venezuelan coasts.

Description

Morphology. Some shells of the species from stn DW 4553, showing the same external morphology, pose a problem, because their pr.p. reveals some of the characteristics of *Tichosina solida* with their tiny extensions on the lateral descending branches of the brachidum, but they are of medium size, mainly less than 20 mm, elongate with a strong straight monoplicate anterior margin (Fig. 10I) and a labiate foramen, pedicle collar widely visible and symphytium concave (Fig. 10H–K). The beak is slightly curved to suberect. Some major growth lines mark the external surface (Fig. 10J).

Ventral valve. The separate valves reveal highly impressed muscle scars and elongate teeth detached from the margins (Fig. 10K).

Dorsal valve. The valve interior reveals a brachidium with some peculiarities. If the brachidium shows a classical aspect in some cases, in certain specimens it tends to be an intermediary to that of *Tichosina solida* (see below), e.g., with a thin narrow external extension of the hinge plates up to the level of the crural processes, while all of them possess a nearly narrow fold at the transverse band (Fig. 10L). It is convenient to consider only one species with ± development of this extension along the descending lamellae (see *T. solida* Cooper, 1977).

Microstructure. The species has a punctate three-layered shell like the other species of the genus.

Depth range

111–162 m, Karubenthos 2 expedition; 60–641 m reported by Cooper (1977).

Distribution

The species is recorded from the Yucatan Channel, off Venezuela, W of Isla de la Tortuga, off Trinidad as far as French and British Guiana as well as Surinam (Cooper 1977).

Ecology

The short pedicle keeps the shell attached closely to the substrate.

Tichosina plicata Cooper, 1977
Fig. 11

Tichosina plicata Cooper, 1977: 78, pl. 9 figs 1–17.

Tichosina plicata – Rojas *et al*. 2015: 57, fig. 2a–d.

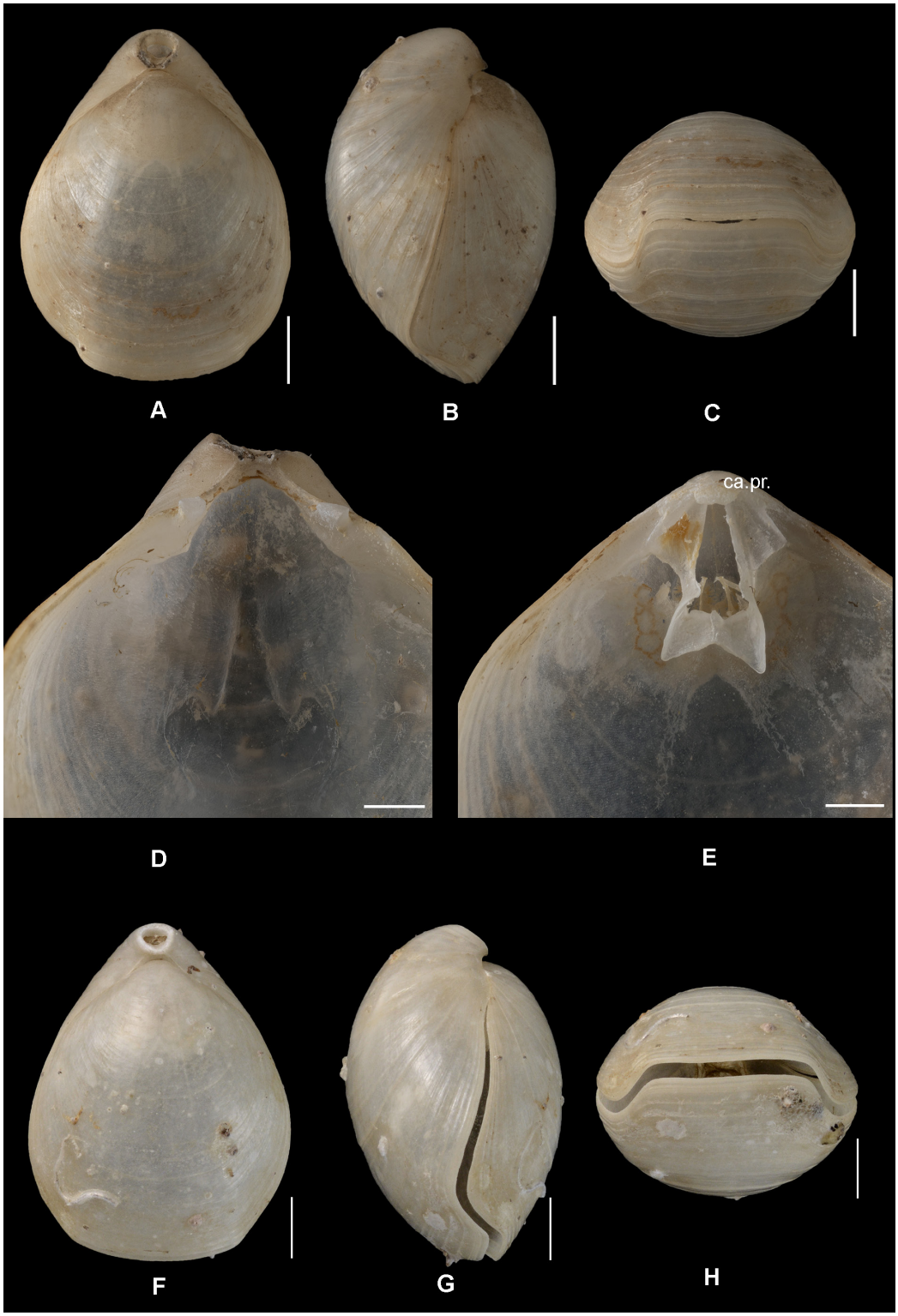

Fig. 11. *Tichosina plicata* Cooper, 1977. **A–C**. Dorsal, lateral and anterior views of an adult specimen, MNHN-IB-2022-991. **D**. Posterior ventral valve interior revealing the deeply impressed cast of muscles (adductor, ventral adjustor and diductor), MNHN-IB-2022-992. **E**. Dorsal valve interior revealing the cardinal process (ca.pr), dental sockets, hinge plates, brachidium, mantle body wall and net of orange gonads, MNHN-IB-2022-992. **F–H**. Dorsal, lateral and anterior views of a slightly open specimen, MNHN-IB-2022-993. Scale bars: A–C, F–H = 5 mm; D–E = 2 mm.

Material examined (including figured material)

GUADELOUPE – **SW of Marie Galante** • 1 shell; stn DW 4636; 15°51′ N, 61°26′ W; depth 262 m; 27 Jun. 2015; Karubenthos 2 exped.; MNHN, MNHN-IB-2022-991 (Fig. 11A–C) • 1 shell; same data as for preceding; MNHN, MNHN-IB-2022-992 (Fig. 11D–E). – **S of Marie Galante** • 1 shell; stn DW 4646; 15°51′ N, 61°18′ W; depth 250–254 m; 29 Jun. 2015; Karubenthos 2 exped.; MNHN, MNHN-IB-2022-993 (Fig. 11F–H).

Type locality

Trinidad.

Description

Morphology. The shell is relatively large but more elongate than that of *T. bullisi*, with a length averaging 27 mm. The maximum width is at the anterior half of the shell length (Fig. 11A), nearly biconvex with maximum convexity posteriorly (Fig. 11B). The symphytium is concave most often hidden by the dorsal convexity. The lateral margins are sinuate (Fig. 11B, G), and the anterior margin is relatively broad and monoplicate (Fig. 11C, H). The ventral umbo is suberect, widely and obliquely truncated by the wide foramen with a tendency to be labiate. Major growth lines mark the surface and faint radial capillae are revealed laterally.

Ventral valve. The valve interior possesses small strong teeth and impressed muscular scars (Fig. 11D).

Dorsal valve. The valve interior presents a short brachial loop, a small transverse cardinal process, dental sockets covered posteriorly and relatively wide anteriorly, large and slightly concave hinge plates limited by the crural base that forms a high inner edge for these plates. The curved crural processes overhang the posterior transverse band, the latter flaring slightly anteriorly, and being moderately folded (Fig. 11E). A remarkable detail of this species is the relatively short crural bases, the crural processes appearing very soon after the anterior of the hinge plates (Fig. 11E).

Microstructure. This species presents a punctate three-layered shell as do the other species of the genus.

Depth range

Karubenthos 2 expedition (206–254 m); 93–115 m (Cooper 1977, 1983).

Distribution

The species is known from E of Trinidad and off Venezuela (Cooper 1977, 1983), see also the comments of Rojas *et al*. (2015) for Colombia.

Ecology

A short pedicle, through the wide worn foramen, attached the shell close to the substrate.

Tichosina solida Cooper, 1977
Fig. 12

Material examined (including figured material)

GUADELOUPE – **E of La Désirade** • 1 shell; stn DW 4578; 16°21′ N, 60°54′ W; depth 119–250 m; 18 Jun. 2015; Karubenthos 2 exped.; MNHN, MNHN-IB-2022-994 (Fig. 12) • 1 shell; stn 4614; 16°23′ N, 60°50′ W, depth 260–270 m; 26 Jun. 2015; Karubenthos 2 exped.; MNHN.

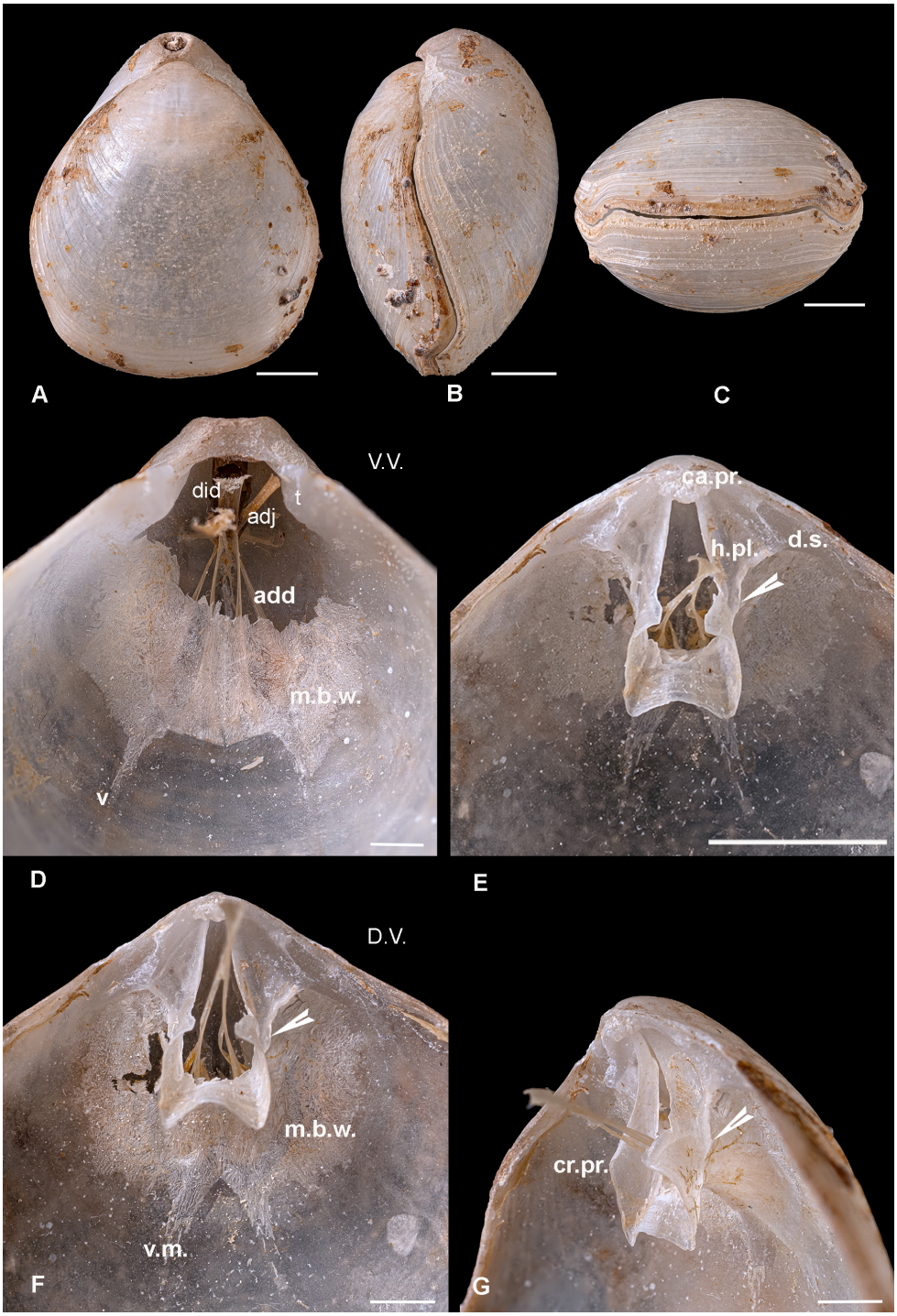

Fig. 12. *Tichosina solida* Cooper, 1977, MNHN-IB-2022-994. **A**–**C**. Dorsal, lateral and anterior views of an adult specimen. **D**. Ventral valve interior (V.V.) of the previous shell showing the teeth (t), withdrawn pedicle, muscles attached to the pedicle and valve floor (adductors = add; adjustor = adj; didductor = did) protected by the spiculate mantle body wall (m.b.w.). **E**. Dorsal valve interior revealing the cardinal process (ca.pr.), dental sockets (d.s.), hinge plates (h.pl.), and the brachidium with lateral extensions (arrowhead). **F**. Same dorsal valve (D.V.) slightly tilted posteriorly to reveal the spiculate mantle body wall (m.b.w.), vascula media (v.m.) and the lateral extensions at the external anterior part of the hinge plates (arrowhead). **G**. Semi-lateral view of the same dorsal valve revealing the length of the lateral extension (arrowhead) and crural process (cr.pr.). Scale bars: A–C, E = 5 mm; D, F–G = 2 mm.

Type locality

Off Floridan coasts.

Description

Morphology. Shell somewhat ventri-biconvex, rather large for the genus, wider at mid-length, elongate posterior part (Fig. 12A). Slightly inclined lateral margins (Fig. 12B) followed by a sudden but small dorsal change of direction, while the anterior margin is broadly and very slightly monoplicate (Fig. 12C). The foramen is large, round to slightly labiate, it cuts obliquely the suberect ventral umbo and is limited dorsally by a concave and inclined symphytium (Fig. 12A, D). Shell with the external surface marked by apparent concentric growth lines (Fig. 12B).

Ventral valve. The valve interior reveals a short pedicle collar, sometimes bordering the remaining pedicle through the foramen with attaching muscles as well as solid teeth and mantle body wall protecting the soft parts, including the muscles (Fig. 12D).

Dorsal valve. This valve possesses a relatively large (protruding) cardinal process, a loop around ¼ of valve length, with concave wide outer hinge plates bordered by elevated crural bases. The dental sockets are posteriorly covered, and the crural processes face each other. The broad transverse band that flares slightly anteriorly reveals a narrow fold bordered by two grooves (Fig. 12E). The peculiarity of this species, compared to the others included in the genus, is the marked extension of a narrow ribbon at the external anterior end of each hinge plate reaching the level beneath the crural processes (Fig. 12E–G). Notice that the position of the imaged valve is of importance, particularly for assessing the shape of the brachidium (regardless of the species concerned, cf. here Fig. 12 E–F). The fragile mantle body wall is best observed when the dorsal valve is tilted posteriorly (Fig. 12F), revealing details of the spicules and the origin of the mantle canals. The body wall and spicules are like those of the other species in the genus.

Microstructure. The shell of this species is three-layered as for all species of the genus.

Depth range

119–268 m Karubenthos 2 expedition; 220–302 m (Cooper 1977).

Distribution

In addition, the species was reported by Cooper (1977) from Sand Key, Florida, and Straits of Florida, SE of Key West and W of Key West.

Genus ***Erymnia*** Cooper, 1977

Type species

Erymnia muralifera Cooper, 1977: 94, pl. 12 figs 3–4, pl. 13 figs 1–22, pl. 14 figs 1–10.

Erymnia muralifera Cooper, 1977
Fig. 13

Material examined (including figured material)

GUADELOUPE – **W of Marie Galante** • 1 shell; stn DW 4634; 15°48′ N, 61°26′ W; depth 304–310 m; 27 Jun. 2015; Karubenthos 2 exped.; MNHN, MNHN-IB-2022-995 (Fig. 13A–C) • 1 shell + 1 juv.; stn DW 4647; 15°51′ N, 61°26′ W; depth 263–264 m; 29 Jun. 2015; Karubenthos 2 exped.; MNHN.

– **S of Marie Galante** • 1 juv.; stn DW 4638; 15°50′ N, 61°19′ W; depth 305–312 m; 28 Jun. 2015; Karubenthos 2 exped.; MNHN, MNHN-IB-2022-996 (Fig. 13D) • 1 juv.; same data as for preceding; MNHN, MNHN-IB-2022-997 (Fig. 13E–F). – **E of La Désirade** • 1 shell; stn DW 4574; 16°22′ N, 60°54′ W; depth 140–340 m; 18 Jun. 2015; Karubenthos 2 exped; MNHN, MNHN-IB-2022-998 (Fig. 13G–I).

Type locality

S of Grand Bahama and NE side of Straits of Florida.

Description

Morphology. Wide ventri-biconvex shell, rather subcircular in outline, ventral umbo suberect and cut obliquely by a rounded or slightly labiate medium foramen (Fig. 13A). The symphytium is partly hidden and the pedicle collar relatively short. The external surface exhibits strong major growth lines. The lateral margins are nearly straight until the very anterior part of the shell (Fig. 13B); in contrast to juveniles, the shell margins of adults are thick with a tendency to be slightly incurved towards the inner side. The anterior margin is rectimarginate to slightly monoplicate (Fig. 13C). The shells were white or greyish when found, the brown colour probably being due to pollution.

Dorsal valve. The valve interior reveals a relatively small cardinal process (Fig. 13D–E, H), short dental sockets narrow and semi-covered posteriorly, but deep and enlarged anteriorly. Short outer hinge plates barely concave attached to the crural bases, themselves attached to the valve floor by means of two vertical plates (Fig. 13D–E, H). The rather close crural processes are short and curved a little bit towards the median plane (Fig. 13D–E, H–I). The brachial loop is short with a large slightly folded transverse band with two short lateral projections (Fig. 13D–E, H–I). The adductor muscle scars are narrow, close to the median plane (Fig. 13D–E). Mantle canals (vascula media and vascula lateralis) are deeply impressed in some specimens, visible beneath the transverse band protected by elongate spicules starting from the anterior part of the body wall itself with large, obviously thick, spicules revealing differences from those of the genus *Tichosina* (Fig. 13H–I).

Ventral valve. The ventral valve reveals a curved partly visible symphytium (Fig. 13A, F–G) and a well-marked pedicle collar in the juveniles, rather abraded in adults (Fig. 13G) indicating a short pedicle, medium strong disengaged hinge teeth (Fig. 13F–G) and a wide multi-muscles cast. The limited soft parts are protected by a body wall consisting here in wide self-locking spicules (Fig. 13F, H–I).

Microstructure. SEM observations reveal a punctate three-layered shell as for species of the genus *Tichosina*.

Depth range

140–340 m, Karubenthos 2 exped.; 205–575 m (Cooper 1977).

Distribution

The species is recorded elsewhere by Cooper (1977), in the Caribbean Sea and adjacent waters: S of Grand Bahama Island, Straits of Florida and N of Virgin Islands.

Ecology

Owing to the heavily abraded margin of the foramen, the shells are closely connected to hard substrates.

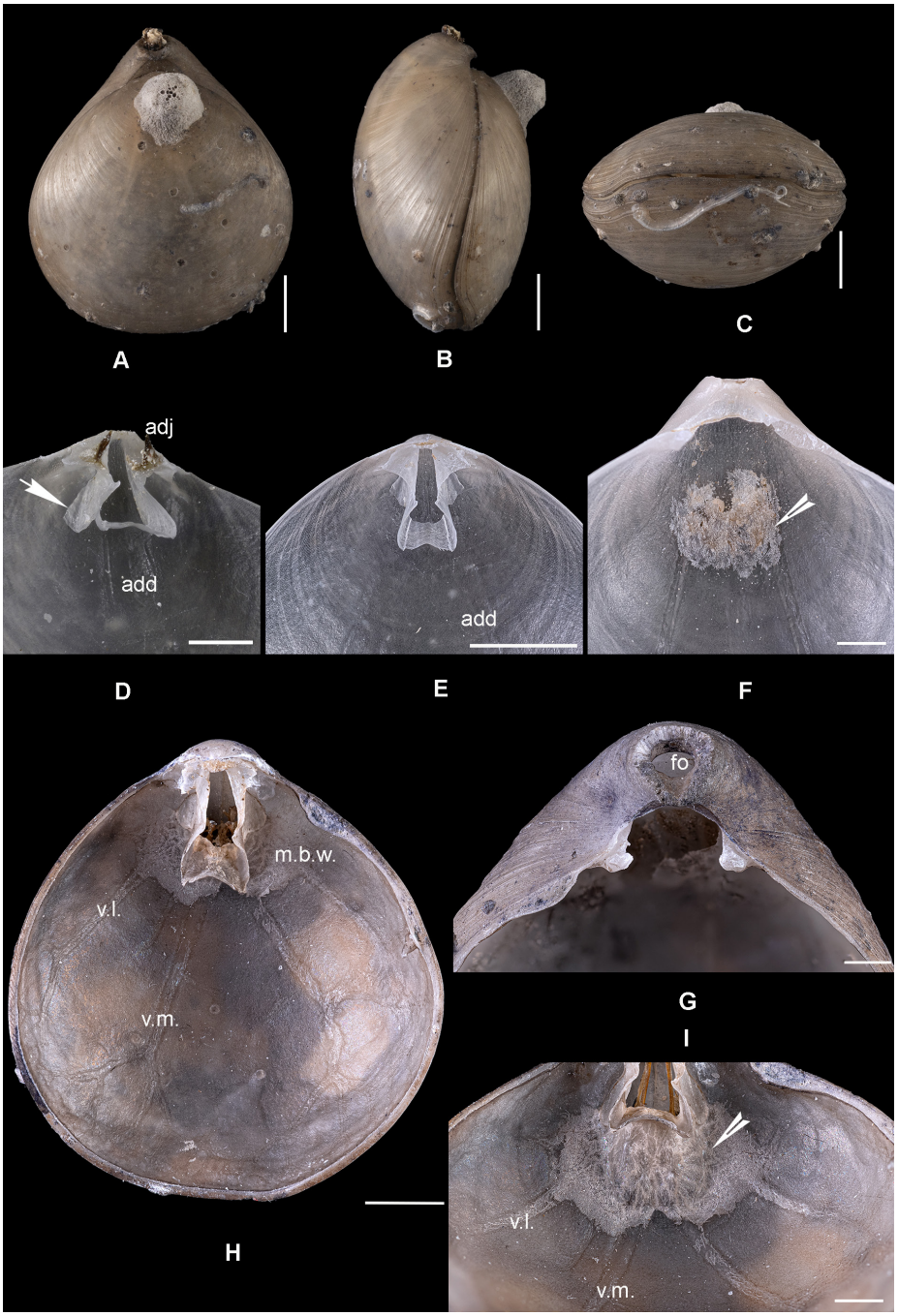

Fig. 13. *Erymnia muralifera* Cooper, 1977. **A–C**. Specimen with epibionts and traces of pollution, MNHN-IB-2022-995. **D**. Dorsal valve tilted semi-laterally revealing the plate (arrow) that links the crural base to the valve floor, adductors (add) and adjustor muscles (adj), MNHN-IB-2022-996. **E**. Dorsal valve interior of a juvenile from the same location, MNHN-IB-2022-997. **F**. Ventral valve interior from the same juvenile specimen, mantle body wall (arrowhead). **G**. Posterior ventral valve interior with traces of pollution, showing small thick teeth and an abraded margin of the foramen (fo), MNHN-IB-2022-998. **H**. Dorsal valve interior of the same shell, with small cardinal process, deep short dental sockets, brachidium, mantle body wall (m.b.w.) and branched vascula media (v.m.) and vascula lateralis (v.l.). **I**. Close-up view of the spiculate mantle body wall (arrowhead) and departure of the vascula media and lateralis, beneath the brachial transverse band, of the previous dorsal valve slightly tilted posteriorly. Scale bars: A–C, H = 5 mm; D–G, I = 2 mm.

Subfamily Dallithyridinae Katz & Popov, 1974

Genus ***Stenosarina*** Cooper, 1977

Type species

Stenosarina angustata Cooper, 1977: 95–97, pl. 31 figs 26–33, pl. 33 figs 7–11.

Stenosarina nitens Cooper, 1977
Fig. 14

Material examined (including figured material)

GUADELOUPE – **N of Grande Terre** • 1 shell; stn DW 4550; 16°37′ N, 61°31′ W; depth 432–482 m; 16 Jun. 2015; Karubenthos 2 exped.; MNHN, MNHN-IB-2022-999 (Fig. 14A–B) • 1 shell; same data as for preceding; MNHN, MNHN-IB-2022-1001 (Fig. 14E–F) • 1 shell; stn DW 4549; 16° 38′ N, 61°35′ W; depth 343–402 m; 14 Jun. 2015; Karubenthos 2 exped; MNHN, MNHN-IB-2022-1000 (Fig. 14C–D) • 1 shell; same data as for preceding; MNHN, MNHN-IB-2022-1002 (Fig. 14G–H). – **? E of La Désirade** • 1 shell; stn DW 4613; 16°25′ N, 60°50′ W; depth 210–240 m; 25 Jun. 2015; Karubenthos 2 exped.; MNHN. – **N of Île des Saintes** • 1 shell; stn DW 4626; 15°57′ N, 61°37′ W; depth 210–233 m; 26 Jun. 2015; Karubenthos 2 exped.; MNHN.

Type locality

NE Island of Dominica.

Description

Morphology. Very few specimens were found. Shell of medium size for the genus, subtriangular-rounded in outline (Fig. 14A, C) and ventri-biconvex. The short suberect ventral beak is truncated by a medium pseudo-labiate foramen, the symphytium is slightly concave, the lateral margins nearly sigmoidal, and the anterior margin rectimarginate. The maximum width is situated at the ¼ anterior shell length. The few shells observed are white, nearly translucent and empty. Faint capillae are best revealed laterally at the external surface (Fig. 14B, D). The convexity of the dorsal valve is more important in its posterior part venturing to hide the symphytium.

Ventral valve. The inner valve shows small teeth and main muscle imprints (Fig. 14E).

Dorsal valve. The valve interior reveals a small cardinal process, a narrow loop of approximately ¼ dorsal valve length. The outer hinge plates are narrow and long, tapering, the parallel crural bases are elevated along the inner margins of outer hinge plates, the crural processes are blunt and the brachial transverse band heavily folded medially owing to its tightness (Fig. 14F). Delicate spicules are observed laterally and beneath the brachidium (Fig. 14G).

Microstructure. The shell of this species is very thin, composed of two layers under the periostracum (primary and fibrous secondary layers). Minute punctae are observed. The inner margins of the valves reveal brown setae from invaginated follicles along mantle grooves, generally protruding beyond the shell margin (Fig. 14D, H).

Depth range

210–482 m, Karubenthos 2 exped.; 549–608 m (Cooper 1977).

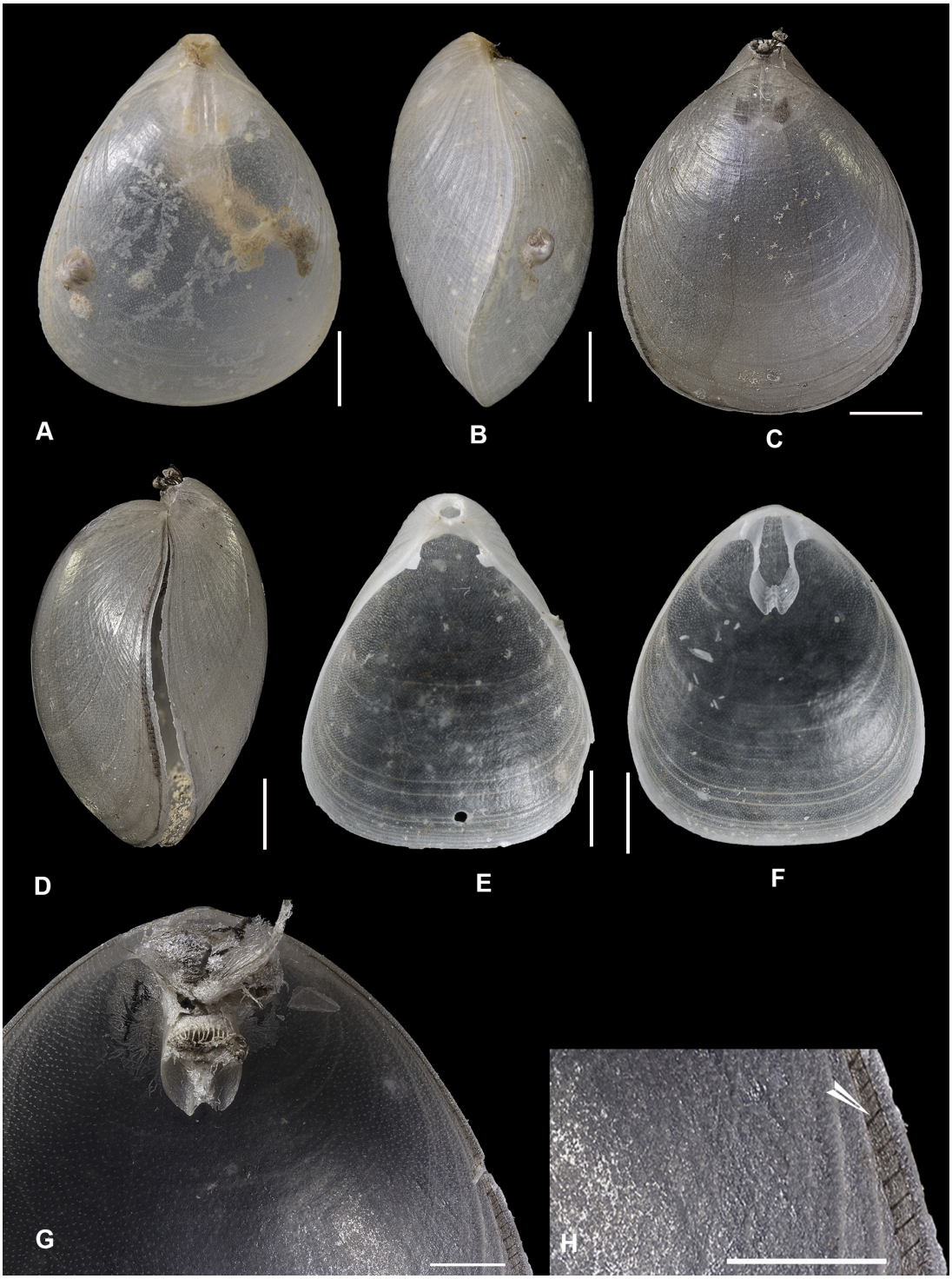

Fig. 14. *Stenosarina nitens* Cooper, 1977. **A**–**B**. Dorsal and lateral views of an adult specimen, MNHN-IB-2022-999. **C**–**D**. Dorsal and lateral views of another specimen with muscles and setae revealed by transparency, MNHN-IB-2022-1000. **E**. Ventral valve interior with the teeth, MNHN-IB-2022-1001. **F**. Dorsal valve interior of the same shell, with the brachidium, MNHN-IB-2022-1001. **G**. Dorsal valve interior with the brachidium, fragment of lophophore between the crural processes, and some spicules hiding the hinge plates, MNHN-IB-2022-1002. **H**. Close-up view of the same shell at the inner lateral margin to highlight the presence of setae (white arrowhead). Scale bars: A–F = 2 mm; G = 1 mm; H = 1 mm.

Distribution

The species is known from the NE side of Dominica Island, N of the east end of the Dominican Republic (Cooper 1977), and banks of the Ibero-Morrocan Gulf (Gaspard 2003).

Ecology

Even though the shells are of medium size, epibionts (small crustaceans) are observed attached to the valves.

Superfamily Cancellothyridoidea Thomson, 1926
Family Cancellothyrididae Thomson, 1926
Subfamily Cancellothyridinae Thomson, 1926

Genus ***Terbratulina*** d'Orbigny, 1847

Type species

Terebratulina retusa (Linnaeus, 1758).

Terebratulina cailleti Crosse, 1865
Figs 15–16, 17A–B

Terebratulina cailleti Crosse, 1865: 27, pl. 1 figs 1–3

Terebratulina cailleti – Dall 1871: 10. — Davidson 1886: 26, pl. 5 figs 41–42. — Cooper 1977: 99–100, pl. 25 figs 1–16, pl. 28 figs 4–27. — Logan 1987: 49, pl. 12 figs 14–22. — Rojas *et al*. 2015: 58, fig. 2j–k.

Material examined (including figured material)

GUADELOUPE – **W of Basse Terre** • 2 shells; stn DW 4510; 16°15′ N, 61°51′ W; depth 660–690 m; 7 Jun. 2015; Karubenthos 2 exped.; MNHN • 4 juvs; stn CP 4513; 16°13′ N, 61°54′ W; depth 406–644 m; 8 Jun. 2015; Karubenthos 2 exped.; MNHN • 3 shells; stn DW 4514; 16°12′ N, 61°51′ W; depth 792–800 m; 8 Jun. 2015; Karubenthos 2 exped.; MNHN • 1 shell; stn DW 4518; 16°34′ N, 61°37′ W; depth 426–441 m; 9 Jun. 2015; Karubenthos 2 exped.; MNHN. – **W of Marie Galante** • 3 shells + juvs; stn DW 4586; 16°00′ N, 61°23′ W; depth 204–251 m; 21 Jun. 2015; Karubenthos 2 exped.; MNHN • 1 juv.; same data as for preceding; MNHN, MNHN-IB-2022-1004 (Fig. 15B) • 7 shells + 3 juvs; stn DW 4518; 15°59′ N, 61°27′ W; depth 150–221 m; 21 Jun. 2015; Karubenthos 2 exped.; MNHN • 40 shells; stn DW 4590; 15°57′ N, 61°27′ W; depth 83–135 m; 21 Jun. 2015; Karubenthos 2 exped.; MNHN • 2 shells; stn DW 4594; 15°58′ N, 61°23′ W; depth 200–206 m; 22 Jun. 2015; Karubenthos 2 exped; MNHN • 1 juv.; same data as for preceding; MNHN, MNHN-IB-2022-1006 (Fig. 15D) • 4 shells; stn DW 4597; 15°26′ N, 61°23′ W; 208–210 m; 22 Jun. 2015; Karubenthos 2 exped.; MNHN • 32 shells; stn DW 4599; 15°53′ N, 61°25′ N; depth 262–266 m; 22 Jun. 2015; Karubenthos 2 exped.; MNHN • 2 preadult shells; same data as for preceding; MNHN, MNHN-IB-2022-1009, MNHN-IB-2022-1010 (Fig. 16A–B) • 6 shells; stn DW 4622; 15°55′ N, 61°30′ W; depth 182–203 m; 26 Jun. 2015; Karubenthos 2 exped.; MNHN • 5 shells; stn DW 4630; 15°48′ N, 61°28′ W; depth 379–428 m; 27 Jun. 2015; Karubenthos 2 exped.; MNHN • 4 shells + 2 juvs; stn DW 4632; 15°49′ N, 61°28′ W; depth 376–393 m; 27 Jun. 2015; Karubenthos 2 exped.; MNHN • 5 shells; stn DW4633; 15°48′ N, 61°28′ W; depth 378–432 m; 27 Jun. 2015; Karubenthos 2 exped.; MNHN • 3 shells + 4 juvs; stn DW 4634; 15°48′ N, 61°26′ W; depth 304–310 m; 27 Jun. 2015; Karubenthos 2 exped.; MNHN • 1 shell + 9 juvs; stn DW 4635; 15°50′ N, 61°26′ W; depth 265–268 m; 27 Jun. 2015; Karubenthos 2 exped; MNHN • 3 shells; stn DW

4647; 15°51′ N, 61°26′ W; depth 263–264 m; 29 Jun. 2015; Karubenthos 2 exped.; MNHN • 1 valve; stn DW 4649; 16°30′ N, 61°27′ W; depth 367–389 m; 29 Jun. 2015; Karubenthos 2 exped.; MNHN. – **N of Marie Galante** • 1 shell + 4 juvs; stn DW 4600; 16°02′ N, 61°18′ W; depth 557–680 m; 23 Jun. 2015; Karubenthos 2 exped; MNHN • 1 shell; stn DW 4602; 16°02′ N, 61°17′ W; depth 507–670 m; 23 Jun. 2015; Karubenthos 2 exped.; MNHN. – **S of Marie Galante** • 1 juv.; stn DW4638; 15°50′ N, 61°19′ W; depth 305–312 m; 28 Jun. 2015; Karubenthos 2 exped.; MNHN • 4 shells + 1 juv.; stn DW 4639; 15°48′ N, 61°20′ W; depth 485–496 m; 28 Jun. 2015; Karubenthos 2 exped.; MNHN • 22 shells; stn DW 4642; 15°47′ N, 61°12′ W; depth 550–562 m; 28 Jun. 2015; Karubenthos 2 exped.; MNHN • 1 juv. shell; stn DW 4639; 15°48′ N, 61°20′ W; depth 485-496 m; 28 Jun. 2015; Karubenthos 2 exped.; MNHN, MNHN-IB-2022-1075 (Fig. 15G-I; Fig. 17a-B) • 6 shells; stn DW 4644; 15°49′ N, 61°06′ W; depth 835–898 m; 28 Jun. 2015; Karubenthos 2 exped.; MNHN • 4 shells; stn DW 4646; 15°51′ N, 61°18′ W; depth 250–254 m; 29 Jun. 2015; Karubenthos 2 exped.; MNHN. – **E of La Désirade** • 29 shells; stn DW 4553; 16°21′ N, 60°54′ W; depth 111–162 m; 15 Jun. 2015; Karubenthos 2 exped.; MNHN • 1 shell; same data as for preceding; MNHN, MNHN-IB-2022-1005 (Fig. 15C) • 2 shells + 3 juvs; stn DW 4554; 16°21′ N, 60°56′ W; depth 300–370 m; 15 Jun. 2015; Karubenthos 2 exped.; MNHN • 1 shell; same data as for preceding; MNHN, MNHN-IB-2022-1003 (Fig. 15A) • 1 shell; same data as for preceding; MNHN, MNHN-IB-2022-10012 (Fig. 16E–F) • 16 shells + 8 juvs; stn DW 4555; 16°24′ N, 60°51′ W; depth 100–258 m; 15 Jun. 2015; Karubenthos 2 exped.; MNHN • 9 shells; stn DW 4556; 16°24′ N, 60°49′ W; depth 367–428 m; 15 Jun. 2015; Karubenthos 2 exped.; MNHN • 4 shells; stn DW 4558; 16°22′ N, 60°50′ W; depth 312–385 m; 15 Jun. 2015; Karubenthos 2 exped.; MNHN • 2 shells; stn DW 4560; 16°25′ N, 60°52′ W; depth 185–250 m; 16 Jun. 2015; Karubenthos 2 exped.; MNHN • 1 shell; stn DW 4561; 16°25′ N, 60°50′ W; depth 278–446 m; 16 Jun. 2015; Karubenthos 2 exped.; MNHN • 1 juv.; stn DW 4566; 16°21′ N, 60°51′ W; depth 165–260 m; 16 Jun. 2015; Karubenthos 2 exped.; MNHN • 6 shells; 1 stn, DW 4572; 6°19′ N, 60°55′ W; depth 396–399 m; 17 Jun. 2015; Karubenthos 2 exped.; MNHN • 17 shells + 5 valves; stn DW 4573; 16°20′ N, 60°55′ W; depth 389–413 m; 17 Jun. 2015; Karubenthos 2 exped.; MNHN • 1 valve; same data as for preceding; MNHN, MNHN-IB-2022-1008 (Fig. 15F) • 1 valve; same data as for preceding; MNHN, MNHN-IB-2022-1011 (Fig. 16C) • 2 shells; stn DW 4575; 16°21′ N, 60°53′ W; depth 79–165 m; 18 Jun. 2015; Karubenthos 2 exped.; MNHN • 11 shells; stn DW 4577; 16°20′ N, 60°54′ W; depth 358–402 m; 18 Jun. 2015; Karubenthos 2 exped.; MNHN • 2 shells; stn DW 4579; 16°21′ N, 60°54′ W; depth 228–264 m; 18 Jun. 2015; Karubenthos 2 exped.; MNHN • 3 shells; stn DW 4581; 16°19′ N, 60°52′ W; depth 221–450 m; 18 Jun. 2015; Karubenthos 2 exped.; MNHN • 2 shells; stn DW 4607; 16°15′ N, 60°50′ W; depth 600–608 m; 24 Jun. 2015; Karubenthos 2 exped.; MNHN • 2 shells; stn DW 4609; 16°15′ N, 60°49′ W; depth 535–673 m; 24 Jun. 2015, Karubenthos 2 exped.; MNHN • 1 shell + 4 valves; stn DW 4611; 16°20′ N, 60°52′ W; depth 242–263 m; 24 Jun. 2015; Karubenthos 2 exped.; MNHN • 17 shells; stn DW 4613; 16°25′ N, 60°50′ W; depth 210–240 m; 25 Jun. 2015; Karubenthos 2 exped.; MNHN • 1 shell; stn DW 4615; 16°23′ N, 60°50′ W; depth 226–270 m; 25 Jun. 2015; Karubenthos 2 exped.; MNHN • 3 shells; stn DW 4618; 16°21′ N, 60°45′ W; depth 780–828 m; 25 Jun. 2015; Karubenthos 2 exped.; MNHN. – **N of Île Les Saintes**: 4 juvs; stn DW 4626; 15°67′ N, 61°37′ W; depth 210–233 m; 26 Jun. 2015; Karubenthos 2 exped.; MNHN • 1 shell; stn DW 4627; 15°56′ N, 61°38′ W; depth; 277–304 m; 26 Jun. 2015; Karubenthos 2 exped.; MNHN. – **N of Grande Terre** • 2 shells; stn DW 4518; 16°34′ N, 61°37′ W; depth 426–441 m; 9 Jun. 2015; Karubenthos 2 exped.; MNHN • 1 juv.; stn DW 4527; 16°24′ N, 61°34′ W; depth 180 m; 10 Jun. 2015; Karubenthos 2 exped.; MNHN • 3 shells; stn DW 4537; 16°38′ N, 61°31′ W; depth 495–570 m; 12 Jun. 2015; Karubenthos 2 exped.; MNHN • 6 shells; stn DW 4540; 16°42′ N, 61°36′ W; depth 618–627 m; 13 Jun. 2015; Karubenthos 2 exped.; MNHN • 1 shell; stn DW 4541; 16°42′ N, 61°37′ W; depth 615–630 m; 13 Jun. 2015; Karubenthos 2 exped.; MNHN • 1 shell; stn DW 4642; 16°42′ N, 61°34′ W; depth 394–400 m; 13 Jun. 2015; Karubenthos 2 exped.; MNHN • 2 shells + 5 juvs; stn DW 4544; 16° 38′ N, 61°37′ W; depth 413–423 m; 13 Jun. 2015; Karubenthos 2 exped; MNHN • 1 shell; stn DW 4545; 16°29′7″ N, 61°31′4″ W; depth 60–82 m; 14 Jun. 2015; Karubenthos 2 exped.; MNHN • 10 shells + 5 juvs; stn DW 4549; 16°38′ N, 61°35′ W; depth 343–402 m; 14 Jun. 2015; Karubenthos 2 exped.; MNHN • 1 shell; same data as for preceding; MNHN, MNHN-IB-2022-1007 (Figs 15E, 16D) • 2 juvs; stn DW 4550; 16°37′ N, 61°31′ W; depth 432–482 m;

14 Jun. 2015; Karubenthos 2 exped.; MNHN. – **E of Petite Terre (Grand Cul de sac marin, facing Fajou)** • 1 shell; stn GN 13; 16°23′ N, 61°37′ W; depth 138 m; 6 May 2012; Karubenthos 1 exped.; MNHN • 3 shells; 16°12′1″ N, 61°03′9″ W; depth 95 m; 26 May 2012; Karubenthos 1 exped.; MNHN.

Type locality

Lee side of Guadeloupe.

Description

Morphology. Common small shell (~ 10 mm and sometimes slightly more) described for the first time from Guadeloupe, elongate, rather narrow oval in juveniles, slightly widened at the anterior part in adults (Fig. 15A). The posterior dorsal valve is auriculate (Fig. 15A–B). A white to orange colour is often observed (Fig. 15C). The shell is multicostellate with some finer intercalations from the anterior margin (Fig. 15A–B, D). These costellae are strongly beaded in juveniles and less in older individuals, i.e., such that adults possess this aspect only at their posterior part. The ventral umbo is erect to suberect, cut by a large open foramen bordered by rudimentary disjunct deltidial plates. The anterior margin is rectimarginate to very slightly folded at the anterior dorsal valve. The shell is attached by means of the pedicle rootlets to (or through) foraminifers as well as to wider and immobile substrates (Fig. 15A, C), including corals and congeners.

Ventral valve. The valve interior shows a relatively large pedicle collar and strong hinge teeth (Fig. 15E–F). Interlocking spicules are revealed in the mantle, strengthening the body wall, and thinner ones protecting the mantle canals (Figs 15E, 16E–F).

Dorsal valve. The valve interior reveals a semi-circular cardinal process, large, wide open dental sockets with a high internal ridge fused to the crural bases, and absence of hinge plates. Crura converging, crural processes facing each other in young specimens (Fig. 15G–H) then fusing to form a ring with the transverse band shaping a median fold (Fig. 16A–B). The latter often presents a projection oriented anteriorly (Fig. 15G). This ring (Fig. 16C) supports the lophophore (Fig. 16D) with spicules at the basal part of their arms (Fig. 16G). When the brachidium is broken or the lophophore removed, it is easy to see the wide mantle canals. The inner margin of the two valves presents interlocking eminences marked by a follicule in the middle highlighted by a line of punctae, intercalated with follicular embayments where the setae appear (Figs 15E, 16D–E, H). The later appear at the shell margins. Each seta arises from an invaginated follicle along mantle grooves (Figs 15E, 16E).

Microstructure. Two-layered shell (primary and secondary layers). The fibrous mosaic of the secondary layer presents modifications in shape and size according to their position at the different internal parts: pedicle collar (Fig. 17A–B), cardinal process, dental sockets, crural processes (Fig. 15G–I) and valve floor: from the margin to the valve centre (Fig. 16H). The punctae are not equally distributed in the shell, their position is mostly related to the location of the costellae. Their diameter decreases rapidly from the margins.

Depth range

60–828 m, Karubenthos 2 exped.; 18–1089 m (Cooper 1977); 32–1163 m (Logan 2007) (see also Logan 1977, 1990; Asgaard & Stentoft 1984; Zezina 2000).

Distribution

The species is common in the Caribbean Sea and the Gulf of Mexico: Straits of Florida, Grand Bahama, Yucatan Channel, Cuba, Jamaica, Dominican Republic, Nevis, Guadeloupe, Dominica Island, St Lucia, Barbados, St Vincent, Grenada, Trinidad, Isla de la Tortuga, as far as the northeastern coasts of South America (Venezuela, French Guiana) (Cooper 1977); Columbia (Rojas *et al*. 2015).

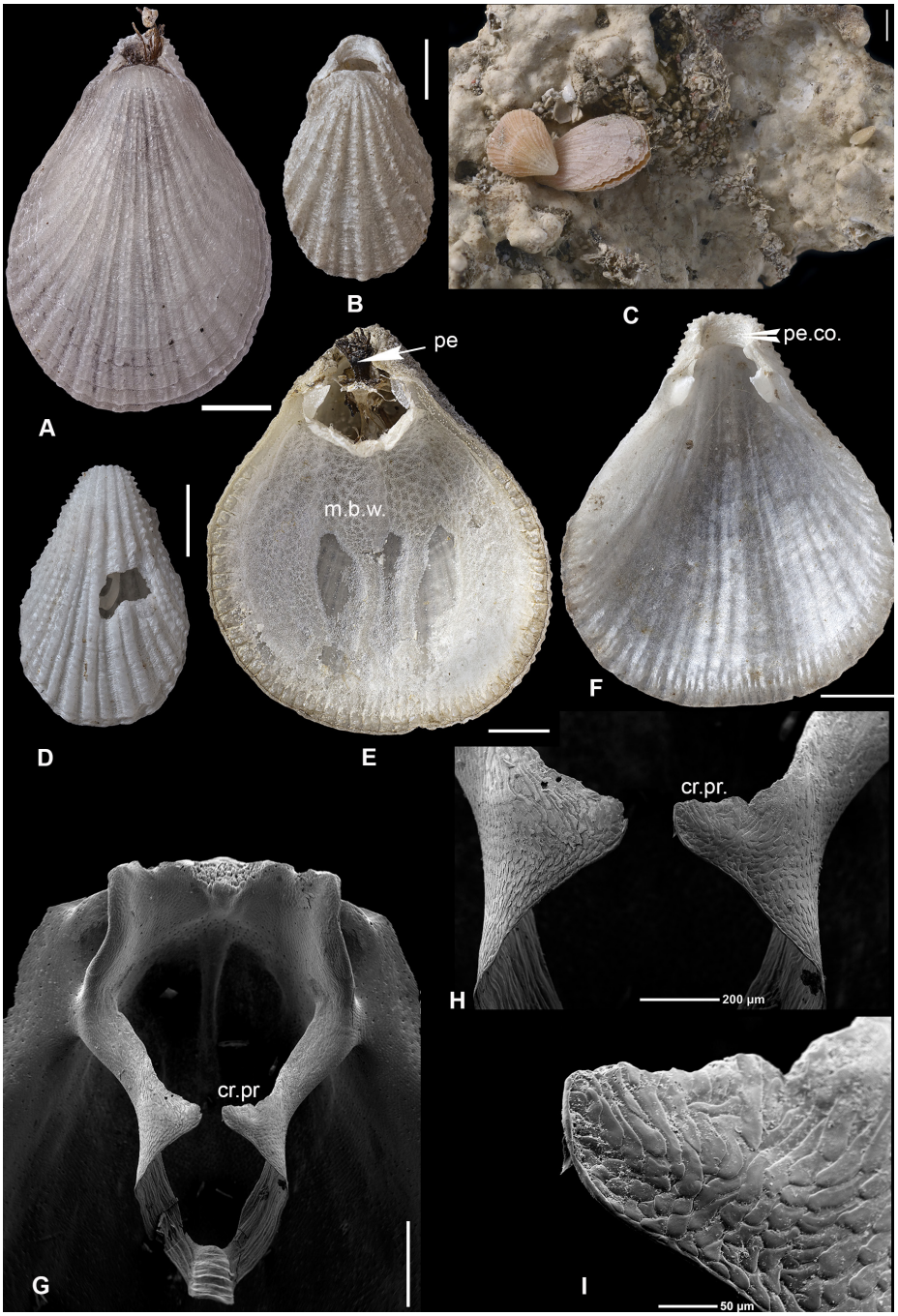

Fig. 15. *Terebratulina cailleti* Crosse, 1865. **A**. Adult specimen, MNHN-IB-2022-1003. **B**. Juvenile specimen, MNHN-IB-2022-1004. **C**. Pink specimen attached to a congener, itself attached to a calcareous substrate and, a few centimetres away, a very young one, MNHN-IB-2022-1005. **D**. Juvenile specimen bored by a predator, MNHN-IB-2022-1006. **E**. Adult ventral valve interior with its frayed pedicle (pe), large teeth, widely extended mantle strengthen by interlocking spicules protecting the soft parts (m.b.w.) and the mantle canals, and setae at the inner margins, MNHN-IB-2022-1007. **F**. Ventral valve interior without the mantle body wall and the pedicle, exposing the pedicle collar (pe.co.) and the teeth, MNHN-IB-2022-1008. **G–I**. SEM views of a juvenile shell, MNHN-IB-2022-1075. **G**. Dorsal valve interior revealing the cardinal process, deep concave dental sockets, high inner socket ridges and an incomplete brachial loop. **H**. Detail of the crural processes (cr.pr.) not yet fused. **I**. Close-up view of distal part of a crural process with its fibrous mosaic. Scale bars: A, C–F = 2 mm; B = 1 mm; G = 500 µm; H = 200 µm; I = 50 µm.

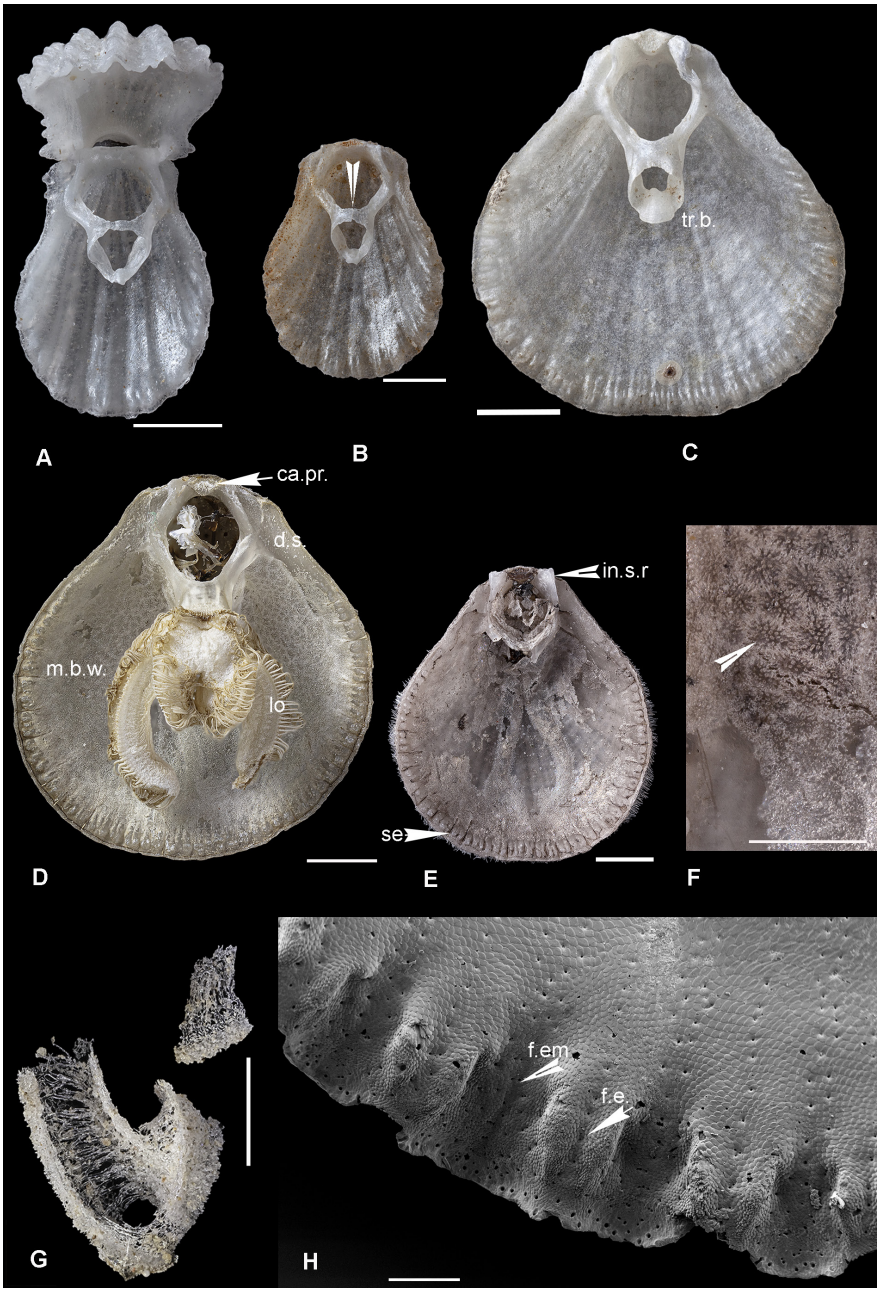

Fig. 16. *Terebratulina cailleti* Crosse, 1865. **A–B**. Subadult specimens with their just developed brachial ring, a junction mark (arrowhead) of the two crural processes still being visible, MNHN-IB-2022-1009 and MNHN-IB-2022-1010, respectively. **C**. Adult dorsal valve interior with its complete ring and a transverse band (tr.b.) projected anteriorly, MNHN-IN-2022-1011. **D**. Dorsal valve interior from the shell, the ventral valve of which is illustrated in Fig. 15E, with the lophophore (lo) supported by the brachidium, the spiculate mantle body wall (m.b.w.) and some setae at the inner margin, and cardinal process (ca.pr.), MNHN-IB-2022-1007. **E**. Dorsal valve interior without the brachidium and the lophophore. The inner socket ridge (in.s.r.) and mantle canals are clearly visible as are the brown setae (se) at the inner margin, MNHN-IB-2022-1012. **F**. Close-up view of the interlocking spicules (white arrowhead) of the previous shell. **G**. Spicules at the basal arms of the lophophore, MNHN-IB-2022-1007. **H**. Close-up view near the inner shell margins revealing the details of crenulations: follicular eminence (f.e.), follicular embayment (f.em.), MNHN-IB-2022-1075. Scale bars: A–B, F–G = 1 mm; C–E = 2 mm; H = 200 µm.

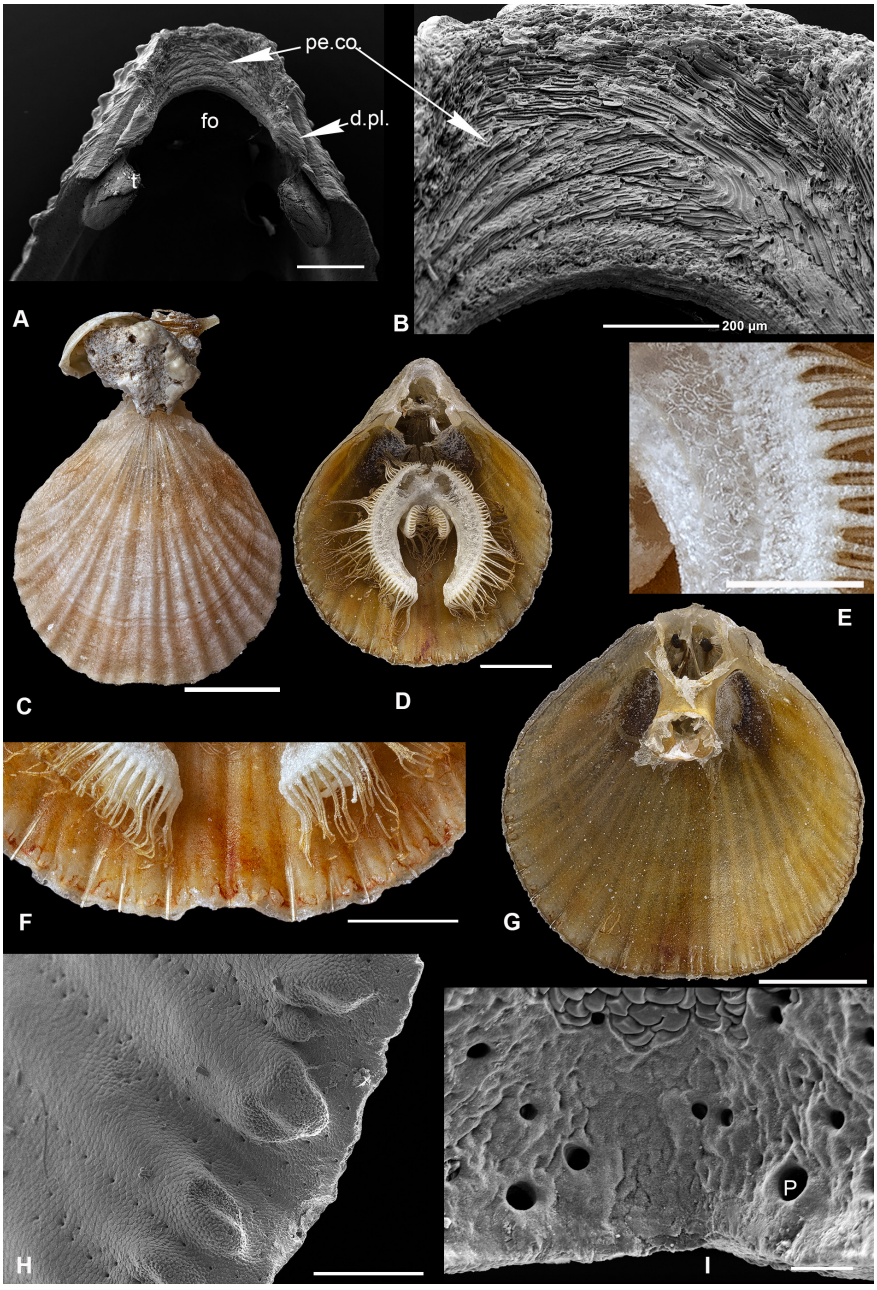

Fig. 17. A–**B**. *Terebratulina cailleti* Crosse, 1865. **A**. SEM view of the posterior ventral valve of a juvenile specimen with its pedicle collar (pe.co.), limited deltidial plates (d.pl.) on each side of the foramen (fo), and strong teeth (t), MNHN-IB-2022-1075. **B**. Close-up view of the fibrous pedicle collar of the preceding valve. — **C**–**I**. *Terebratulina latifrons* Dall, 1920. **C**. Adult fascicostellate shell, MNHN-IB-2022-1013. **D**. Ventral valve interior coloured orange (pollution), with a pedicle collar, brown gonads beneath the mantle body wall, setae and lophophore detached from the dorsal valve, MNHN-IB-2022-1014. **E**. Close-up view of the spicules at the basal lophophore arms, MNHN-IB-2022-1014. **F**. Close-up view on the anterior part of the lophophore and the setae at the inner anterior margin, MNHN-IB-2022-1083. **G**. Dorsal valve interior with the brachidium differing from *Terebratulina cailleti*, with a wide transverse band (same shell as D), MNHN-IB-2022-1014. **H**. SEM view of crenulations near the inner margins to be compared with that of *T. cailleti*, MNHN-IB-2022-1076. **I**. Close-up view of the inner margin, revealing juvenile fibres in course of secretion and different sizes of punctae (P), MNHN-IB-2022-1076. Scale bars: A= 500 µm; B, H = 200 µm; C–D, F–G = 2 mm; E = 1 mm; I = 20 µm.

Ecology

The medium length of the pedicle with its rootlets allows a stable attachment to different kinds of substrate.

Terebratulina latifrons Dall, 1920
Fig. 17C–I

Terebratulina cailleti var. *latifrons* Dall, 1920: 309.

Terebratulina latifrons – Cooper 1977: 100, pl. 17 fig. 1–13.

Material examined (including figured material)

GUADELOUPE – **W of Basse Terre** • 1 juv.; stn CP 4516; 16°13′ N, 61°51′ W; depth 749–768 m; 8 Jun. 2015; Karubenthos 2 exped.; MNHN. – **E of La Désirade** • 25 shells; stn DW 4553; 16°21′ N, 60°54′ W; depth 111–162 m; 15 Jun. 2015; Karubenthos 2 exped; MNHN • 2 shells; stn DW 4555; 16°24′ N, 60°51′ W; depth 100–258 m; 15 Jun. 2015; Karubenthos 2 exped.; MNHN, MNHN-IB-2022-1013 (Fig. 17C), MNHN-IB-2022-1083 (Fig. 17F) • 1 shell; stn DW 4574; 16°22′ N, 60°54′ W; depth 140–340 m; 18 Jun. 2015; Karubenthos 2 exped.; MNHN, MNHN-IB-2022-1014, MNHM-IB-2022-1015 (Fig. 17D–G). – **W of Marie Galante** • 3 juvs; stn DW 4589; 15°59′ N, 61°27′ W; depth 150–221 m; 21 Jun. 2015; Karubenthos 2 exped.; MNHN • 1 shell; stn DW 4590; 15°57′ N, 61°27′ W; depth 83–135 m; 21 Jun 2015; Karubenthos 2 exped.; MNHN, MNHN-IB-2022-1076 (Fig. 17H–I) • 1 shell; stn DW 4596; 15°57′ N, 61°22′ W; depth 164–185 m; 22 Jun. 2015; Karubenthos 2 exped.; MNHN. – **N of Les Saintes** • 1 shell; stn DW 4628; 15°24′ N, 61°39′ W; depth 260–320 m; 26 Jun. 2015; Karubenthos 2 exped.; MNHN. – **S of Marie Galante** • 1 shell; stn DW 4639; 15°48′ N, 61°20′ W; depth 485–496 m; 28 Jun. 2015; Karubenthos 2 exped.; MNHN.

Type locality

Off Barbados.

Description

Morphology. The shell is generally longer than that of *T. cailleti*, with a wider anterior margin. The characteristics of the foramen area are those of *Terebratulina*. The ornamentation differs from that of *T. cailleti* and is rather fascicostellate in trio (i.e., a primary cotellae and two accessory ones from the anterior shell part (Fig. 17C). The anterior margin shows a faint fold. A straight and minor bulge exists at the posterior dorsal valve bordered by ears. The inner shell is often orange/salmon coloured (Fig. 17D–G). Spicules are observed at the basal part of the lophophore arms (Fig. 17E). Slight differences appear in the shape of the interlocking excrescences at the inner margins compared to those of *T. cailleti* (Figs 16H, 17G–H), and in the thickness of setae (Fig. 17F). Lines of punctae are observed at the inner shell side (Fig. 17H). These punctae reveal an irregular diameter between the excrescences near the inner shell margin (Fig. 17I). The cardinal process is semi-oval, and the muscle fields not strongly impressed. The ring of the brachidium is wider than in the previous species and the transverse band presents a wide and less pronounced fold (Fig. 17G).

Depth range

72–768 m, Karubenthos 2 exped.; 37–292 m (Cooper 1977).

Distribution

The species was recorded from the Caribbean Sea (cf. Cooper 1977): northeast Mexico, Straits of Florida, Key West, E of St. Vincent, southwest side of Great Inagua, British Guiana.

Ecology

The orange colour seen at the inner valves is not considered to have the same origin as the colour observed on/in inner parts of shells of *Terebratulina cailleti* and *Argyrotheca* (see below); it could be due to the decomposition of *Sargassum* Agardh, 1820 (see Boisnoir 2025).

Family Clidonophoridae Muir-Wood, 1959
Subfamily Eucalathinae Muir-Wood, 1965

Genus ***Eucalathis*** Fischer & Oehlert, 1890

Type species

Eucalathis murrayi Dall (not Davidson), 1920: 323.

Eucalathis cubensis Cooper, 1977
Fig. 18A–C

Material examined (including figured material)

GUADELOUPE – **W of Basse-Terre** • 4 shells; stn DW 4511; 16°14′ N, 61°52′ W; depth 630–660 m; 8 Jun. 2015; Karubenthos 2 exped.; MNHN • 1 shell; same data as for preceding; MNHN, MNHN-IB-2022-1016 (Fig. 18A) • 1 valve; stn DW 4507; 16°13′ N, 61°52′ W; depth 700–750 m; 7 Jun. 2015; Karubenthos 2 exped.; MNHN, MNHN-IB-2022-1017 (Fig. 18B–C) • 1 shell; stn CP 4512; 16°13′ N, 61°54′ W; depth 409–532 m; 8 Jun. 2015; Karubenthos 2 exped; MNHN • 1 shell; stn CP 4513; 16°13′ N, 61°54′ W; depth 406–644 m; 8 Jun. 2015; Karubenthos 2 exped.; MNHN. – **N of Grande Terre** • 1 valve; stn DW 4518; 16°34′ N, 61°37′ W; depth 426–441 m; 9 Jun. 2015; Karubenthos 2 exped.; MNHN. – **E of La Désirade** • 1 valve; stn DW 4555; 16°24′ N, 60°51′ W; depth 100–258 m; 15 Jun. 2015; Karubenthos 2 exped.; MNHN • 1 shell; stn 4556; 16°24′ N, 60°49′ W; depth 367–428 m; 15 Jun. 2015; Karubenthos 2 exped.; MNHN • 2 shells; stn DW 4572; 16°19′ N, 60°55′ W; depth 396–399 m; 17 Jun. 2015; Karubenthos 2 exped.; MNHN. – **N of Marie Galante** • 1 shell; stn DW 4600; 16°02′ N, 61°18′ W; depth 557–680 m; 23 Jun. 2015; Karubenthos 2 exped.; MNHN. – **W of Marie-Galante** • 1 shell; stn DW 4630; 15°48′ N, 61°28′ W; depth 379–428 m; 27 Jun. 2015; Karubenthos 2 exped.; MNHN • 1 shell; stn DW 4632; 15°49′ N, 61°28′ W; depth 376–393 m; 27 Jun. 2015; Karubenthos 2 exped.; MNHN • 1 shell; stn DW 4634; 15°48′ N, 61°26′ W; depth 304–310; 27 Jun. 2015; Karubenthos 2 exped.; MNHN. – **S of Marie-Galante** • 2 shells; sta. DW 4642; 15°47′ N, 61°12′ W; depth 550–562 m; 28 Jun. 2015: Karubenthos 2 exped; MNHN.

Type locality

Off Havana, Cuba.

Description

Morphology. White small shell, sometimes triangular in outline, with a rounded anterior margin. The surface is ornamented by round beaded costellae, between which median ones are more pronounced; two generations of intercalations are observed. The anterior margin is rectimarginate and the maximum width is at the ½–⅓ anterior shell length.

Ventral valve. The ventral valve presents a large foramen, revealing an important pedicle collar, no obvious deltidial plates or rudimentary ones, and prominent and strong teeth (Fig. 18A–B). The ventral umbo is slightly curved.

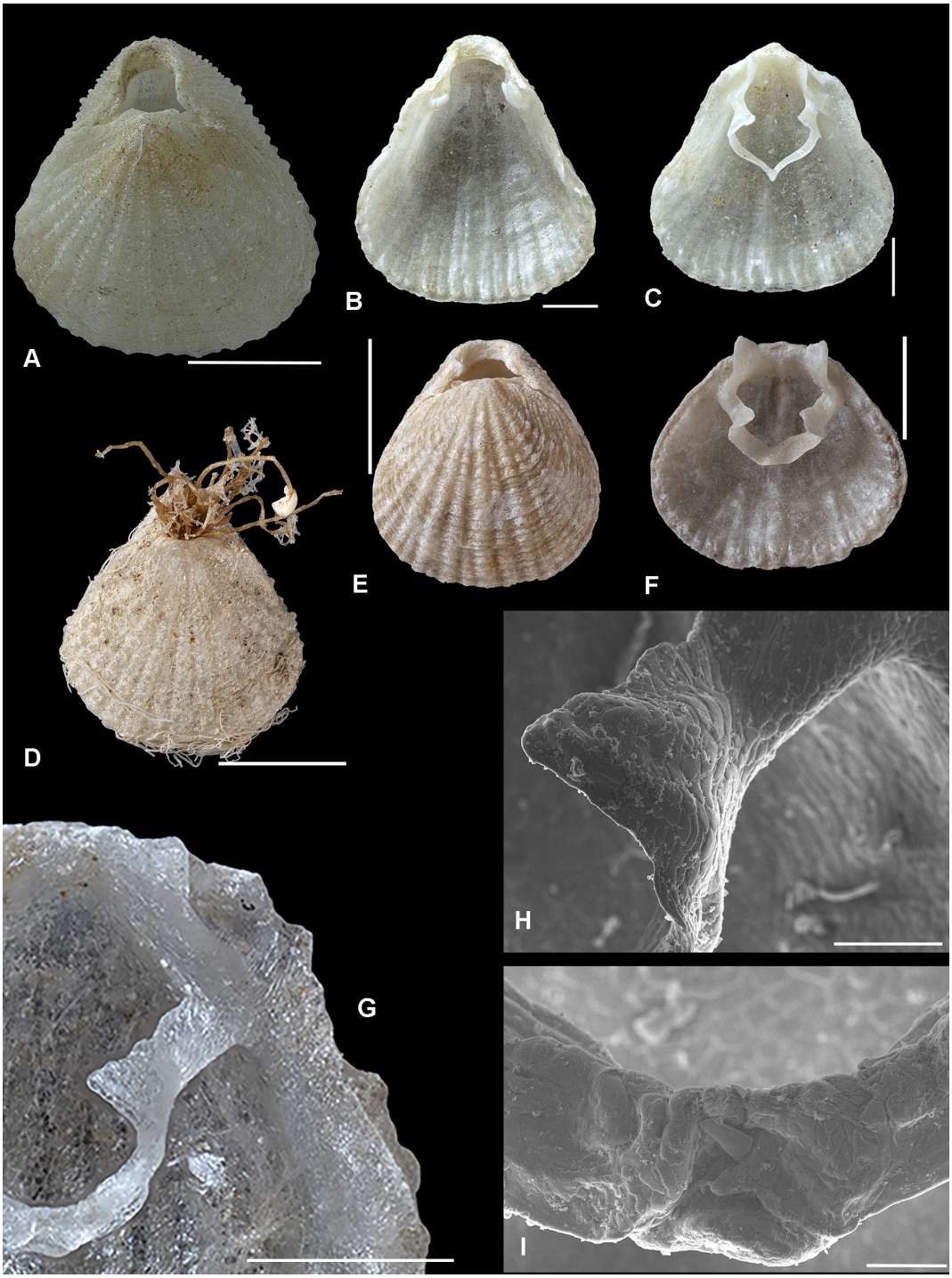

Fig. 18. A–C. *Eucalathis cubensis* Cooper, 1977. **A**. Rounded shell, beaded costellate, MNHN-IB-2022-1016. **B–C**. Elongate shell, MNH-IB-2022-1017. **B**. Ventral valve interior. **C**. Dorsal valve interior. — **D–I**. *Notozyga lowenstami* Cooper, 1977. **D**. Specimen with frayed pedicle, MNHN-IB-2022-1018. **E**. Costellate shell with intermediaries, MNHN-IB-2022-2-1019. **F**. Ventral valve interior revealing elevated inner socket ridges and a stout brachidium, MNHN-IB-2022-2-1020. **G**. Half posterior of dorsal valve interior with inner socket ridge, crural process and transverse band of a translucent juvenile shell, MNHN-IB-2022-1077. **H**. SEM view of left fibrous crural process, MNHN-IB-2022-1077. **I**. SEM close-up view of the junction mark of the branches in the middle of the transverse band from G. Scale bars: A, D–F = 2 mm; B–C = 1 mm; G = 500 µm; H = 100 µm; I = 50 µm.

Dorsal valve. The dorsal valve presents small ears at the posterior part. The valve interior reveals a cardinal process in the shape of half a cup, wide open dental sockets with straight inner socket ridges, stout and relatively long crural plates, large curved crural processes and a thin brachial loop with a deep angulation between the descending lamellae directed dorsi-anteriorly (Fig. 18C). The two valves present marked interlocking crenulations at the inner anterior margin.

Depth range

100–768 m, Karubenthos 2 exped.; 320 to 2005 m (Cooper 1977; Logan 1990).

Distribution

The species was recorded from Key west (Florida), off Havana (Cuba) (Cooper 1977) as well as near Bonaire, and Saba-bank (Logan 1990).

Ecology

The long pedicle rootlets increase the ability of the shell to move.

Genus ***Notozyga*** Cooper, 1977

Type species

Notozyga lowenstami Cooper, 1977.

Notozyga lowenstami Cooper, 1977
Fig. 18D–I

Material examined (including figured material)

GUADELOUPE – **W of Basse Terre** • 1 shell; stn DW 4511; 16°14′ N, 61°52′ W; depth 630–660 m; 8 Jun. 2015; Karubenthos 2 exped.; MNHN, MNHN-IB-1022-1018 (Fig. 18D). – **E of la Désirade** • 1 shell; stn DW 4555; 16°24′ N, 60°51′ W; depth 100–258 m; 15 Jun. 2015; Karubenthos 2 exped.; MNHN • 1 shell; same data as for preceding; MNHN, MNHN-IB-2022-1077 (Fig. 18G–I) • 1 shell; stn DW 4572; 16°19′ N, 60°55′ W; depth 396–399 m; 17 Jun. 2015; Karubenthos 2 exped.; MNHN, MNHN-IB-2022-1019 (Fig. 18E) • 1 shell; same data as for preceding; MNHN, MNHN-IB-2022-1020 (Fig. 18F).

Type locality

California Institute of Technology station 1484.

Description

Morphology. Small biconvex shell, roughly pentagonal with a wide rounded anterior part, ornamented with coarsely beaded primary costellae, between them two generations of intercalated ones are observed (Fig. 18D–E), the median costella and one on each side are stronger than the others, the anterior margin is rectimarginate. The deltidial plates are rudimentary. The ventral umbo is suberect, and a large open foramen cuts most of its posterior part. The maximum width is anterior to mid valve length. The frayed pedicle ends seem obviously longer than what is seen in *Terebratulina cailleti* (Fig. 18D), the different rootlets penetrate shells of foraminifers. Sponge spicules can sometimes cover one valve or the entire shell. The dorsal valve is slightly auriculate at the posterior part. The shell of this species is roughly fascicostellate and growth lines regularly mark the surface (Fig. 18E).

Ventral valve. The valve interior has a well-preserved pedicle collar, a more pointed umbo in juveniles becoming rounded later, and disengaged hinge teeth.

Dorsal valve. The valve interior reveals very high inner socket ridges, a stout brachidium with short and thick distant crural processes pointing to the median plan (Fig. 18F) but never uniting to form a ring (Fig. 18F), and a thick transverse band medially directed toward the valve floor with the trace of the junction of the two halves (Fig. 18G, I). This loop is unlike that of *Eucalathis cubensis*. Both inner valve margins show the characteristic interlocking features of the Cancellothyridoidea, larger and flatter than in *T. cailleti* (Fig. 18F).

Microstructure. In this two-layered shell, the fibrous secondary layer is clearly visible as it is nearly translucent in very young specimens (Fig. 18G), and the fibrous mosaic there reveals differences in shape and size according to their location: crura and crural processes (Fig. 18H), transverse band (Fig. 18G) where the junction of the descending branches is revealed (Fig. 18G–I), and near the margins.

Depth range

100–660 m, Karubenthos 2 exped.; 320–732 m (Cooper 1977; Logan 1990; Zezina 2000).

Distribution

The species is known elsewhere in the Caribbean Sea: Bermuda platform, Cuba, Bonaire, Curaçao, Saba Bank (Cooper 1977; Logan 1990; Zezina 2000).

Ecology

The very long pedicle rootlets increase the ability of the shell to move and so that the shell can adopt an optimal orientation in the currents.

Suborder Terebratellidina Muir-Wood, 1959
Superfamily Megathyridoidea Dall, 1870
Family Megathyrididae Dall, 1870

Genus ***Argyrotheca*** Dall, 1900

Type species

Terebratula cuneata Risso, 1826.

Argyrotheca beaumalei sp. nov.
urn:lsid:zoobank.org:act:5535E9C5-967C-41BF-B7E8-5294D263909E
Fig. 19

Diagnosis

Only three specimens (partly broken and fragile) were collected during the Karubenthos 1 expedition in 2012, with characteristics of dorsal valve interior with no resemblance to other known species included in the genus. Smooth small, white to brown, tiny shell, rounded in outline. A characteristic aspect is the shape of the septum with its posterior zone comprised of four wide curved lateral extensions enclosing a concave area that could be interpreted as brood pouch.

Differential diagnosis

Argyrotheca beaumalei sp. nov. differs from all other species of the genus *Argyrotheca*. It differs from *A. cuneata* that could be closely related to it by the shape and extensions of the posterior septum; it differs from *A. bermudana* Dall, 1911 and *A. rubrotincta* (Dall, 1871) by the coloured pattern and absence of costae; from *A. schrammi* (Dall, 1871) by the absence of wide round costae and no spines on

the posterior septum (see below); from *A. johnsoni* Cooper, 1934 and *A. lutea* (Dall, 1871) by the absence of a fan-shaped septum when viewed laterally and from all other species of the genus by the number and/or size of protuberances at the anterior septum.

Etymology

This new species is dedicated to Mr J. Beaumale for his help when testing Atomic Force Microscopy (AFM Bruker ©).

Type material

Holotype

GUADELOUPE – **Basse Terre** (Pointe à Lézard) • shell; stn GR 10; 16°08′4″ N, 61°46′9″ W; depth 90 m; 7 May 2012; Karubenthos 1 exped.; MNHN, MNHN-IB-2022-1026a (Fig. 19).

Syntypes

GUADELOUPE – **Basse Terre** (Pointe à Lézard) • 2 fragmented shells; same data as for holotype; MNHN, MNHN-IB-2022-1026b–c.

Type locality

Guadeloupe, Basse Terre: Pointe à Lézard (Guadeloupe); 16°08′4″ N, 61°46′9″ W.

Description

Morphology. Small smooth biconvex shell, rather brown coloured to white, slightly wider than long, with a rectimarginate anterior margin. The hinge line is straight, the beak short with a large foramen.

Ventral valve. The interior reveals a developed pedicle collar supported by a median septum extending for ¾ of the valve length with a wide hollow at the anterior part receiving the anterior protuberance of the dorsal valve (Fig. 19A–B). The deltidial plates are vestigial. Medium elongate teeth as for the genus. A wide depression is observed on each side of the septum at its posterior part where the adductor imprints are located.

Dorsal valve. This valve interior deserves some attention with medium and long dental sockets, short prominent crura, two slender arcuate descending lamellae attached to the inner socket ridges, the valve floor and the anterior end of the median septum (Fig. 19C–D, G). Extravagant wide curved extensions susceptible to be recognised as flanges, rising ventrally (two anterior and two posterior), bound a wide and long concave space that could be related to reproduction (cf. brood pouches, see Kaulfuss *et al*. 2013) reaching the level of the inner socket ridges (Fig. 19C–D). The upper boundary of these extensions reveals spine germinations (Fig. 19F). The median septum ends with an elevated protuberance (Fig. 19C, G).

Microstructure. Wide punctae cross the two-layered shell thickness, except in the brachial descending lamellae, extensions and septum. At the inner valve margins, one can readily observe the canopy localised at the upper head of the punctae (Fig. 19E, H) that highlight the basal part of the tubules of the caecal brush. The extremity of the fibres changes rapidly in size from the inner margin to the middle of the valve; the last fibres being secreted reveal their incomplete state (Fig. 19H). The descending lamellae reveal, on the external side, a regular fibrous mosaic (Fig. 19G) compared to the external side of the flanges of the septum with brachiotest.

Depth range

90 m.

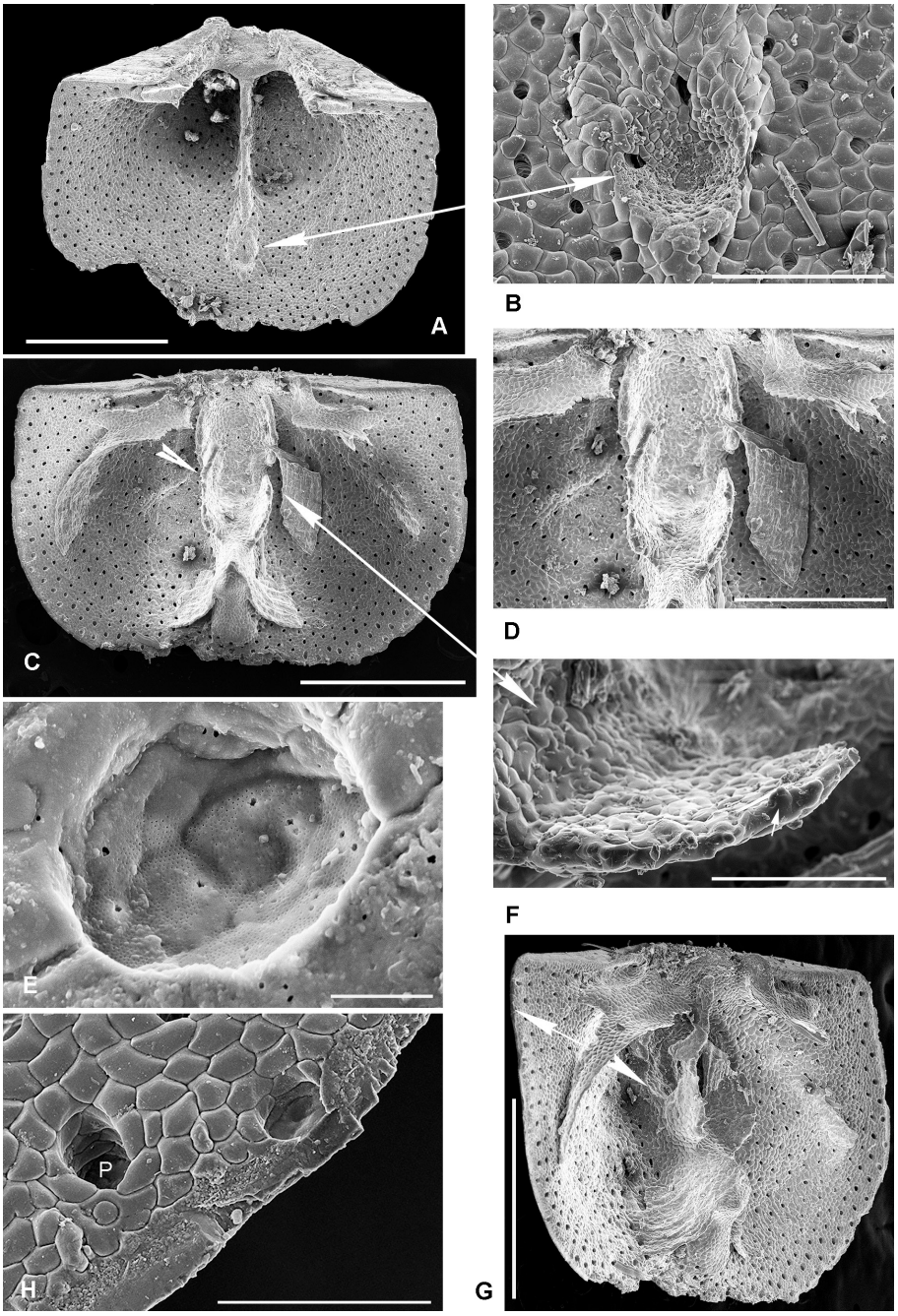

Fig. 19. SEM views of *Argyrotheca beaumalei* sp. nov., holotype, MNHN-IB-2022-1026a. **A**. Ventral valve interior with the pedicle collar, median septum separating the adductor casts and ending with a wide pit. **B**. Detailed pit located by a double arrow. **C**. Dorsal valve interior with large punctae, descending branches of the brachidium widely attached to the valve floor, and double extensions (white arrowhead) on each side of the median septum enclosing a brood-like space between them. **D**. Detail of the brood-like space. **E**. Canopy at the inner head of a puncta, corresponding to the basal caecal brush. **F**. Crest with germinations (small white arrow) and fibrous inner side of a lateral septum extension (located by the double arrow). **G**. Dorsal valve tilted slightly laterally to clearly reveal the path of the right descending brachial branch from the crura to the attachment to the valve floor, then attachment of the ascending part to the high anterior part of the septum. **H**. Inner margin side revealing the proximal part of two punctae (P), and submicrometric granules announcing the first formed fibres. Scale bars: A, C, G = 500 µm; B, F = 100 µm; D = 300 µm; E = 5 µm; H = 50 µm.

Remarks

The same comments made above for the genus *Tichosina* are relevant here with new species (4 + sp. 1 to 5) included in the genus *Argyrotheca* by Cooper (1977), with too small and unfortunately no coloured illustrations (honestly recognised to be infrequently used in 1977) to highlight the coloured patterns on the shell surface and inner parts, most often necessary in tropical regions (see Gaspard *et al*. 2019).

Argyrotheca bermudana Dall, 1911
Fig. 20

Argyrotheca bermudana Dall, 1911: 86.
Cistellla cistellula Verrill, 1900: 592, pl. 70 fig. 7.

Argyrotheca bermudana – Cooper 1977: 107, pl. 3 figs 1–5.

Material examined (including figured material)

GUADELOUPE – **Grand cul de sac Marin (external slope)** • 3 shells; stn GS 04; 14°22′ N, 61°38′ W; depth 11 m; 4 May 2012; Karubenthos 1 exped.; MNHN. – **Grand cul de sac Marin (facing Fajou)** • 3 shells; stn GS 06; 16°21′8″ N, 61°36′1″ W; depth 23 m; 6 May 2012; Karubenthos 1 exped.; MNHN. – **Grand cul de sac Marin (Port St. Louis)** • 1 shell; stn GS 18; 16°23′7″ N, 61°32′1″ W; depth 49 m; 15 May 2012, Karubenthos 1 exped.; MNHN. – **N of Grande Terre** • 3 shells; stn DW 4545; 16°29′7″ N, 61°31′4″ W; depth 62–80 m; 14 Jun. 2015; Karubenthos 2 exped.; MNHN • 1 valve; same data as for preceding; MNHN, MNHN-IB-2022-1078 (Fig. 20E) • 1 shell; same data as for preceding; MNHN, MNHN-IB-2022-1030 (Fig. 20D) • 1 valve; same data as for preceding; MNHN, MNHN-IB-2022-1031 (Fig. 20F–G) • 1 shell; same data as for preceding; MNHN, MNHN-IB-2022-1032 (Fig. 20H–J).

MARTINIQUE – **offshore La Caravelle Peninsula** (St. Aubin islet) • 1 shell; stn AB301; 14°47′3″ N, 60°57′4″ W; depth 19 m; 21 Sep. 2016; Madibenthos exped.; MNHN, MNHN-IB-2022-1027 (Fig. 20A) • 1 shell; same data as for preceding; MNHN, MNHN-IB-2022-1028 (Fig. 20B). – **La Caravelle Peninsula (Table du Diable)** • 10 shells; stn AB 350; 14°56′5″ N, 60°51′5″ W; depth 15 m; 21 Sep. 2016; Madibenthos exped.; MNHN • **Le Robert (Le Loup Bordelais)** • 3 shells; stn AB 405; 14°43′2″ N, 60°50′6″ W; depth 23 m; 25 Sep. 2016; Madibenthos exped.; MNHN. – **E of Le Robert (Cayes Mitan)** • 1 shell; stn AS 255; 14°40′1″ N, 60°51′1″ W; depth 16 m; 18 Sep. 2016; Madibenthos exped.; MNHN • 7 shells; stn AB 191; 14°40′1″ N, 60°51′1″ W; depth 14 m; 18 Sep. 2016; Madibenthos exped.; MNHN. – **Bay of Saint Pierre (Roumaïra wreck)** • 12 shells; sta. AS 572; 14°44′5″ N, 61°10′8″ W; depth 44–47 m; 8 Oct. 2016; Madibenthos exped.; MNHN. – **off Pointe du Diamant** • 1 shell; stn AD 214; 14°27′ N, 60°04′1″ W; depth 70 m; 9 Sep. 2016; Madibenthos exped.; MNHN. – **Les Anses d'Arlet (Morne Jacqueline)** • 3 shells; stn AD 616; 14°28′1″ N, 61°05′3″ W; depth 72 m; 8 Oct. 2016; Madibenthos exped.; MNHN, MNHN-IB-2022-1029 (Fig. 20C). – **Sainte Luce (Grand Caye)** • 1 shell; stn AB 062, 14°27′3″ N, 60°55′5″ W; depth 15 m; 10 Sep. 2016; Madibenthos exped.; MNHN • 8 shells; stn AB 169; 14°27′3″ N, 60°55′5″ W; depth 22 m; 10 Sep. 2016; Madibenthos exped.; MNHN. – **Le Marin channel (Pointe Borgnesse)** • 1 shell; stn AD 067; 14°26′9″ N, 60°54′ W; depth 15 m; 11 Sep. 2016; Madibenthos exped; MNHN.

Type locality

Bermuda.

Description

Morphology. Small to tiny biconvex shell, obviously smooth and thin, bilobate while a light sulcus marks the median anterior valves (Fig. 20A–C). A yellowish/scarlet pattern ornaments the shell as stripes

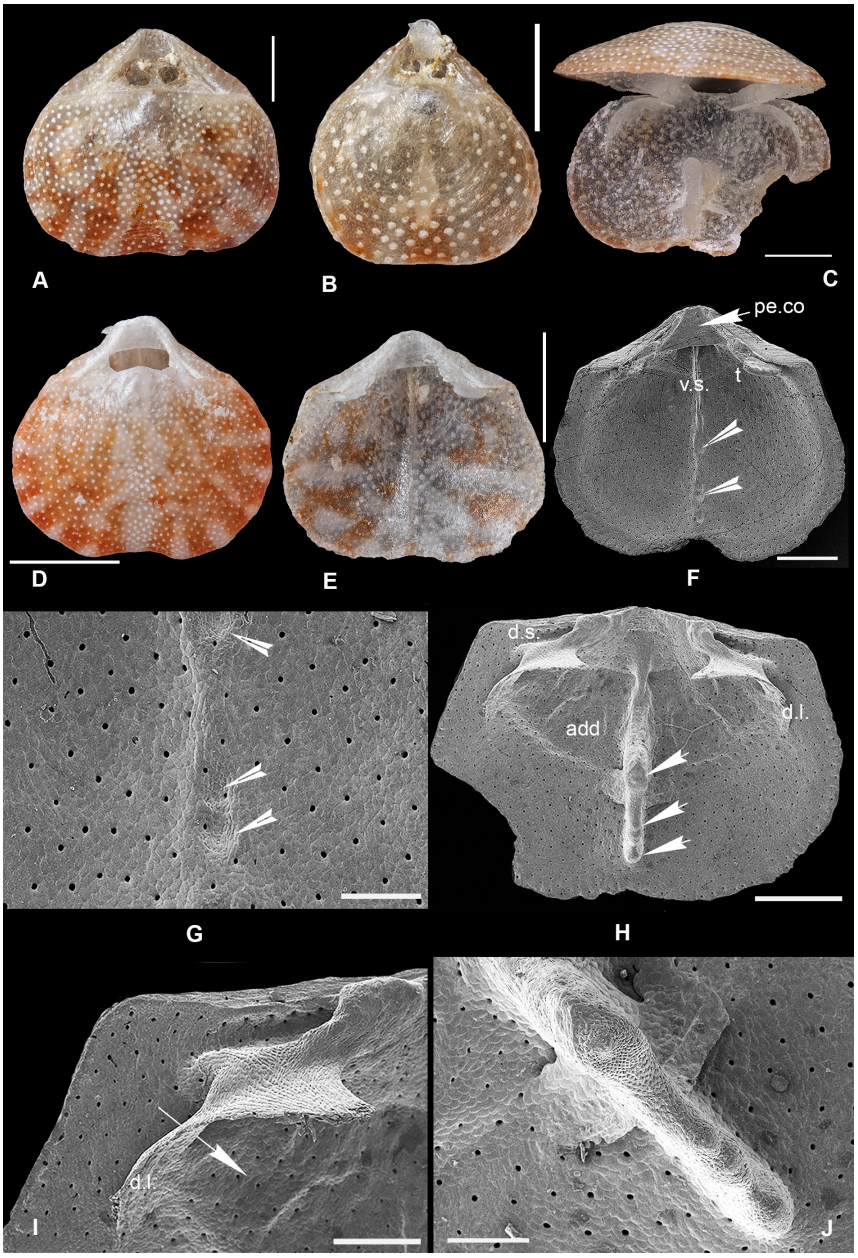

Fig. 20. *Argyrotheca bermudana* Dall, 1911. **A–B**. Coloured adult and juvenile specimens, MNHN-IB-2022-1027 and MNHN-IB- 2022-1028, respectively. **C**. Semi-open articulated shell to reveal the dorsal valve interior, MNHN-IB-2022-1029. **D**. Shell with a bright colour pattern, MNHN-IB- 2022-1030. **E**. Ventral valve interior of a shell from the same station, MNHN-IB-2022-1078. **F–G**. SEM views, MNHN-IB- 2022-1031. **F**. Ventral valve interior of a shell from the same station, with the pedicle collar (pe.co.), teeth (t), and ventral septum (v.s.) with several pits (arrowheads). **G**. Close-up view of the pits of the septum. **H–J**. SEM views of a dorsal valve interior, MNHN-IB-2022-1032. **H**. Valve interior with the widely open dental sockets (d.s.), thick posterior inner socket ridges, adductor imprints (add), median septum with protuberances (white arrows), and path of the descending lamellae (d.l.) of the brachidium, from the crura to the valve floor followed by the attachment over the higher protuberance of the septum. **I**. Close-up view of the right lateral dorsal valve revealing the long and wide dental socket and part of the descending lamellae not attached to the valve floor (white arrow). **J**. Close-up view of the anterior median septum with the protuberances and part of the ascending lamellae attached to it. Scale bars: A, D–E = 1 mm; B–C, F, H = 500 µm; G = 150 µm; I = 200 µm; J= 150 µm.

larger at nearly right angles from the lateral margins, while parallel to the hinge line at the posterior part of the shell, alternating with faded zones (Fig. 20D). The foramen is wide, rounded triangular. The hinge line is wide, approximately straight, and the narrow deltidial plates are wide apart.

Ventral valve. The interior reveals a developed pedicle collar, flattened and long teeth (Fig. 20D–E), and a thin median septum, the anterior part of which is impressed by several pits (Fig. 20E–G) for the reception of the protuberances of the dorsal median septum (Fig. 20H, J).

Dorsal valve. The interior reveals a short transverse cardinal process, long wide dental sockets (Fig. 20H–I), absence of outer hinge plates, crural processes pointed and short crural bases from which is attached the loop consisting of two arcuate ribbon-like descending lamellae mainly fused with the valve floor (Fig. 20H–I), then converging to the thick prominent anterior median septum (Fig. 20H, J).

Microstructure. Two-layered shell with punctae relatively wide for this small shell, visible by transparency (Fig. 20A–D), wider near the margins. The fibrous mosaic of this two-layered shell illustrates the variation observed on the different internal appendices (Fig. 20G–J) and valve floor.

Depth range

14–72 m, Madibenthos; 11–49 m and 60–82 m respectively Karubenthos 1 and 2 exped.; 1– 46 m (Logan 1975; Cooper 1977; Asgaard & Stentoft 1984).

Distribution

In addition, the species is present on the Bermuda platform (Dall 1920; Logan 1975) as well as E and NE of Grenada (Cooper 1977).

Argyrotheca crassa Cooper, 1977
Fig. 21A–B

Material examined (including figured material)

GUADELOUPE – **E of La Désirade** • 1 shell; stn DW 4559; 16°24′5″ N, 60°51′8″ W; depth 72–111 m; 16 Jun. 2015; Karubenthos 2 exped.; MNHN, MNHN-IB-2022-1033 (Fig. 21A) • 1 shell; stn DW 4607; 16°15′ N, 60°50′ W; depth 600–608 m; 24 Jun. 2015; Karubenthos 2 exped.; MNHN, MNHN-IB-2022-1034 (Fig. 21B).

Type locality

Barbados and Grenada.

Description

Morphology. Sub-pentagonal, strongly ventri-biconvex shell with a rounded anterior margin. The hinge line is narrower than the mid-width. The shell is adorned by few (about five) large round costae enlarged anteriorly on each side of the plane of symmetry, plus a few intercalations (Fig. 21A). The intercostal space is nearly as wide as the costae. A slight median sulcus is observed at the anterior part of both valves.

Dorsal valve. Uncommon specimens were sampled. One specimen was half-open revealing the short and narrow dental sockets, the crural processes, the loop reaching the valve floor at mid valve length remaining attached to it, then extending to the septum that it reaches and climbs onto. The dorsal median septum is concave posteriorly, followed by a high anterior slope with several (four to five) projections the characteristic of which is described as a fan-shaped septum when looking laterally. Two thickened round areas concern adductor muscle attachments laterally bordered by the descending branches (Fig. 21B).

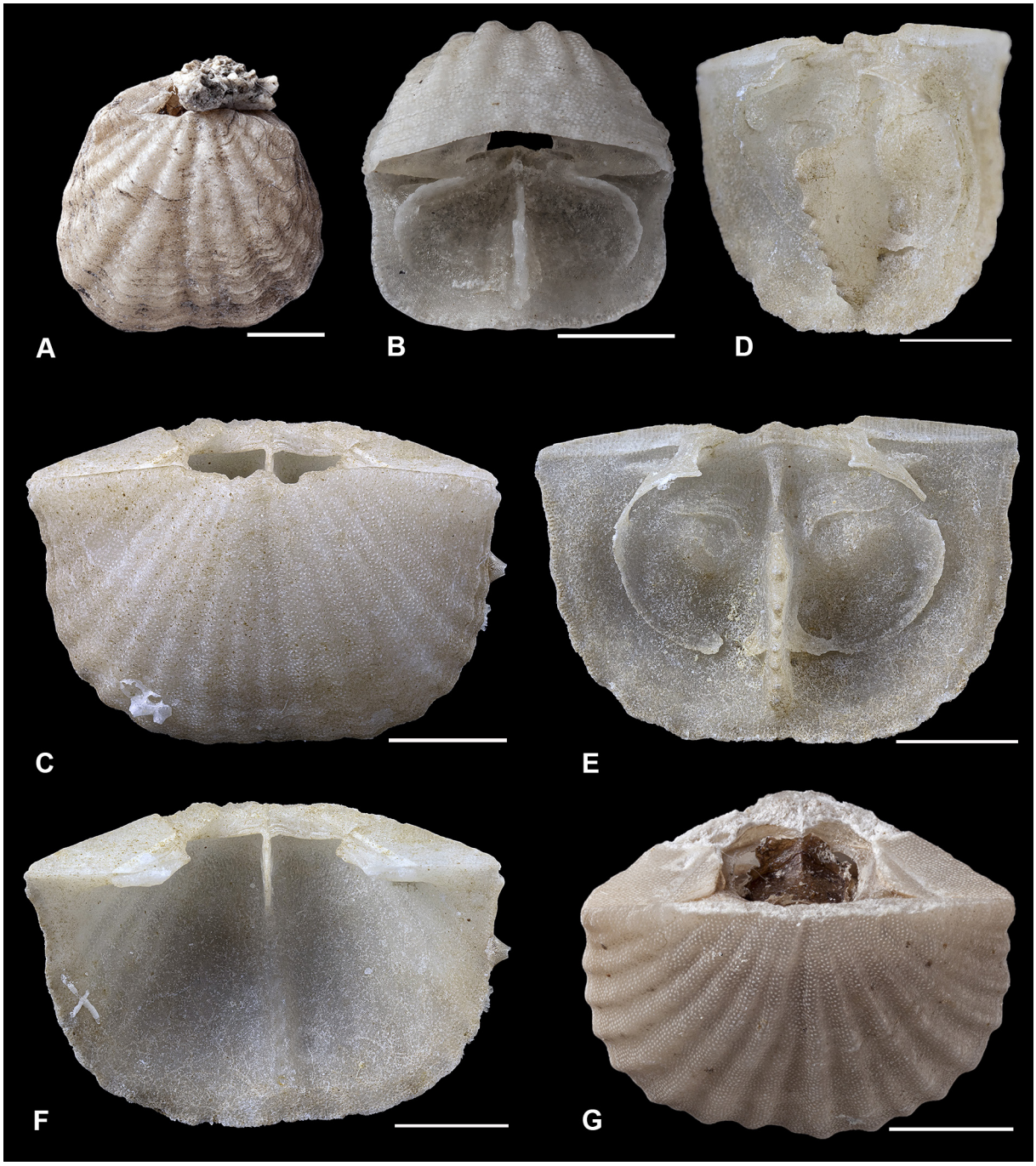

Fig. 21. A–**B**. *Argyrotheca crassa* Cooper, 1977. **A**. Dorsal view of a specimen, MNHN-IB-2022-1033. **B**. Wide open shell to expose the dorsal valve interior, MNHN-IB-2022-1034. — **C**–**F**. *Argyrotheca johnsoni* Cooper, 1934, MNHN-IB-2022-1035. **C**. Dorsal view of a wide costellate shell. **D**. Semi-lateral view of the dorsal valve interior revealing the fan-shape of the septum with small protuberances. **E**. Interior of the same valve with the long dental sockets, small crural processes, brachidium attached to the septum, from its third lateral protuberance, and the muscle imprints. **F**. Ventral valve of the same shell to expose the wide worn pedicle collar, and the septum with several pits accommodating the protuberances of the dorsal septum. **G**. Another adult specimen with a heavily abraded posterior ventral valve, MNHN-IB-2022-1036. Scale bars: A, C–G = 2 mm; B = 1 mm.

Microstructure. Owing to the paucity of the material, no additional examination was made concerning this two-layered shell crossed by wide punctae.

Depth range

72–608 m, Karubenthos 2 exped.; 37–257 m (Cooper 1977); 37–285 m, see Asgaard & Stentoft (1984).

Distribution

The species is recorded from Barbados and NE of Grenada (Cooper 1977).

Ecology

The shell observed reveals a relative short pedicle closely attached to a hard fragment.

Argyrotheca johnsoni Cooper, 1934
Fig. 21C–G

Argyrotheca johnsoni Cooper, 1934: 2, pl. 2 figs 1–12.

Argyrotheca johnsoni – Cooper 1977: 111, pl. 1 figs 2–7.

Material examined (including Figured material)

GUADELOUPE – **S of Marie Galante** • 1 shell; stn DW 4646; 15°51′ N, 61°18′ W; depth 250–254 m; 29 Jun. 2016; Karubenthos 2 exped.; MNHN, MNHN-IB-2022-1035 (Fig. 21C–F). – **N of Grande Terre** • 1 shell; stn CP 4529; 16°24′ N, 61°35′ W; depth 176–183 m; 11 Jun. 2015; Karubenthos 2 exped.; MNHN, MNHN-IB-2022-1036 (Fig. 21G).

MARTINIQUE – **Les Anses d'Arlet (Morne Jacqueline)** • 1 shell; stn AD 616; 14°28′1″ N, 61°05′3″ W; depth 72 m; 8 Oct. 2016; Madibenthos exped.; MNHN.

Type locality

Dominican Republic.

Description

Morphology. Large shell, strongly ribbed, ventral beak which tends to be worn down due to a short disc-like pedicle causing abrasion of the posterior ventral valve against the substrate (Fig. 21C, G). The remaining part of the pedicle collar is close to the posterior part of the septum visible from the wide foramen. The deltidial plates are small and the foramen large. A costa often marks this median wide scalloping anterior margin.

Ventral valve. The interior reveals two elongate teeth and the anterior part of the septum, slightly enlarging on the slope and bearing a line of pits (Fig. 21F) to receive the protuberances of the dorsal septum.

Dorsal valve. The interior reveals the short, shallow but wide-open dental sockets, the short crural processes, the descending brachial branches rapidly attached to the valve floor, then oriented to reach the anterior dorsal septum and overlap it just above the upper projection (Fig. 21E). The anterior part (slope) of the septum bears about seven small projections. These projections were also noted in semi-lateral position of the valve (Fig. 21D). Two marked muscle imprints are on each side of the septum (Fig. 21E).

Microstructure. The very few valves sampled prevent observation of the microstructural details of this punctate two-layered shell.

Depth range

176–254 m, Karubenthos 2 exped.; Madibenthos exped. (72 m); 25–95 m, see Cooper (1977).

Distribution

The species is recorded from the Dominican Republic and Bahama Islands (Cooper 1977), see Jackson *et al*. (1971), and in the Red Sea (Logan *et al*. 2008).

Ecology

The very short pedicle is responsible for the heavy abrasion of the posterior shell appressed to a hard substrate. This species is typical of the genus *Argyrotheca* with the anterior-posterior axis at right angles to the substrate.

Argyrotheca lutea (Dall, 1871)
Fig. 22

Cistella lutea Dall, 1871: 20, pl. 1 figs 5, 5a, pl. 2 figs 4–8.

Cistella lutea – Dall 1886: 203. — Davidson 1887: 142, pl. 23 figs 5–6.
Argyrotheca lutea – Dall 1920: 329. — Cooper 1977: 111, pl. 24 figs 12–28.

Material examined (including figured material)

GUADELOUPE – **N of Grande Terre** • 1 shell; stn DW 4529; 16°24′ N, 61°35′ W; depth 176–183 m; 11 Jun. 2015; Karubenthos 2 exped.; MNHN, MNHN-IB-2022-1037 (Fig. 22). – **W of Marie Galante** • 1 shell; stn DW 4589; 15°59′ N, 61°27′ W; depth 150–221 m; 21 Jun. 1015; Karubenthos 2 exped.; MNHN.

Type locality

Tortugas.

Description

Morphology. Medium size for the genus, nearly wider than long with a pale yellowish colour. Shell surface costate with a wide space between them. The anterior margin is nearly round and slightly indented medially. The shell is gently biconvex.

Ventral valve. The interior reveals the thick median septum, not too elevated but widening anteriorly, with five pits since its mid length (Fig. 22A–B); elongate and flattened teeth (½ of the hinge line on each side), with an undulating upper surface (Fig. 22A, C).

Dorsal valve. The interior reveals the dental sockets with the inner socket ridges marked by the counterparts of the undulating teeth upper surface, the short elevated median septum with the upper part at mid valve length. The anterior of the septum is marked by four to five projections (Fig. 22E). The loop is attached to mid valve floor and to the upper part of the septum above the upper projection (Fig. 22E–I). The adductor imprints are round and deeply marked at the posterior part and do not present a classical fibrous mosaic, while the valve floor lining the anterior part is truly fibrous (Fig. 22G). The external descending branches present a fine fibrous mosaic (Fig. 22D), while it is not the case for the internal side (cf. brachiotest) except when they reach the contact with the valve floor and the septum

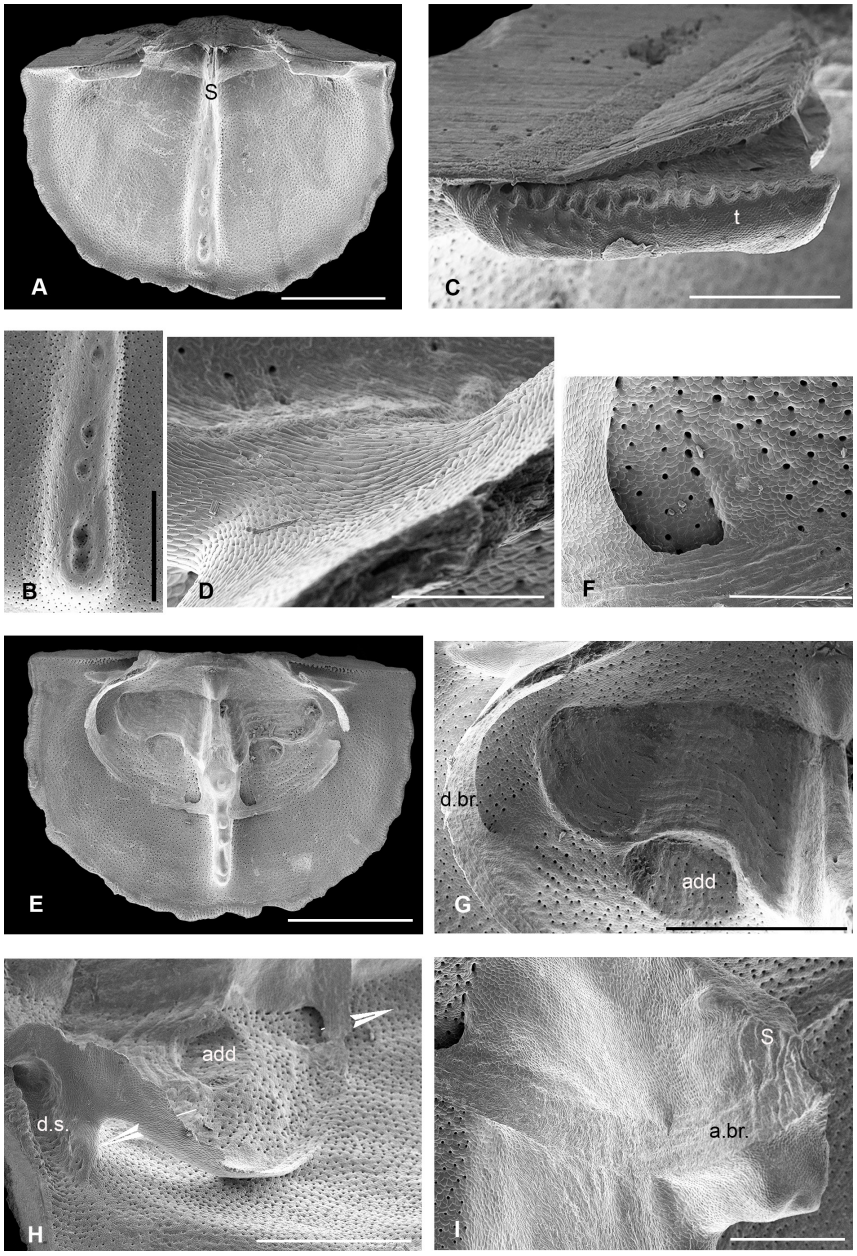

Fig. 22. *Argyrotheca lutea* (Dall, 1871), SEM views of separate valves, MNHN-IB-2022-1037. **A**. Ventral valve interior revealing the pedicle collar, long and flattened teeth, septum (S) enlarging anteriorly with several pits. **B**. Close-up view of the line of pits. **C**. Close-up view of the crenulated upper surface of the right tooth (t). **D**. Fibrous mosaic from the anterior inner socket ridge to the descending lamella. **E**. Dorsal valve interior revealing the long and wide dental sockets, the high inner socket ridges, the descending lamellae till their attachment to the valve floor and then to the high part of the anterior septum with several protuberances, and the deeply impressed muscle casts. **F**. Close-up view illustrating the area where the descending branch, after a short detachment from the valve floor, ascends to become attached laterally to the septum. **G**. Detail of the right half area between the descending branch (d.br) and the lateral posterior septum, with the round imprint of the adductor (add). **H**. Tilted dorsal valve to reveal laterally: the dental socket (d.s.), the adductor (add) and, above all, the locations where the descending and ascending branches are not attached to the valve floor (arrows). **I**. Close-up view to highlight where the ascending branch (a.br) is attached laterally and over the high part to the septum (S). Scale bars: A, E = 2 mm; B, F–H = 1 mm; C, I = 500 µm; D = 200 µm.

(Fig. 22E, G). The external descending branches of the brachidium appear after the inner socket ridges and the anterior dental sockets with a regular mosaic of fibre ends (Fig. 22H). The fibrous mosaic is clearly revealed when looking at the dental pits (Fig. 22C), at the valve floor (Fig. 22F–H), and at the inner shell margin with the punctae.

Depth range

150–221 m, Karubenthos 2 exped.; 55–275 m (Cooper 1977).

Distribution

The species is also recorded from Dry Tortugas, Cuba (Cooper 1977; Logan 1977), Barbados (Dall 1920).

Argyrotheca rubrotincta (Dall, 1871)
Fig. 23

Cistella (? *schrammi* var.) *rubrotincta* Dall, 1871: 19, pl. 1 fig. 6, 6a.

Cistella barrettiana var. *rubrotincta* – Dall 1886: 203.
Cistella barrettiana – Davidson 1887 (part): 145, pl. 23 figs 1–2.
Argyrotheca schrammi – Dall 1920: 330 (part).
Argyrotheca rubrotincta – Cooper 1977: 115, pl. 24 figs 2–11.

Material examined (including figured material)

GUADELOUPE – **E of La Désirade** • 1 shell; stn DW 4555; 16°24′ N, 60°51′ W; depth 100–258 m; 15 Jun. 2015; Karubenthos 2 exped.; MNHN, MNHN-IB-2022-1038 (Fig. 23A) • 1 shell; stn DW 4553; 16°21′ N, 60°54′ W; depth 111–162 m; 15 Jun. 2015; Karubenthos 2 exped.; MNHN, MNHN-IB-2022-1039 (Fig. 23B–D) • 1 shell; same data as for preceding; MNHN, MNHN-IB-2022-1041 (Fig. 23F, H) • 1 shell; stn DW 4574; 16°22′ N, 60°54′ W; depth 140–340 m; 18 Jun. 2015; Karubenthos 2 exped.; MNHN, MNHN-IB-2022-1040 (Fig. 23E, G).

Type locality

West of Dry Tortugas.

Description

Morphology. Very small transverse ventri-biconvex shell, with a rounded scalloped anterior margin and a long straight hinge line (Fig. 23A–B). The dorsal valve is nearly flat while the ventral one is strongly convex (Fig. 23C–D). The ventral umbo is suberect to slightly curved and thick with a large foramen occupying the dorsal side. Small deltidial plates are observed on each side. A distinctive characteristic of the species is its coloured ornamentation: pale yellow on costae and orange even strongly scarlet in intercostae (Fig. 23A–D), plus the bright colour of the internal characters.

Ventral valve. At the valve interior (Fig. 23E–F), the teeth are flat and long, sometimes coloured, the pedicle collar is visible via the foraminal aperture, the median septum thin in its posterior part is thicker anteriorly with several pits, the posterior one at nearly mid valve length accommodates the high projection of the dorsal median septum. Ventral adjustor muscles can be sometimes revealed as well as yellow gonads (Fig. 23F).

Dorsal valve. At the valve interior, the dental sockets are narrow and long with a high inner socket ridge. The dorsal septum, thin posteriorly, is high at nearly mid valve with a scarlet round projection bounded

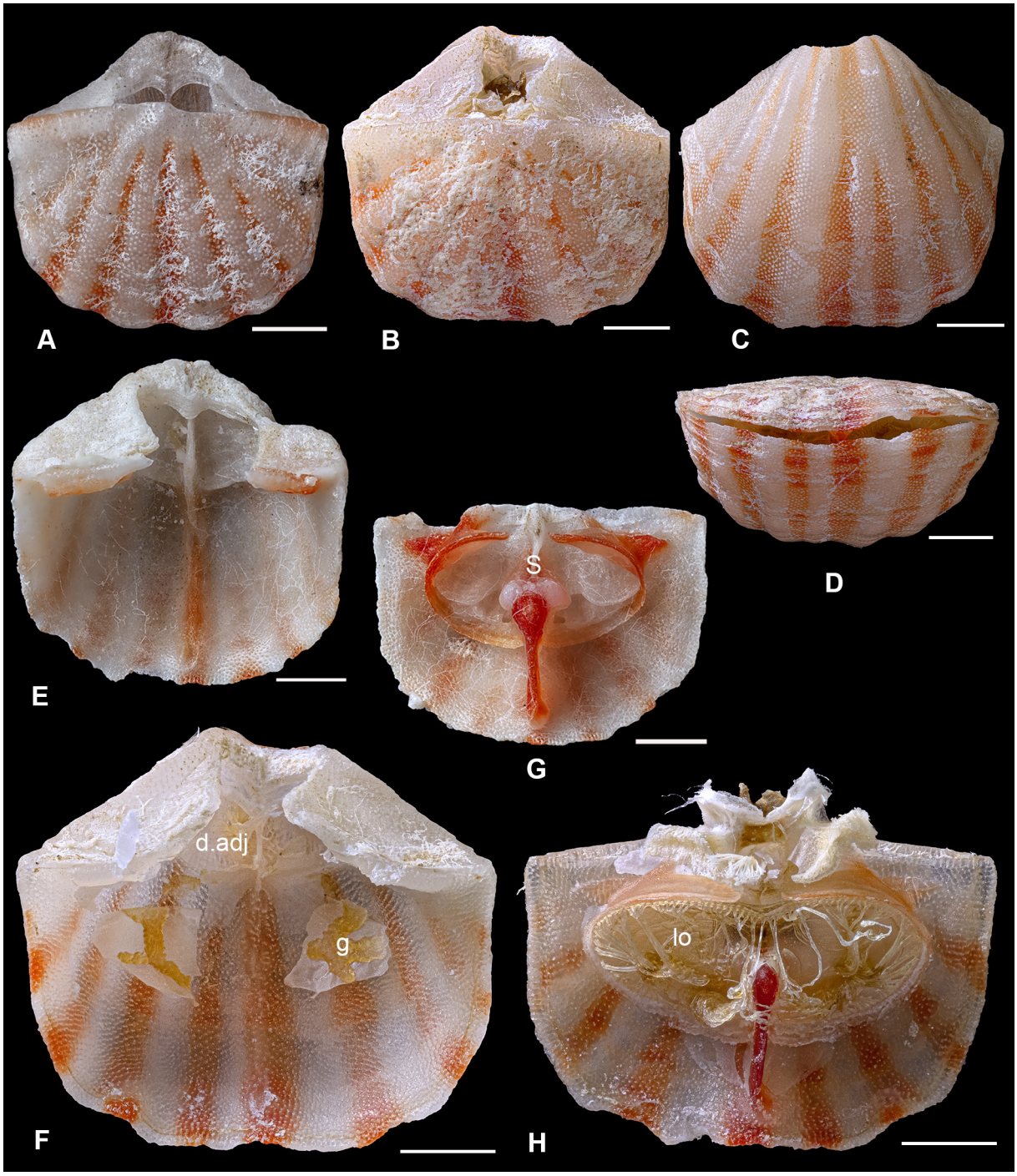

Fig. 23. *Argyrotheca rubrotincta* (Dall, 1871). **A**. Adult shell, MNHN-IB-2022-1038. **B–D**. Dorsal, ventral and anterior views of a shell with brightly coloured intercostae, MNHN-IB-2022-1039. **E**. Ventral valve interior, MNHN-IB-2022-1040. **F**. Another ventral valve interior revealing the long teeth, dorsal adjustors (d.adj), and gonads (g), MNHN-IB-2022-1041. **G**. Brightly coloured dorsal valve interior revealing the red anterior median septum (S), long crural processes and dental sockets (same shell as in E). **H**. Dorsal valve interior (same shell as in F), slightly less coloured, lophophore (lo) still attached to the inner crural processes, inner descending branches and upper septum, MNHN-IB-2022-1041. Scale bars = 1 mm.

by another round pale or pink expansion on each side (Fig. 23G–H). Adductors strongly impressed were observed (Fig. 23G). The inner socket ridges, long crural processes, and loop branches can be coloured red or pink as well as the slope of the anterior septum (Fig. 23G–H). The brachial loop never grows beyond the mid valve length. The lophophore is visible in one of the two coloured specimens sampled (Fig. 23H).

Depth range

100–340 m, Karubenthos 2 exped.; 55–140 m (Cooper 1977).

Distribution

Elsewhere the species is recorded from Barbados, Florida Keys, Dry Tortugas, Bonaire, Curaçao, Grenada (Cooper 1977; Asgaard & Stentoft 1984; Logan 1990).

Ecology

This species, like others included in the genus, has a thick short pedicle that can lead to abrasion at the posterior shell when the specimen is moving.

Argyrotheca schrammi (Crosse & Fischer, 1866)
Figs 24–25

Argyope schrammi Crosse & Fischer 1886: 269, pl. 8 fig. 6.

Cistella schrammi – Davidson 1887: 148, pl. 22 figs 3–4.
Argyrotheca schrammi – Dall 1920: 329. — Cooper 1977: 117, pl. 16 figs 12–16. — Alvarez *et al*. 2008: fig. 7d–e.

Material examined (including figured material)

MARTINIQUE **– La Pointe du Diamant**: 1 shell; stn AD 214; 14°27′ N, 61°04′1″ W; depth 70 m; 9 Sep. 2016; Madibenthos exped.; MNHN, MNHN-IB-2022-1042 (Fig. 24A). – **Sainte Luce (Grand Caye)** • 1 shell; stn AB 062; 14°27′3″ N, 60°55′5″ W; depth 15 m; 10 Sep. 2016; Madibenthos exped.; MNHN.

GUADELOUPE **– S of La Désirade (N of Petite Terre)** • 4 shells; no precise geographical coordinates; depth 90 m; Dive 2019; D. Lamy leg.; MNHN • 1 shell; same data as for preceding; MNHN, MNHN-IB-2022-1043 (Fig. 24B) • 2 valves; same data as for preceding; MNHN, MNHN-IB-2022-1079, MNHN-IB-2022-1044 (Fig. 24C–D) • 3 valves; same data as for preceding; MNHN, MNHN-IB-2022-1083, MNHN-IB-2022-1084, MNHN-IB-2022-1085 (Fig. 25A–B, D–E). **– E of Petite Terre** • 1 shell; stn GD 61; 16°12′ N, 61°04′ W; depth 80 m; May 2012; Karubenthos 1 exped.; MNHN, MNHN-IB-2022-1080 (Fig. 24E–G). **– Grande Terre (Banc des Vaisseaux)** • 1 shell + 1 valve; stn GD 67; 16°08′ N, 61°17′ W; depth 110 m; 27 May 2012; Karubenthos 1 exped.; MNHN.

Type locality

Guadeloupe.

Description

Morphology. Small salmon reddish shell, obviously wider than long and somewhat bilobate, ornamented by three costae on each valve side. The colour varies over the shell, but the intercostae are widely brightly coloured (Fig. 24A–B). Very small deltidial plates are positioned on each side of the foramen and the pedicle collar is visible at the foramen opening.

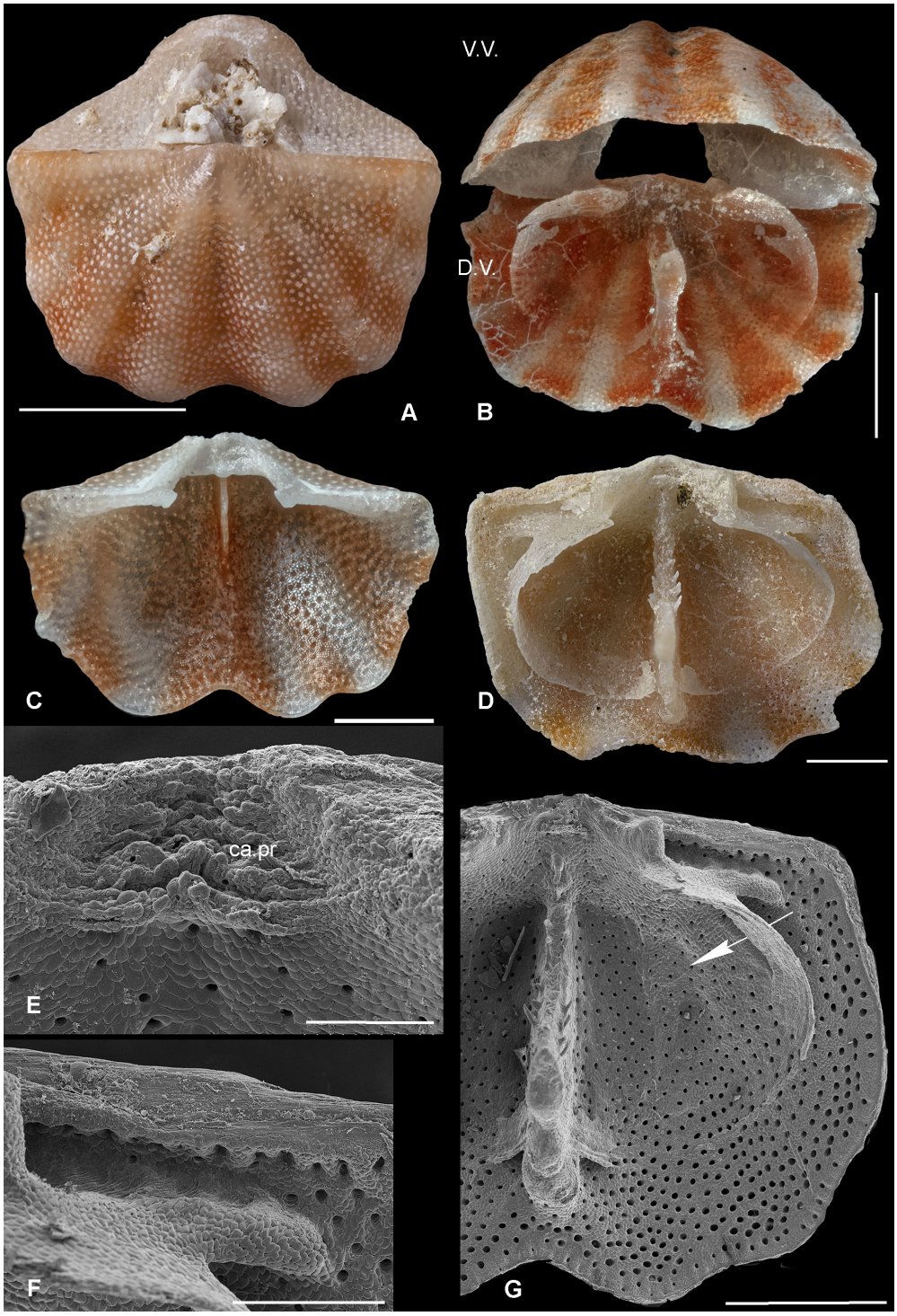

Fig. 24. *Argyrotheca schrammi* (Crosse & Fischer, 1866). **A**. Adult shell, MNHN-IB-2022-1042. **B**. wide open articulated shell to reveal the dorsal valve interior, MNHN-IB-2022-1043. **C**. Ventral valve interior with long teeth, MNHN-IB-2022-1079. **D**. Dorsal valve interior with wide open dental sockets, the brachial ribbons, and the median septum with a line of spines on each of its upper sides, MNHN-IB-2022-1044. **E–G**. SEM views, MNHN-IB-2022-1080. **E**. Cardinal process (ca.pr.). **F**. Punctate dental socket. **G**. Left part of the dorsal valve interior showing the attachment of the brachial descending branch with the part unattached to the valve floor (arrow) and the spines on the septum. Scale bars: A–C, G = 1 mm; D = 500 µm; E–F = 100 µm.

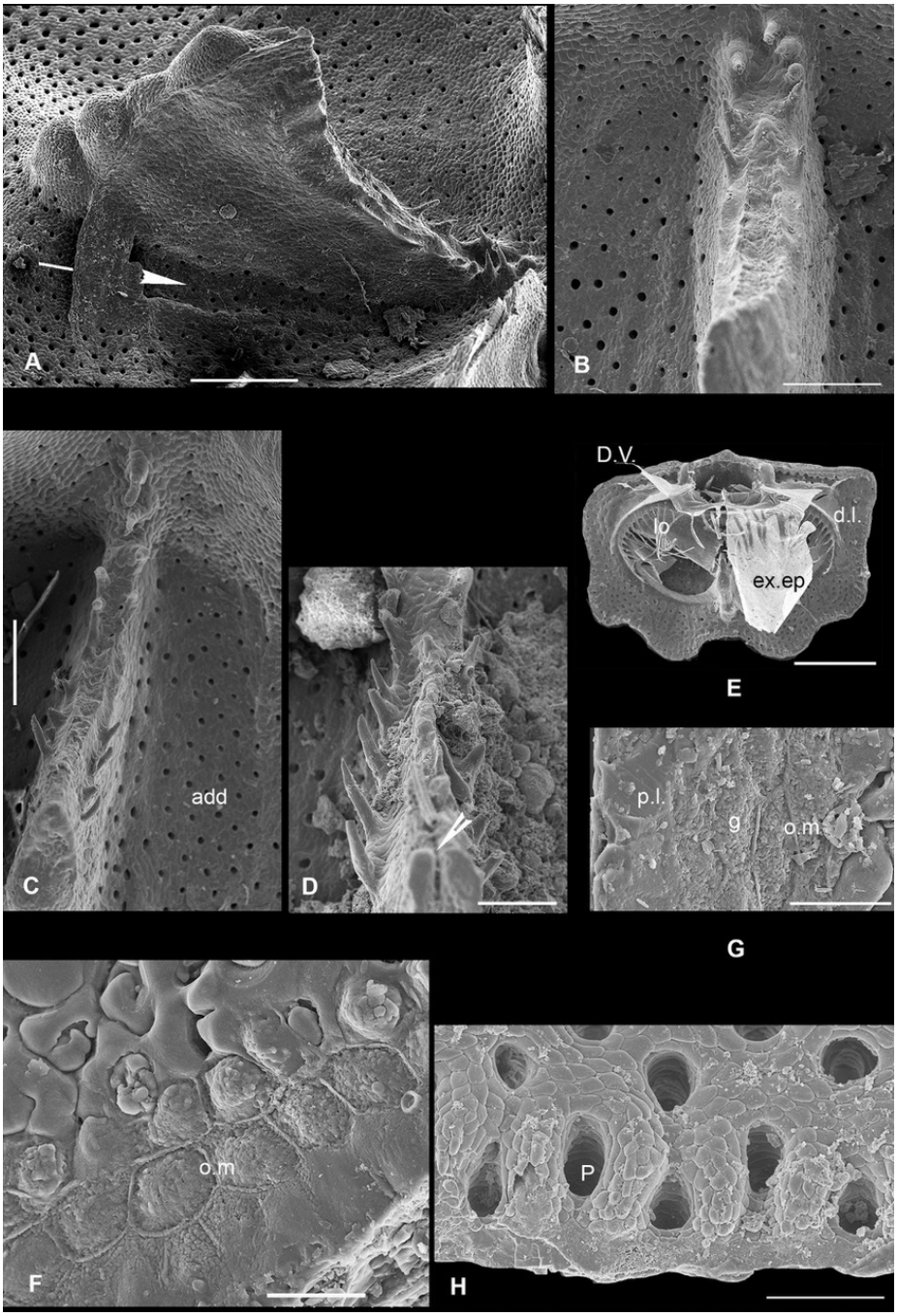

Fig. 25. *Argyrotheca schrammi* (Crosse & Fischer, 1866), SEM views. **A**. Lateral view of a juvenile dorsal valve interior tilted to reveal the high septum with the first spines and the ascending brachial ribbon attached to it, MNHN-IB-2022-1083. **B**. Posterior part of the same median septum, MNHN-IB-2022-1083. **C**. Septum of an adult shell with spines along each side of the upper posterior part (add = adductor), MNHN-IB-2022-1080. **D**. Unusual divided high anterior point of the septum (arrowhead), MNHN-IB-2022-1084. **E**. Dorsal valve with lophophore (lo) partly covered with a fragment of external epithelium (ex.ep.) (d.l. = descending lamellae), MNHN-IB-2022-1085. **F–G**. Close-up view at the inner margin, with submicrometric granules (g) surrounded by organic membranes (o.m.) at the limit between the secondary and the primary layers (p.l.), MNHN-IB-2022-1080. **H**. Inner margin with light fibrous crenulations separated from each other by a wide puncta (P), MNHN-IB-2022-1080. Scale bars: A = 250 µm; B–D = 150 µm; E = 500 µm; F–G = 10 µm; H = 50 µm.

Ventral valve. The ventral valve interior reveals long and narrow teeth, and the short posterior septum starting under the pedicle collar (Fig. 24C).

Dorsal valve. The dorsal valve interior reveals a shallow cardinal process with the imprints of the diductor muscle (Fig. 24D–E), very long dental sockets densely punctate (Fig. 24D, F), no real crural processes, but crura oriented slightly ventri-medially, descending branches of the brachidium in continuity with the inner socket ridges, closely attached to the valve floor (Fig. 24B, D, G) and to the flanks and summit of the anterior median septum (Figs 24G, 25A). The plateau of the posterior septum is occupied by two rows of spines (Fig. 24D, G): curved at the posterior part, first visible in juveniles (Fig. 25A–B) and ± erect on each side of the septum plate in adults (Figs 24G, 25C) as also illustrated in Alvarez *et al*. (2008: fig. 7d–e). Along the slope of the elevated anterior septum are four round protuberances susceptible to fit to the pits of the ventral septum (Figs 24G, 25A) and, sometimes, the upper septum can be cloven (Fig. 25D). When observed, the schizolophous lophophore appears to be attached at the internal surface of the slender curved descending branches (Fig. 25E).

Microstructure. As for all species of *Argyrotheca*, the diameter of the punctae is wide, but their distribution reveals a gentle decrease in size from the margins to the middle valve, particularly near the adductor imprints (Figs 24G, 25A, C). The last fibres secreted at the inner margins reveal submicrometric elements and the first formed organic membranes in relation with them (Fig. 25F–G). Just prior to this zone, at the inner margin boundary, crenulations appear in both valves, each of which is separated by a very wide puncta and the orientation of the fibre ends there is nearly at right angle to the margin line (Fig. 25H).

Depth range

80–110 m, Karubenthos 1 exped.; 15–70 m, Madibenthos exped.; elsewhere from 6 to 981 m (Logan 1975, 1977; Cooper 1977; Asgaard & Stentoft 1984).

Distribution

The species was also recorded by Crosse & Fischer 1866: Caribbean Sea, Yucatan; from Guadeloupe, Barbados (Davidson 1887; Dall 1920); Florida Keys, Tortugas, Barbados, Antigua, Grenada (Cooper 1977); Grenada; Barbados (Alvarez *et al*. 2008).

Superfamily Platidioidea Thomson, 1927
Family Platidiidae Thomson, 1927
Subfamily Platidiinae Thomson, 1927

Genus ***Platidia*** Costa, 1852

Type species

Orthis anomioides Scacchi & Philippi, 1844.

Platidia anomioides (Scacchi & Philippi, 1844)
Fig. 26A–I

Orthis anomioides Scacchi & Philippi, 1844: 69, pl. 18 fig. 9a–g.

Platidia anomioides – Costa 1852: 48, pl. 3 fig. 4, pl. 3bis fig. 6. — Dall 1870: 14, figs 20–21. — Davidson 1880: 55, pl. 4 figs 10–11. — Cooper 1977: 122, pl. 20 figs 11–19, pl. 33 figs 15–17. — Gaspard 2024: fig. 1, table 1.

Platidia (*Morrisia*) *anomioides* – Davidson 1870: 405, pl. 21 figs 15, 15a.

Material examined (including figured material)

FRENCH GUIANA – 1 shell; stn CP 4374; 06°40′ N, 52°29′ W; depth 240 m; 3 Aug. 2014; Convention APA-973-1; Acoupa exped.; MNHN, MNHN-IB-2017-224.

GUADELOUPE – **N of Grande Terre** • 2 shells; stn DW 4518; 16°34′ N, 61°37′ W; depth 426–441 m; 9 Jun. 2015; Karubenthos 2 exped.; MNHN • 1 shell; stn DW 4524; 16°29′ N, 61°42′ W; depth 500–550 m; 10 Jun. 2015; Karubenthos 2 exped.; MNHN • 1 shell; stn DW 4530; 16°27′ N, 61°35′ W; depth 275–292 m; 11 Jun. 2015; Karubenthos 2 exped.; MNHN • 1 shell; stn DW 4538; 16°38′ N, 61°31′ W; depth 320–338 m; 12 Jun. 2015; Karubenthos 2 exped.; MNHN, MNHN-IB-2022-1045 (Fig. 26A–B) • 2 juvs; stn DW 4545; 16°29′7″ N, 61°31′4″ W; depth 60–82 m; 14 Jun. 2015; Karubenthos 2 exped.; MNHN, MNHN-IB-2022-1086 (Fig. 26H), MNHN-IB-2022-1048 (Fig. 26I). – **W of Basse Terre** • 2 shells; stn CP 4512; 16°13′ N, 61°54′ W; depth 409–532 m; 8 Jun. 2015; Karubenthos 2 exped.; MNHN, MNHN-IB-2022-1047 (Fig. 26D–G) • 7 shells; stn CP 4513; 16°13′ N, 61°54′ W; depth 406–644 m; 8 Jun. 2015; Karubenthos 2 exped.; MNHN. – **E of La Désirade** • 3 shells; Sta. DW 4560; 16°25′ N, 60°52′ W; depth 185–250 m; 16 Jun. 2015; Karubenthos 2 exped.; MNHN • 2 shells; stn DW 4580; 16°19′ N, 60°50′ W; depth 412–500 m; 18 Jun. 2015; Karubenthos 2 exped.; MNHN • 1 shell; stn DW 4607; 16°15′ N, 60°50′ W; depth 600–608 m; 24 Jun. 2015; Karubenthos 2 exped.; MNHN, MNHN-IB-2022-1046 (Fig. 26C) • 3 shells; stn DW 4608; 16°14′ N, 60°49′ W; depth 618–632 m; 24 Jun. 2015; Karubenthos 2 exped.; MNHN • 1 shell; stn DW 4610; 16°17′ N, 60°55′ W; depth 513–528 m; 24 Jun. 2015; Karubenthos 2 exped.; MNHN.

Type locality

Sicily.

Description

Morphology. Small shell nearly subcircular, plano-convex, thin and quasi-transparent, allowing observation of the punctae and predicting the lophophore shape (Fig. 26A–B, E). The external surface is smooth, the hinge line is nearly half the shell width and the amphithyrid foramen is very wide (an unusual embayment encroaching also the dorsal valve), covered by a solid integument (Fig. 26A, D). The deltidial plates are narrow, widely disjunct and the pedicle collar short.

Ventral valve. The ventral valve interior reveals strong teeth supported by short dental plates (Fig. 26C). The muscles are strong and the diductors, while short, may attach the integument over the pedicle opening. Spicules are visible around the gonads (Fig. 26G).

Dorsal valve. The dorsal valve interior reveals no cardinal process, shallow and widely open dental sockets (Fig. 26H), and an uncommon brachial apparatus with no hinge plates. A septal pillar is erected near the dorsal embayment, ending in a pair of flanges forming a U shape directed slightly posteriorly. Two long and thin crura with short processes are present, two arcuate descending branches are united to the lateral side of the flanges of the high septal pillar. The lophophore supported by the brachidium is zygolophous (Fig. 26F) and its basal arm parts are protected by spicules.

Microstructure. This species presents a thin two-layered shell with numerous small punctae.

Depth range

176–644 m, Karubenthos 2 exped.; 240 m, Acoupa exped.; this species is also recorded by Cooper 1977 (18– 963 m); 8–2190 m (Logan 2007: 3108).

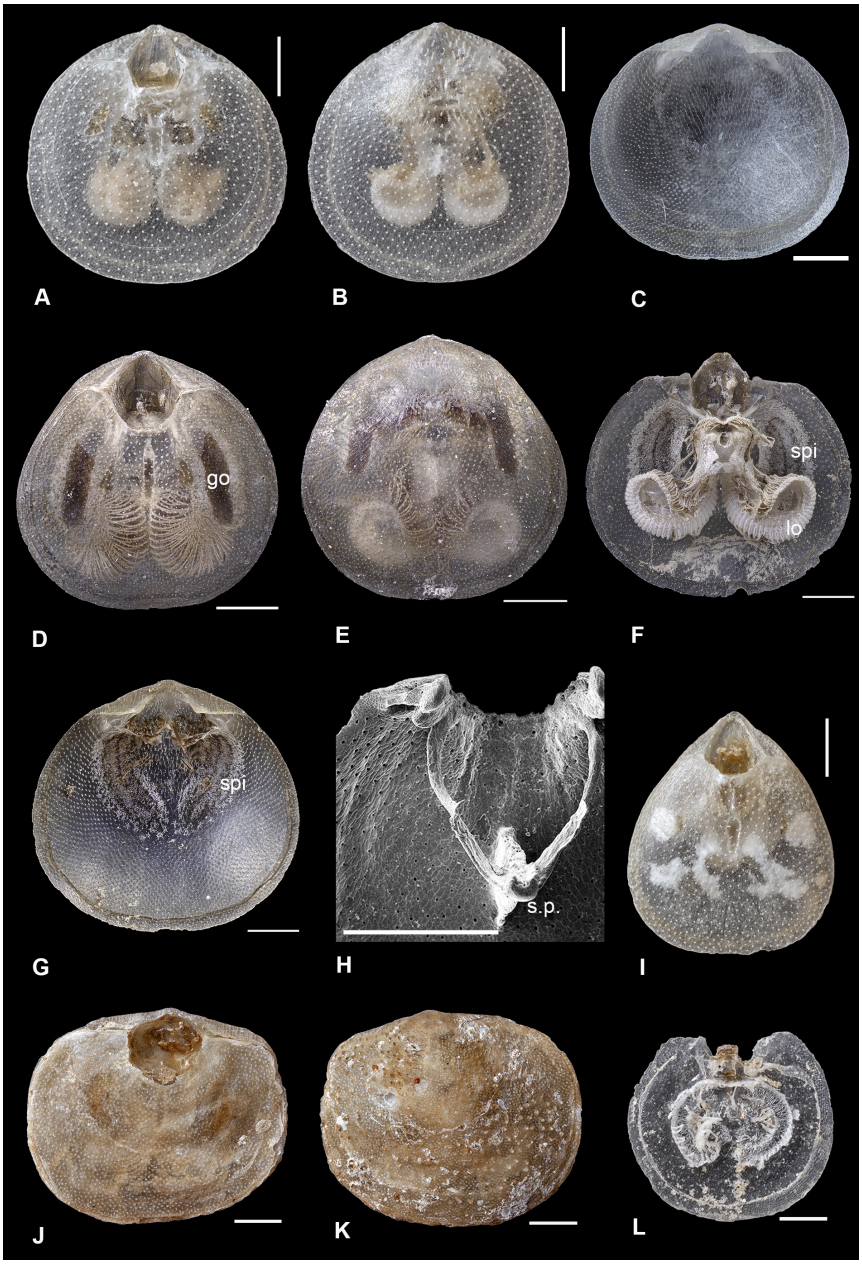

Fig. 26. A–I. *Platidia anomioides* (Scacchi & Philippi, 1844). **A–B**. Dorsal and ventral views of a shell, revealing punctae and the lophophore by transparency, MNHN-IB-2022-1045. **C**. Ventral valve interior of a shell, MNHN-IB-2022-1046. **D–E**. Dorsal and ventral views of a shell, the septum, lophophore and brown gonads (go) are seen by transparency. The shell retains its integument covering the foramen, MNHN-IB-2022-1047. **F–G**. Interior views of separate dorsal and ventral valves of the preceding shell. The integument is still attached to the dorsal valve, the upper part of the septum, lophophore (lo), brown gonads and spicules (spi) around them are revealed (F). The teeth, spicules around the gonads and setae at the inner margins are seen at the ventral valve (G). **H**. Detail of the brachidium, with the crura, descending branches attached to the lateral parts of the high septal pillar (s.p.) and the departure of the U-shaped broken flanges, MNHN-IB-2022-1086. **I**. Juvenile specimen, MNHN-IB-2022-1048. — **J–K**. *Platidia davidsoni* (Deslongchamps, 1855), MNHN-IB-2022-1049. Dorsal (J) and pustulous external ventral surface (K). — **L**. *Amphithyris buckmani* (Thomson, 1918), MNHN-IB-2022-1050, dorsal valve interior with the lophophore curled differently compared to that of species of *Platidia* Costa, 1852. Scale bars: A–B, H–I = 500 µm; C–G, J–K = 1 mm; L = 300 µm.

Distribution

Worldwide distribution. In the Caribbean Sea: off Cuba, Columbia, SE Florida shelf, NW of Cap San Antonio, SW Yucatan Channel, NE of Porto de Morelos, NE of Caracas, NE of Grenada, St. Vincent, NW side of Ste Lucia, E of Dominica Island (Cooper 1977); French Guiana; in the Atlantic Ocean (Gaspard 2003; Logan 2007); Mediterranean Sea (Brunton & Curry 1979; Logan 1979); Sub-Antarctic and Antarctic: Marion Island, Crozet Islands (Foster 1974; Gaspard 2018, 2024); Pacific Ocean (Zezina 1990) among the locations.

Ecology

The movements generated by the pedicle system, in relation with no clearly differentiated pedicle muscles for members of the Platidiidae, are restricted to raising and lowering the shells, with the loss of capacity to twist them. The amphithyrid foramen is associated with this type of pedicle system.

Platidia davidsoni (Deslongchamps, 1855)
Fig. 26J–K

Morrisia davidsoni Eudes-Deslongchamps, 1855: 443, pl. 10 fig. 20a–d.

Terebratula (*Morrisia*) *davidsoni* – Reeve 1861: pl. 10 fig. 42.
Platidia davidsoni – Dall 1870: 143. — Fischer 1872: 160, pl. 6 fig. 3–9. — Davidson 1887: 154, pl. 21 figs 23–27. — Fischer & Oehlert 1891: 100, pl. 8 figs 15a–d. — Cooper 1977: 123, pl. 18 figs 18–22, pl. 27 figs 3–6.

Material examined (including figured material)

GUADELOUPE – **N of Grande Terre** • 1 shell; stn DW 4541; 16°42′ N, 61°37′ W; depth 615–630 m; 13 Jun. 2015; Karubenthos 2 exped.; MNHN, MNHN-IB-2022-1049 (Fig. 26J–K).

Description

Morphology. Subcircular to subquadrate small shell, plano- to slightly concavo-convex. The hinge line is wide, almost as wide as the shell, located at mid valve. As for *P. anomioides*, the foramen opening is shared by the two valves (mostly by the dorsal one), and an integument is also present here (Fig. 26J). The deltidial plates appear to be absent. The external surface of the ventral valve is adorned by pustules (small nodules) partly worn (Fig. 26K). The specimen is pale brown and not very transparent like *P. anomioides*.

Depth range

615–630 m, Karubenthos 2 exped.; 485–496 (Cooper 1977); 90–142 m and 1238 m (Fischer & Oehlert 1891); 82–897 m elsewhere.

Distribution

The species was recorded elsewhere in the Caribbean Sea [Gd. Bahama, West end of Cuba] and in the Atlantic Ocean [off Brazil (Kowalewski *et al*. 2002; Rodland *et al*. 2004, confused with *P. anomioides*), off Portugal and Ibero-Morrocan Gulf (Gaspard 2003, confused with *P. anomioides*), the Gulf of Biscay, Canaries]; in the Mediterranean Sea (Logan 1979); in the Pacific Ocean among other locations (see Logan 2007: 3108).

Genus ***Amphithyris*** Thomson, 1918

Type species

Amphithyris buckmani Thomson, 1918.

Obviously, a species of this genus has not previously been reported in the Caribbean Sea.

Amphithyris buckmani Thomson, 1918
Fig. 26L

Amphithyris buckmani Thomson, 1918: 22, pl. 15 fig. 9.

Amphithyris buckmani – Bitner 2006: 28, fig. 6, pl. 16 fig. 35; 2008s: 440, fig. 11.

Material examined (including figured material)

GUADELOUPE – **W of Basse Terre** • 1 shell; stn CP 4513; 16°13′ N, 61°54′ W; depth 406–644 m; 8 Jun. 2015; Karubenthos 2 exped.; MNHN, MNHN-IB-2022-1050 (Fig. 26L).

Type locality

Cook Straits near Wellington (New Zealand).

Description

One tiny shellsampled. This shell is suborbicular, plano-convex. The foramen is amphithyrid, the hinge teeth without dental plates. The cardinalia consist only of socket ridges, and the dorsal median septum is low. In contrast to species of *Platidia*, the schizolophous lophophore of this species presents branches curled to the symmetry plane, towards the upper part of the septum (Fig. 26L).

Depth range

406–644 m, Karubenthos 2 exped.; 91–1865 m (see Logan 2007).

Distribution

The species is recorded from New Zealand (see Logan 2007).

Subfamily Phaneroporinae Zezina, 1981

Genus ***Phaneropora*** Zezina, 1981

Type species

Phaneropora galatheae Zezina, 1981.

Phaneropora aff. ***galatheae*** Zezina, 1981
Fig. 27A–C

Material examined (including figured material)

GUADELOUPE – **W of Basse Terre** • 1 shell, stn CP 4512; 16°13′ N, 61°54′ W; depth 409–532 m; 8 Jun. 2015; Karubenthos 2 exped.; MNHN, MNHN-IB-2022-1051 (Fig. 27A) • 1 open shell; stn CP 4513; 16°13′ N, 61°54′ W; depth 406–644 m; 8 Jun. 2015; Karubenthos 2 exped; MNHN, MNHN-IB-2022-1052 (Fig. 27B–C).

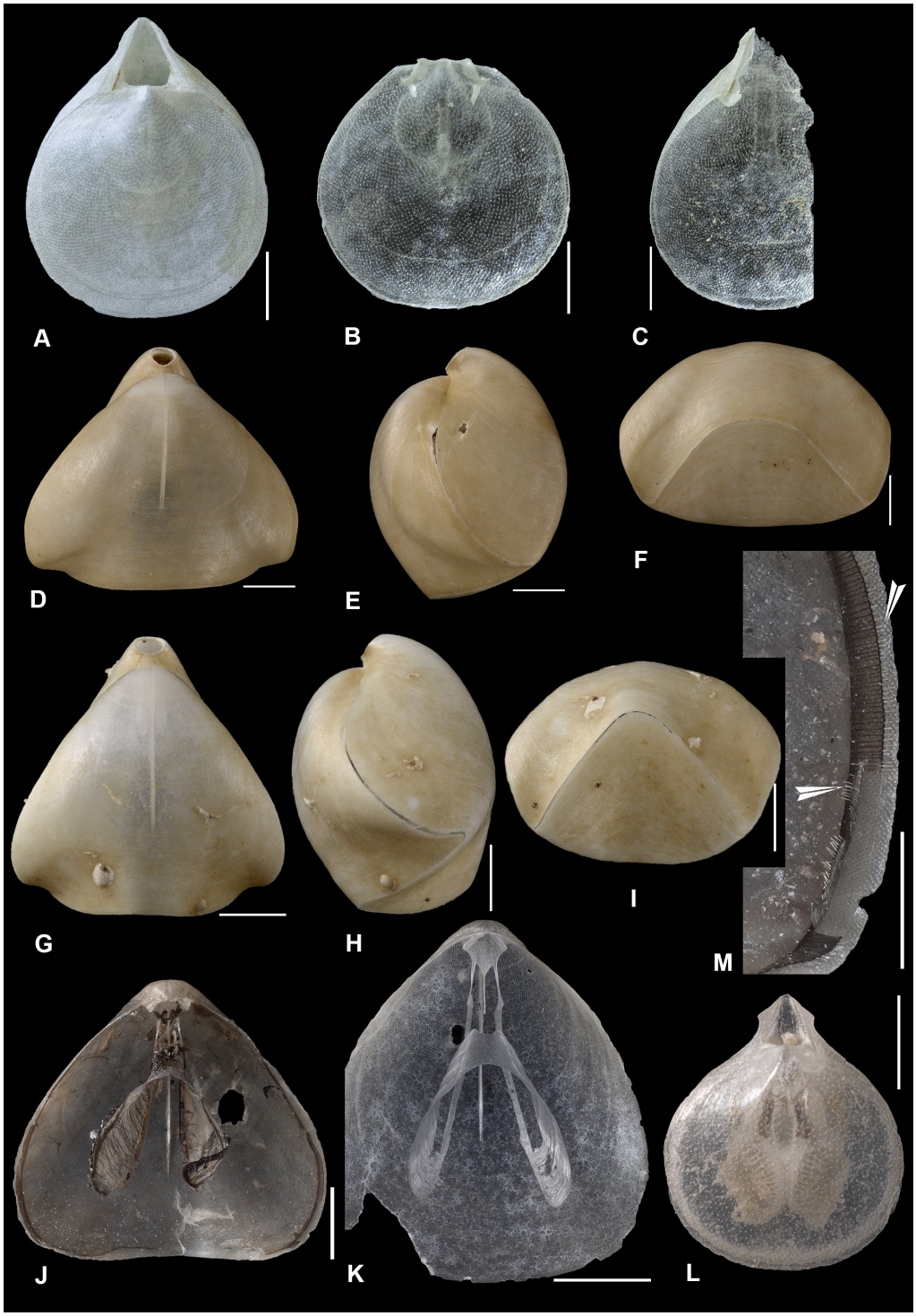

Fig. 27. A–C. *Phaneropora galatheae* Zezina, 1981. **A**. Tiny specimen, MNHN-IB-2022-1051. **B–C**. Interior dorsal and ventral valves, MNHN-IB-2022-1052. — **D–M**. *Dallina floridana* (Pourtalès, 1868). **D–I**. Dorsal, lateral and anterior views of two morphotypes of the species (wide and elongate), MNHN-IB-2022-1053 (D–F) and MNHN-IB-2022-1054 (G–I). **J**. Dorsal valve interior with its brachidium, MNHN-IB-2022-1055. **K**. Dorsal valve interior to observe the septalium and the long loop brachidium free from the septum, MNHN-IB-2022-1056. **L**. Juvenile shell of the species, MNHN-IB-2022-1057. **M**. Close-up view at the brown margin line of specimen (J) to reveal the setae (arrowhead). Scale bars: A–C, L = 1 mm; D–K = 5 mm; M = 2 mm.

Type locality

Great Australian Bight.

Description

Morphology. Subcircular smooth and tiny single shell, slightly biconvex, with a rectimarginate anterior margin (Fig. 27A). In the dorsal valve interior: high inner socket ridges, no crural processes and long crura converging somewhat antero-ventrally. The proportionally high septal pillar is plate-like in its basal part, ending by a narrow extremity (Fig. 27B). Erect ventral beak, foramen large, very small and disjunct deltidial plates, pedicle collar barely visible (Fig. 27A), teeth emerging from the antero-dorsal side of the ventral valve (Fig. 27C).

Depth range

406–644 m, Karubenthos 2 exped.; 225–3493 m (see Logan 2007).

Distribution

The species is recorded from the E Atlantic Ocean, W Pacific Ocean, New Zealand, Indian Ocean, and Antarctica (Zezina 1981, 1987; Foster 1989; Laurin 1997; Gaspard 2003).

Superfamily Terebratelloidea King, 1850
Family Dallinidae Beecher, 1893
Subfamily Dallininae Beecher, 1893

Genus ***Dallina*** Beecher, 1893

Type species

Terebratula septigera Lovén, 1846.

Dallina floridana (Pourtalès, 1868)
Figs 27D–M, 28

Waldheimia floridana Pourtalès, 1868: 127.

Waldheimia floridana – Dall 1871: 12, pl. 1 fig. 3, pl. 2 figs 1–3. — Davidson 1887: 59, pl. 12 figs 1–5.
Dallina floridana – Beecher 1893: 382, pl. 1 fig. 45. — Dall 1920: 358. — Cooper 1977: 128, pl. 4 figs 1–4, pl. 11 figs 20–27, pl. 29 figs 14–24.

Material examined (including figured material)

GUADELOUPE – **E of La Désirade** • 2 shells + 1 dorsal valve; stn DW 4573; 16°20′ N, 60°55′ W; depth 389–413 m; 17 Jun. 2015; Karubenthos 2 exped.; MNHN, MNHN-IB-2022-1053 (Fig. 27D–F) • 1 shell; same data as for preceding; MNHN, MNHN-IB-2022-1054 (Fig. 27G–I) • 1 valve; same data as for preceding; MNHN, MNHN-IB-2022-1056 (Fig. 27K) • 3 shells + 1 valve; stn DW 4554; 16°21′ N, 60°56′ W; depth 300–370 m; 15 Jun. 2015; Karubenthos 2 exped.; MNHN, MNHN-IB-2022-1055 (Fig. 27J, M) • 1 juv.; stn DW 4555; 16°24′ N, 60°51′ W; depth 100–258 m; 15 Jun. 2015; Karubenthos 2 exped.; MNHN • 3 juvs; stn CP 4608; 16°14′ N, 60°59′ W; depth 618–632 m; 24 Jun. 2015; Karubenthos 2 exped.; MNHN • 1 juv.; same data as for preceding; MNHN, MNHN-IB-2022-1057 (Fig. 27L) • 1 juv.; same data as for preceding; MNHN-IB-2022-1061 (Fig. 28H–J) • 1 juv.; same data as for preceding; MNHNIB-2022-1059a–b (Fig. 28B–D, F–G) – **N of Grande Terre** • 2 juvs; stn DW 4518; 16°34′ N, 61°37′ W; depth 426–441 m; 9 Jun. 2015;

Karubenthos 2 exped.; MNHN, MNHN-IB-2022-1058 (Fig. 28A) • 1 juv.; same data as for preceding; MNHN, MNHN-IB-2022-1060 (Fig. 28E) • 3 juvs; stn 4544; 16°38′ N, 61°37′ W; depth 413–423 m; 13 Jun. 2015; Karubenthos 2 exped.; MNHN • 2 juvs; stn 4549; 16°38′ N, 61°35′ W; depth 343–402 m; 14 Jun. 2015; Karubenthos 2 exped.; MNHN • 6 juvs; stn DW 4550; 16°37′ N, 61°31′ W; depth 432–482 m; 14 Jun. 2015; Karubenthos 2 exped; MNHN. – **W of Basse Terre** • 1 juv.; stn CP 4513; 16°13′ N, 61°54′ W; depth 406–644 m; 8 Jun. 2015; Karubenthos 2 exped.; MNHN.

Type locality

Florida Reefs.

Description

Morphology. Large biconvex shell, easily recognised by its triangular outline and the greatest width in a very anterior position (Fig. 27D–I). A certain degree of dimorphism is clearly present in the different populations (Fig. 27D, G). The ventral beak is suberect (Fig. 27E, H), obliquely cut by a wide foramen. The deltidial plates are fused in a slightly concave symphytium. The lateral margins are very sinuous and the anterior margin paraplicate (Fig. 27E–F, H–I). Juvenile specimens with a rectimarginate anterior margin could be confused at first sight with *Cryptopora rectimarginata*, but the presence of punctae and the length of the lophophore seen by transparency help to make the difference as do the shape of the deltidial plates (Figs 27L, 28A).

Ventral valve. The ventral valve interior is notable for the absence of dental plates and reveals small hinge teeth (Fig. 28D), a slight excrescence could probably be equivalent to the septum or a septal node (Fig. 28B–C).

Dorsal valve. The dorsal valve interior displays a long loop (Fig. 27J–K). The inner hinge plates converge to form a septalium that unite with the posterior part of the median septum (Fig. 27K). Narrow crural bases separate the inner and outer hinge plates, and discrete crural processes are observed. The descending branches are thin, then enlarge rapidly with the appearance of the conspicuous ascending branches. The ontogeny of the loop deserves attention. In the juvenile stage a ring appears and develops on the septal pillar (Fig. 28E–G), different from the one with the hollow on the septum of the ventral valve (Fig. 28A–C). The continuous growth of this similar hood enlarges the ring as explained by Gaspard (2003). At the same time, the descending branches reach the septal pillar. When the ring is enlarged, a resorption or lysis appears at this place of the septum, the enlarging ring giving origin to the ascending branches which will form, with the descending branches, a long and complete loop free from the septum (Fig. 27J–K). The lack of intermediate stages about the ontogeny of the loop is noticeable here. The lophophore is clearly visible even in the juvenile stage (Fig. 28H), with details of the basal part of the arms (Fig. 28I–J).

Microstructure. Punctate two-layered shell. The fibrous mosaic is visible on the valve floor, the teeth (Fig. 28D) and septa (Fig. 28C, G). Setae are revealed on the inner side of the margins (Fig. 27J, M).

Depth range

100–632 m, Karubenthos 2 exped.; 64–595 m (Cooper 1977); 64–724 (Logan 2007: 3111).

Distribution

The species is recorded from the Gulf of Mexico, the Yucatan Channel and Peninsula, Straits of Florida, Key West Florida, Grand Bahama, Cuba, Dominican Republic, Porto Rico, Island of Aves, Dry Tortugas (Dall 1920; Cooper 1977).

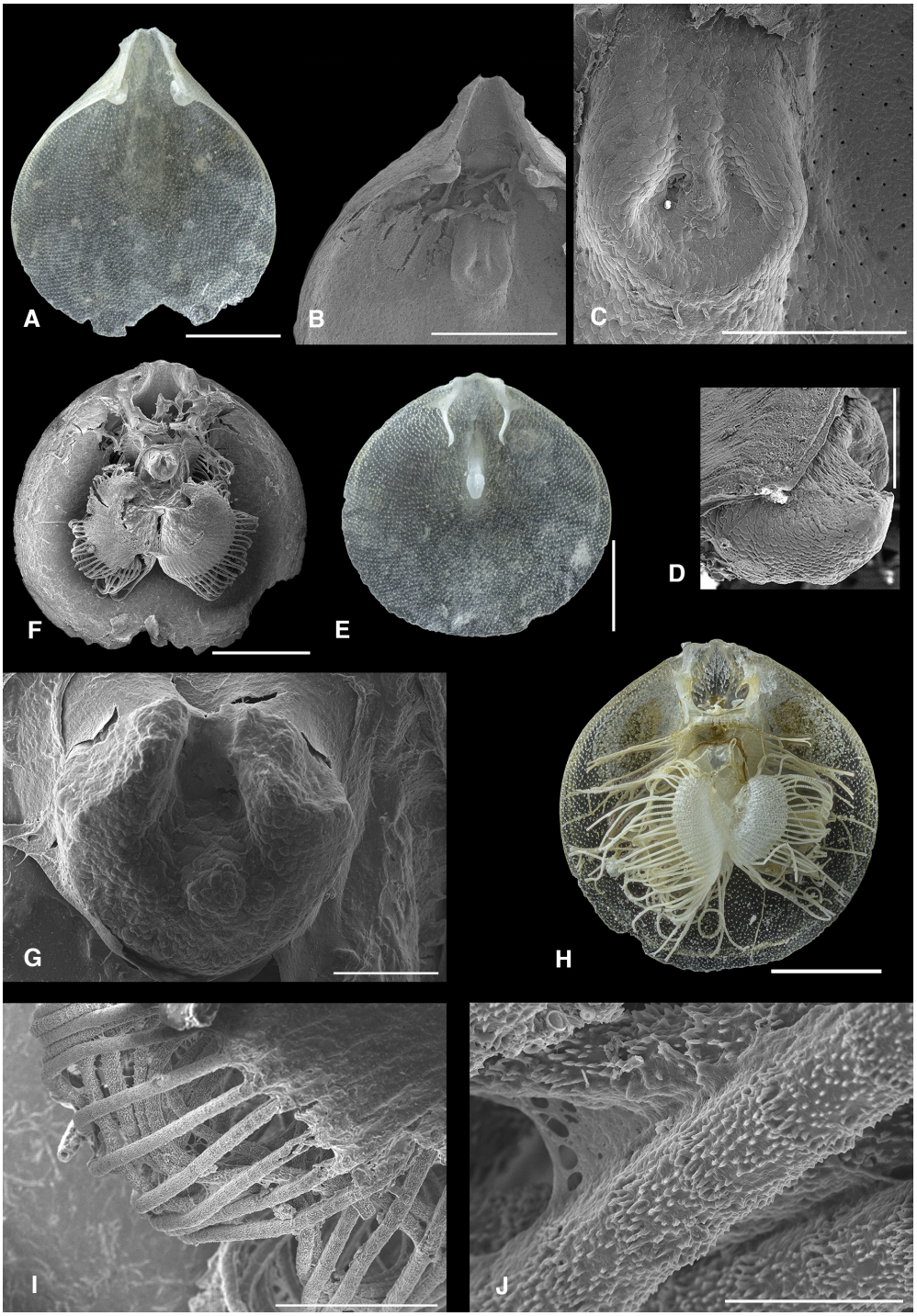

Fig. 28. *Dallina floridana* (Pourtalès, 1868). **A**. Juvenile ventral valve, MNHN-IB-2022-1058. **B–D**. SEM views of a posterior juvenile ventral valve, MNHN-IB-2022-1059a. **B**. With the minute deltidial plates, teeth and septal pillar. **C**. Detail of the ventral septal pillar. **D**. Detail of the right tooth. **E**. Juvenile dorsal valve interior with the beginning descending branches and the hood-like septal pillar, MNHN-IB-2022-1060. **F–G**. SEM views of a juvenile stage of dorsal valve interior (same shell as B–D), MNHN-IB-2022-1059b. **F**. Juvenile with the septal pillar and the lophophore. **G**. Close-up view of the hood-like septal pillar. **H**. Juvenile specimen with its lophophore, MNHN-IB-2022-1061. **I–J**. SEM details of the lophophore cirri (same valve as H). Scale bars: A–B, F, H = 1 mm; C = 400 µm; D = 150 µm; E = 500 µm; G = 100 µm; I = 200 µm; J = 30 µm.

Superfamily Kraussinoidea Dall, 1870
Family Kraussinidae Dall, 1870

Genus ***Megerlia*** King, 1850

Type species

Megerlia truncata (Linnaeus, 1767).

Megerlia echinata (Fischer & Oehlert, 1890)
Fig. 29

Mülfeldtia echinata Fischer & Oehlert, 1890: 73.

Mülfeldtia echinata – Fischer & Oehlert 1891: 90, pl. 7 fig. 13a–g.
Pantellaria echinata – Dall 1920: 336.
Megerlia echinata – Atkins 1961: 89–94. — Cooper 1977: 125, pl. 17 figs 14–22. — Gaspard 2003: 299, pl. 5 figs 1–8.

Material examined (including figured material)

GUADELOUPE – **W of Marie Galante** • 1 shell; stn DW 4598; 15°55′ N, 61°24′ W; depth 207–211 m; 22 Jun. 2015; Karubenthos 2 exped.; MNHN • 1 shell; stn DW 4635; 15°50′ N, 61°26′ W; depth 265–268 m; 27 Jun. 2015; Karubenthos 2 exped.; MNHN. – **N of Grande Terre** • 4 shells + 1 juv.; stn CP 4529; 16°24′ N, 61°35′ W; depth 176–183 m; 11 Jun. 2015; Karubenthos 2 exped; MNHN, MNHN-IB-2022-1062 (Fig. 29A–B) • 1 shell; same data as for preceding; MNHN, MNHN-IB-2022-1063 (Fig. 29C–D, G). – **E of La Désirade** • 1 shell + 1 ventral valve; stn DW 4578; 16°21′ N, 60°54′ W; depth 119–250 m; 18 Jun. 2015; Karubenthos 2 exped.; MNHN • 1 shell; stn DW 4611; 16°20′ N, 60°52′ W; depth 242–263 m; 24 Jun. 2015; Karubenthos 2 exped.; MNHN, MNHN-IB-2022-1064 (Fig. 29F, H–I) • 1 fragmented valve; same data as for preceding; MNHN, MNHN-IB-2022-1087 (Fig. 29E).

Type locality

Off Marseille, Mediterranean Sea.

Description

Morphology. White to brown slightly biconvex to gently concavo-convex shell, wider than long, with a cardinal line almost as short as the shell width and with rounded margin (Fig. 29A–C). The external ventral valve is adorned with radial lines of nodules oriented anteriorly (Fig. 29A, C). The umbo of the ventral valve is rather curved to suberect, dominating a wide foraminal embayment that touches the posterior dorsal valve (Fig. 29B). The foramen is amphithyrid-like. Two brown ribbons of gonads are revealed on both valves by transparency (Fig. 29A–B). The close and strong attachment of the shell to the substrate leads to an abraded posterior dorsal valve due to the position of the integument over the pedicle opening (Fig. 29B).

Ventral valve. Small divergent disjunct deltidial plates are observed. The valve interior reveals small teeth in the anterior part of two excavated plates, well-developed pedicle adjustor muscles (Fig. 29D), and a short median septum (Fig. 29E). When the mantle is still present, one can observe setae at the inner margin, which are obviously located in the same alignment as the external nodules (Fig. 29D).

Dorsal valve. At the valve interior, no cardinal process, crura attached to the inner sides of socket ridges and no real crural processes. The two descending branches join, at the anterior septum, two extensions growing toward the ventral valve and latero-anteriorly that unite to form the ascending branches of the

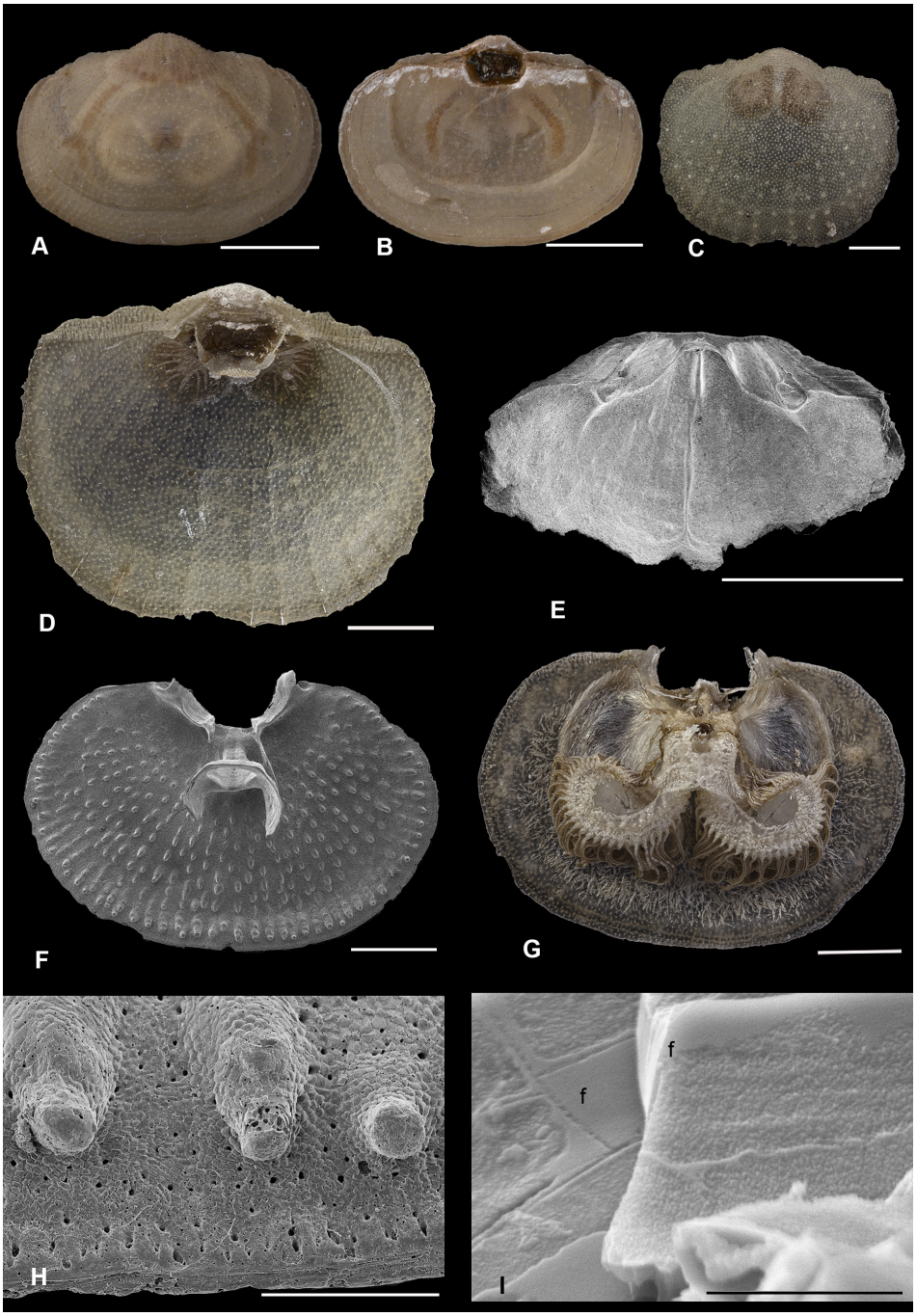

Fig. 29. *Megerlia echinata* (Fischer & Oehlert, 1890). **A–B**. Adult ventral and dorsal valves of a shell, MNHN-IB-2022-1062. **C**. Shell with pustulous external ventral valve (same station), muscle areas are visible by transparency, MNHN-IB-2022-1063. **D**. Inner side of the same valve, the strong ventral adjustors are visible as well as the integument and some setae at the inner anterior margin. **E**. SEM inner view of a fragmented posterior ventral valve, revealing the teeth and short septum, MNHN-IB-2022-1087. **F**. Dorsal valve interior, from the same location, adorned with radial lines of protuberances, revealing a ring-like brachidium attached to the septum, MNHN-IB-2022-1064. **G**. Dorsal valve interior from same shell as in (D) with the lophophore and heavily spiculate mantle. **H**. SEM view of the inner margin of a valve, highlighting the proximal double protuberances and the distribution of punctae, MNHN-IB-2022-1064. **I**. SEM view of fibres (f) composed of submicrometric granules, MNHN-IB-2022-1064. Scale bars: A–B = 5 mm; C–D, G = 1 mm; E = 3 mm; F = 2 mm; H= 300 µm; I = 4 µm.

loop (Fig. 29F). At first sight, it is easy to see the radial alignments of tubercules in the valve floor, the rows ending by larger ones before the margin line (Fig. 29F, H). The plectolophous lophophore, like the remaining parts of the mantle, is strongly spiculate (Fig. 29G).

Microstructure. The two-layered shell is densely punctate. In the SEM images, the secondary layer partly reveals the submicrometric granules that compose the fibres (Fig. 29I).

Depth range

119–268 m, Karubenthos 2 exped.; 10–1970 m (Logan 2007).

Distribution

The species was recorded from the Straits of Florida, off Sand Key, off Barbados, off Venezuela (Cooper 1977) and, elsewhere, Cape of Good Hope, Africa; off Portugal and the Ibero-Morrocan Gulf (Gaspard 2003); Australia; New South Wales.

Discussion

The expeditions conducted around the French Caribbean islands of Guadeloupe and Martinique revealed the presence of previously unknown or overlooked representatives of the phylum Brachiopoda in the region. All three brachiopod subphyla are represented, with Rhynchonelliforms being the most diverse. Among the collected material, the genera *Argyrotheca* and *Tichosina* display the highest species richness. Of the thirty taxa recovered, *Terebratulina cailleti* is the most frequently encountered species and was first recognised in the Guadeloupe area.

Several species exhibit a broad bathymetric distribution within the Caribbean Sea, including *Terebratulina cailleti* (60–898 m) and *Cryptopora rectimarginata* (185–800 m), In contrast, other taxa, particularly species of *Argyrotheca*, prefer shallow water environments, e.g., *A. bermudana* (14–82 m). Similarly restricted depth ranges are observed for *Discradisca antillarum* (67 m) and *Novocrania anomala* (11–23 m). Minor differences in species composition were also observed between the Atlantic-facing and lee sides of the islands suggesting an influence of local hydrodynamic or environmental conditions.

Within this tropical setting, brachiopod shells span a wide range of sizes, from relatively wide forms (e.g., *Tichosina*, *Erymnia*, *Dallina*) to medium-sized (*Stenosarina*, *Terebratulina*, *Megerlia*) or very small to tiny taxa (*Cryptopora*, *Eucalathis*, *Argyrotheca*, *Platidia*, *Amphithyris*, *Phaneropora*). All brachiopod species are suspension feeders and attach to substrates using a pedicle or by cementation. Pedicle morphology varies markedly among taxa and includes massive structures (*Tichosina*, *Erymnia*); thin and elongated pedicles (*Cryptopora*); rootlets or frayed pedicles (*Terebratulina*, *Eucalathis*, *Notozyga*), attachment via an integument (*Platidia*, *Megerlia*), or ± complete cementation (*Novocrania*).

Differences in attachment mode reflect distinct life strategies among rhynchonelliform brachiopods. Pedicle morphology plays a key role in orienting the shell relative to the substrate and surrounding environment, enabling species to exploit different surface types and microhabitats. This functional diversity explains why taxa such as *Argyrotheca* and *Platidia* are never positioned in the same manner as species of *Tichosina*, even when occurring in similar environments.

Attachment strategies also influence ecological interactions. In *Terebratulina cailleti*, a wide range of relationships with surrounding organisms was observed, including associations with conspecifics, sponges, bryozoans, and especially corals such as *Stylaster roseus* Pallas, 1766 or *Scolymia* aff. *cubensis* Milne Edwards & Haime, 1848. These interactions occur among filter feeding organisms sharing the same habitat. In some cases, the frayed pedicle of *T. cailleti* penetrated living substrates such as corals or

foraminifers, while in other instances the shells themselves host epibionts, including sessile foraminifers and hemichordates such as *Rhabdopleura* aff. *compacta* Hincks, 1880.

Species of *Argyrotheca* show a comparable substrate specificity. *Argyrotheca bermudana*, for example, commonly occurs on or beneath coralline algae-coral assemblages, including taxa such as *Monstracea* sp. or *Agaricia fragilis* Dana, 1848. Some species, such as *A. johnsoni*, exhibit cryptic behaviour, inhabiting the undersides of foliaceous corals or caves. These habitats likely reduce grazing pressure and occur at depths below the photic zone. Previous studies suggest that such species may be sensitive to low light levels (cf. Jackson *et al*. 1971), and intolerant of enclosed cavities with muddy substrates.

In cryptic coral reef niches, species of *Argyrotheca* are frequently found attached to heavily encrusted dead coral branches, encrusting foraminifers (e.g., *Homotrema rubrum* Lamarck, 1816), or coralline algae. Similar ecological settings have been reported in the Red Sea (Zuschin & Mayrhofer 2009), noticeably indicating convergent habitat use across tropical regions.

Several Caribbean species of *Argyrotheca*, including *A. bermudana*, *A. rubrotincta* and *A. schrammi* (the latter species having been first described from Guadeloupe) display attractive shell colouration. Brightly coloured brachiopods have also been reported from the Coral Sea and the Red Sea, suggesting a broader tropical trend. What are the pigments involved in the colouration of these benthic shells of the Caribbean Sea? To answer this question, a work in progress applying several methods including the Raman Spectroscopy indicates the presence of carotenoids (see also Gaspard *et al*. 2019, 2025).

In coastal environments influenced by mangroves, decomposition of *Sargassum* as well as elevated temperatures and salinities may promote microbial growth, potentially resulting in secondary pigmentation associated with bacterial carotenoid production (Boisnoir 2025). This hypothesis could explain the colouration observed on the inner surfaces of certain shells of *Terebratulina cailleti* and *T. latifrons* (Fig. 17C–G).

In contrast, some specimens of *Tichosina* and *Erymnia* exhibit a brown to dark shell colouration, which is more likely related to environmental pollution, including oil contamination or *Sargassum* decomposition. Such conditions may interfere with feeding during prolonged valve closure or respiration by obstructing shell punctae. The impact of the chlordecone contamination in coastal areas of the French Caribbean may also contribute to these observations.

Several species collected during the expeditions, including *Argyrotheca beaumalei* sp. nov. provide additional data relevant to previous studies (Kaulfuss *et al*. 2013) on micromorphism and brooding strategies in Caribbean *Argyrotheca*. These findings contribute to a broader understanding of reproductive and developmental variability within the group.

Climate change represents an additional and growing threat to Caribbean brachiopod assemblages. Coral bleaching, driven primarily by rising sea temperatures, leads to the loss of symbiotic algae and weakens coral frameworks. As corals degrade, species that depend on them for attachments and habitat, including *Argyrotheca*, *Terebratulina cailleti*, and *Novocrania anomala*, lose critical substrates, potentially resulting in declines in abundance and diversity. Given the role of coral reefs as biodiversity hotspots, such losses may have cascading ecological consequences. It is crucial to address climate change and implement conservation measures to protect reefs and the species that rely on them.

Overall, these observations highlight the ecological diversity, adaptability, and environmental sensitivity and interactions of the Caribbean brachiopods. Beyond their ecological significance, brachiopod shells serve as valuable bio-archives recording environmental parameters such as temperature that can be reconstructed using geochemical analyses (Letulle *et al*. 2023).

Finally, the present-day Caribbean fauna reflects a long history of larval dispersal and adaptation, originating from the Neotethys Ocean and northeastern boreal Sea since the Late Cretaceous (see Scotese 2017). The successful colonisation of the North Atlantic underscores the resilience and evolutionary persistence of brachiopods in changing marine environments.

Acknowledgments

Specimens were obtained during research expeditions organised by the MNHN and ProNatura International as part of the "Our Planet Reviewed" program, as well as by the MNHN and the Institut de Recherche pour le Développement as part of the "Tropical Deep-Sea Benthos program" (KARUBENTHOS 1 in 2012, KARUBENTHOS 2 in 2015, and MADIBENTHOS in 2016, in Martinique and Guadeloupe, and ACOUPA in 2014 in French Guiana). I am grateful to numerous cruise leaders and co-PIs: Philippe Bouchet, and Laure Corbari. I thank Prof. Ph. Bouchet (MNHN, Paris) who proposed the study of the brachiopod material collected and the team of the RV *L'Antea*, as well as Prof. D. Lamy (Borea, University of French Caribbean, Guadeloupe). Thanks are due to L. Corbari (MNHN) who provided information on the localisation of the sampling stations and P. Lozouet and Ph. Maestrati (DGD.C, MNHN) for their help. I warmly thank the two photographers L. Cazes and Ph. Loubry for help in the studio imagery (CR2P, MNHN-SU), A. Lethiers (CR2P, Sorbonne Université) for help in the final drawing of the map with the sampled stations, and G. Toutirais (MNHN, MEB platform) for help using the SEM. I gratefully thank Prof. Ch. Lecuyer (LGL-TPE, Univ. Lyon1) who proposed to add some of the Caribbean species collected as part of a doctoral project, mainly including geochemical analyses, brought to a successful conclusion by Th. Letulle. M. Thoury (Dir. IPANEMA), and Cl. Hairie (IPANEMA, Synchrotron Soleil, Paris-Saclay) are also thanked for the beginning collaboration in the analyses of the pigments involved in the colour patterns of shells of *Argyrotheca*. I would not like to forget Prof. J. Webb (Swinburne Univ., Australia) and M. Pickford (MNHN) for helpful comments, as well the Editors and the two anonymous reviewers.

Funding

This research has not received any specific grant from funding agencies in the public, commercial, or non-profit sector.

Conflict of interest

No conflicts of interest are declared; no use of AI was made.

References

Agassiz A. 1888. *Three Cruises of the United States Coast and Geodesic Survey Steamer "Blake" in the Gulf of Mexico and the Caribbean Sea and along the Atlantic Coast of United States from 1877 to 1880*. Houghton, Mifflin and Company, Boston and New York; The Riverside Press, Cambridge. https://doi.org/10.5962/bhl.title.26524

Alvarez F., Brunton C.H.C. & Long S.L. 2008. Loop ultrastructure and development in Recent Megathyridoidea, with description of a new genus *Joina* (type species *Terebratula cordata* Risso, 1826). *Earth and Environmental Science – Transactions of the Royal Society of Edinburgh* 98: 391–403. https://doi.org/10.1017/S1755691008075130

Asgaard U. & Stentoft N. 1984. Recent micromorph brachiopods from Barbados. Palaeontological and evolutionary implications. *Géobios* MS 8: 29–37. https://doi.org/10.1016/S0016-6995(84)80153-9

Atkins G. 1961. The generic position of the brachiopod *Megerlia echinata* (Fischer & Oehlert). *Journal of the Marine Biological Association of the United Kingdom* 41: 89–94.

Beecher C.E. 1893. Revision of the families of loopbearing Brachiopoda. The development of *Terebratalia obsoleta* Dall. *Transactions of the Connecticut Academy of Arts and Sciences* 9: 392–399.

Bitner M.A. 2006. Recent Brachiopoda from the Fiji and Wallis and Futuna Islands, Southwest Pacific. *In*: Justine J.-L. & Richer De Forges B. (eds) *Tropical Deep Sea Benthos, Vol. 24*. Mémoires du Muséum national d'Histoire naturelle 193: 15–32.

Bitner M.A. 2008. New data on the recent brachiopods from Fiji and Futuna slands, South-West Pacific. *Zoosystema* 30 (2): 419–461.

Boisnoir A. 2025. En Martinique et Guadeloupe, pourquoi les eaux des Mangroves se colorent en rose? *The Conversation*: 6p. https://doi.org/10.64628/AAK.xrch7upxy

Bromley R.G. & Surlyk F. 1973. Borings produced by Brachiopod pedicles, fossil and Recent. *Lethaia* 6: 349–365. https://doi.org/10.1111/j.1502-3931.1973tb01203.x

Brunton C.H.C. & Curry G.B. 1979. British Brachiopods – Keys and Notes for the Identification of the species. *Synopses of the British Fauna (New Series) Linnean Society of London* 17: 1–64.

Checa A.G., Gaspard D., Gonzáles-Segura A. & Ramírez-Rico J. 2009. Crystallography of the calcite foliated-like and semi-nacre microstructures of the brachiopod *Novocrania*. *Crystal Growth and Design* 29 (5): 2464–2469. https://doi.org/10.1021/cg801372j

Cohen B., Kaulfuss A. & Lüter C. 2014. Craniid brachiopods: aspects of clade structure and distribution reflect continental drift (Brachiopoda: Craniiformea. *Zoological Journal of the Linnean Society* 171 (1): 133–150. https://doi.org/10.1111/zoj.12121

Cooper G.A. 1934. New brachiopods. Reports on the collections obtained by the first Johnson-Smithsonian deep-sea expedition to the Puerto Rican Deep. *Smithsonian Miscellaneous Collections* 9 (10): 5p.

Cooper G.A. 1954. Gulf of Mexico, its origin, waters, and marine life. Brachiopoda occurring in the Gulf of Mexico. *Fish and Wildlife Service. Fisheries Bulletin* 55: 363–365.

Cooper G.A. 1959. Tertiary and Recent rhynchonelloid brachiopods. *Smithsonian Miscellaneous Collections* 139 (5): 1–90.

Cooper G.A. 1973. New Brachiopoda from the Indian Ocean. *Smithsonian Contributions to Paleobiology* 16: 1–43. https://doi.org/10.5479/si.00810266.16.1

Cooper G.A. 1977. *Brachiopods from the Caribbean Sea and Adjacent waters*. Studies in Tropical Oceanography 14, University of Miami Press.

Cooper G.A. 1983. The Terebratulacea (Brachiopoda), Triassic to Recent: A study of the brachidia (loops). *Smithsonian Contributions to Paleobiology* 50: 1–445. https://doi.org/10.5479/si.00810266.50.1

Costa O.G. 1852. Classe V, Brachiopodi. *Fauna del Regno di Napoli* 10: 1 60.

Crosse H. 1865. Description d'espèces nouvelles de Guadeloupe: *Terebratulina cailleti, Murex abyssicola*, *Fusus schrammi*, *Pleurotoma jelskii*, *P. antillarum*, *Astralium guadeloupense. Journal de Conchyliologie, Series 3* 5: 27–38.

Crosse H. & Fischer P. 1866. Note sur la distribution géographique des Brachiopodes aux Antilles. *Journal de Conchyliologie*, 3ème edition 6: 265–273.

Dall W.H. 1870. A revision of the Terebratulidae and Lingulidae, with remarks on and description of some recent forms. *American Jounal of Conchology* 6 (2): 86–168.

Dall W.H. 1871. Report of the Straits of Florida on the Brachiopoda obtained by the United States Coast Survey expedition in charge of L.F. de Pourtalès, with a revision of the Craniidae and Discinidae. *Bulletin of the Museum of Comparative Zoology* 3 (1): 1–45.

Dall W.H. 1882. American work on recent Mollusca in 1881. *The American Naturalist* 16(11): 874–887.

Dall W.H. 1886. Report on the results of dredging under the supervisor of A. Agassiz, in the Gulf of Mexico (1877–1878) and in the Caribbean Sea (1879–1880), by the US Coast Survey steamer "Blake" …. and commander J.R. Bartlett XXIX – Report on the Mollusca. Part I. Brachiopoda and Pelecypoda. *Bulletin of the Museum of Comparative Zoology* 12: 171–318.

Dall W.H. 1911. A new brachiopod from Bermuda. *Nautilus* 25: 86–87.

Dall W.H. 1920. Annotated list of the Recent Brachiopoda in the Collection of the United States National Museum, with descriptions of thirty-three new forms. *Proceedings of the United States National Museum* 57: 261–377. https://doi.org/10.5479/si.00963801.57-2314.261

Davidson T. 1870. On Italian Tertiary Brachiopoda. *Geological Magazine* 7: 359–370, 399–408, 460–466.

Davidson T. 1880. Report on the Brachiopoda dredged by H.M.S. "*Challenger*" during the years 1873–1876. *Report of Scientific Result of the Voyage H.M.S. Challenger (Zoology)* 1: 1–67.

Davidson Th. 1886–1888. A monograph of the Recent Brachiopoda. *Transactions of the Linnean Society of London, Second Series, Zoology* IV (1–3): 1–248. https://doi.org/10.1111/j.1096-3642.1886.tb00655.x

Eudes-Deslongchamps E. 1855. On a new species of *Morrisia*. *Annals and Magazine of Natural History* 2 (16): 443–444.

Fischer P. 1872. Brachiopodes des côtes océaniques de France. *Journal de Conchyliologie* 3, ser. 2a: 160–164.

Fischer P. & Oehlert D.P. 1890. Diagnoses de nouveaux Brachiopodes. *Journal de Conchyliologie* 18: 70–74.

Fischer P. & Oehlert D.P. 1891. *Brachiopodes. Expéditions du Talisman et du Travailleur pendant les Années 1880, 1881, 1882, 1883*. Masson Ed., Paris.

Foster M.W. 1974. *Recent Antarctic and Subantarctic Brachiopods*. American Geophysical Union, Antarctic Research Series 21. Washington, USA. https://doi.org/10.1029/AR021

Foster M.W. 1989. Brachiopods from the extreme south Pacific and Adjacent waters. *Journal of Paleontology* 63: 268–301. https://doi.org/10.1017/S0022336000019442

Gaspard D. 2000. Recent brachiopod fauna from the Lesser Antilles (Caribbean Sea) and Guyana coasts — Morphological and Microstructural characters. *In*: Brunton C.H.C. & Long S. (eds) *Abstract Volume of the 4th International Brachiopod Congress, London, UK*. London.

Gaspard D. 2003. Recent brachiopods collected during the "SEAMOUNT 1" Cruise off Portugal and the Ibero-Morrocan Gulf (Northeastern Atlantic) in 1987. *Géobios* 36: 285–304. https://doi.org/10.1016/S0016-6995(03)00033-0

Gaspard D. 2018. Recent brachiopods of the French Insular Caribbean region (Biodiversity). 8th IBC (S6), Milan, Italy, 11–14 Sept. 2018. Abstract Volume. *Permophiles* 66 supplement 1: 51. Angiolini L. & Posenato R. (General Chairs), Milan.

Gaspard D. 2024. Biodiversity and characteristics of Antarctic brachiopods sampled during the CEAMARC expedition. *Polar Biology* 47: 1323–1356. https://doi.org/10.1007/s00300-024-03308-y

Gaspard D., Cazes L. & Loubry Ph. 2018. Brachiopod diversity around the French Lesser Antilles (Caribbean). CARIBAEA Initiative. *3rd Research and Conservation Workshop. Abstract Book*: 38. Cezilly F. (org.), Guadeloupe.

Gaspard D., Paris C., Loubry Ph. & Luquet G. 2019. Raman investigation of the pigment families in Recent and fossil brachiopod shells. *Spectrochimica Acta Part A: Molecular and Biomolecular Spectroscopy* 208: 73–84. https://doi.org/10.1016/j.saa.2018.09.050

Gaspard D., Hairie C. & Thoury M. 2025. Motifs colorés des coquilles de Brachiopodes du Paléozoïque à l'Actuel — Quels pigments sont impliqués? comment les mettre en évidence. *Congrès APF, 5–8 Mai 2025, Lille France. Oral presentation, Volume Abstract*: 26. Servais Th. *et al*. (orgs.), Lille.

Jackson J.B.C., Goreau Th.F. & Hartman W.D. 1971. Recent brachiopod-coralline sponge communities and their paleoecological significance. *Science* 173: 623–625. https://doi.org/10.1126/science.173.3997.623

Jeffreys J.G. 1878. On the Mollusca procured during 'Lightning' and 'Porcupine' Expeditions, 1868–70 (Part I). *Proceedings of the Zoological Society of London* 46 (1): 393–416. https://doi.org/10.1111/j.1469-7998.1878.tb07976.x

Kaesler R.L. 1997–2006 (ed.). *Treatise on Invertebrate Paleontology. Pt H: Brachiopoda Revised Vols 1–5*: 1–2320. The Geological Society of America, Boulder, Colorado and the University of Kansas, Lawrence.

Kaulfuss A., Seidel R. & Lüter C. 2013. Linking micromorphism, brooding, and hermaphrodism in brachiopods: Insights from Caribbean *Argyrotheca* (Brachiopoda). *Journal of Morphology* 274: 361–376. https://doi.org/10.1002/jmor.20093

Kowalewski M., Simões M., Carroll M. & Rodland D. 2002. Abundant brachiopods on a tropical upwelling-influenced shelf (Southeast Brazilian Bight, South Atlantic). *Palaios* 17: 277–286. https://doi.org/fjvtsq

Laurin B. 1997. Brachiopodes récoltés dans les eaux de la Nouvelle-Calédonie et des îles Loyauté, Matthew et Chesterfield. *In*: Crosnier A. (ed.). *Résultats des Campagnes MUSORSTOM 18* 176: 411–471. Mémoires du Muséum national d'Histoire naturelle, Paris.

Lee D.E. & Brunton C.H.C. 1986. *Neocrania* n. gen., and a revision of Cretaceous–Recent brachiopod genera in the family Craniidae. *Bulletin of the British Museum of Natural History (Geology)* 40 (4): 141–160.

Letulle Th., Gaspard D., Daëron M., Suan G., Vinçon-Laugier A., Arnaud-Godet F. & Lecuyer Ch. 2021. Assessing the potential of brachiopod shell geochemistry as a recorder of past sea-water temperature and oxygen isotope composition. *27ème Réunion des Sciences de la Terre, Lyon, 1–5 Nov. 2021. Volume Abstract*: 594. Mattioli E. & Baudin F. (orgs.), SGF, Paris.

Letulle Th., Gaspard D., Daëron M., Arnaud-Godet F., Vinçon-Laugier A., Suan G. & Lecuyer Ch. 2023. Multiproxy assessment of brachiopod shell calcite as a potential archive of sea-water temperature and oxygen isotope composition. *Biogeosciences* 20: 1381–1403. https://doi.org/10.5194/bg-20-1381-2023

Logan A. 1975. Ecological observations on the Recent articulate brachiopod *Argyrotheca bermudana* Dall from the Bermuda platform. *Bulletin of Marine Science* 25 (2): 186–204.

Logan A. 1977. Reef-dwelling articulate brachiopods from Grand Cayman, B.W.I. *Proceedings of the 3rd International Reef Symposium, Miami, 1 Biology*: 87–93. Rosenstiel School of Marine and Atmospheric Science, University of Miami, Miami.

Logan A. 1979. The Recent Brachiopoda of the Mediterranean Sea. *Bulletin de l'Institut Océanographique* 72 (1434): 1–112.

Logan A. 1987. Neogene paleontology in the northern Dominican Republic, 6. The Phylum Brachiopoda. *Bulletins of American Paleontology* 93:44–55.

Logan A. 1990. Recent Brachiopoda from the *Snellius* and *Luymes* expeditions to the Surinam – Guyana Shelf, Bonaire-Curaçao, and Saba Bank, Caribbean Sea, 1966 and 1969–72. *Zoologische Mededelingen* 63 (11): 123–136.

Logan A. 2007. Geographic distribution of extant articulated brachiopods. *In*: Selden P.A. (ed.) *Treatise on Invertebrate Paleontology, Pt H: Brachiopoda Revised 6*: 3082–3115. The Geological Society of America, Boulder, Colorado and the University of Kansas, Lawrence.

Logan A. & Long S.L. 2001. Shell morphology and geographical distribution of *Neocrania* (Brachiopoda, Recent) in the eastern North Atlantic and Mediterranean Sea. *In*: Brunton C.H.C., Cocks L.R.M. & Long S.L. (eds) Brachiopod Past and Present. *Proceedings of the 4th International Brachiopod Congress. The Systematic Association, Special volume Series* 53: 71–79. Taylor & Francis, London and New York.

Logan A., Tomasových A., Zuschin M. & Grill B. 2008. Recent brachiopods from the Red Sea and Gulf of Aden. *Fossil and Strata* 54: 299–309. Wiley-Blackwell, Chichester. https://doi.org/10.18261/9781405186643-2008-33

Orbigny A. d' 1845. Mollusques. *In*: Ramon de la Sagra M. (ed.) *Histoire, Physique, Politique et Naturelle de l'Île de Cuba, Vol. 2*: 1–336.

Orbigny A. d' 1853. Mollusques. *In*: M. Ramon de la Sagra (ed.) *Histoire, Physique, Politique et Naturelle de l'Île de Cuba Vol. 2*. A. Bertrand, Paris.

Philippi R.A. *1844. Fauna Molluscorum Viventium et in tellure Tertiaria via Fossilium Regni Utriusque Siciliae*: 1–303.

Pourtalès L.F. de 1868. Contributions to fauna of the Gulf Stream at great depths. *Bulletin of the Museum of Comparative Zoology* 1 (6): 103–120.

Reeve L.A. 1861. *Conchologia Iconica, or Figures and Descriptions of the Shells of Molluscous Animals*, 1843-178: 23 Vols. London.

Robinson J. 2017. Review of all Recent species in the genus *Novocrania* (Craniata, Brachiopoda). *Zootaxa* 4329 (6): 501–559. https://doi.org/10.11646/zootaxa.4329.6.1

Rodland D.L., Kowalewski M., Carroll M. & Simões M. 2004. Colonization of a 'Lost World': Encrustation patterns in modern subtropical brachiopod assemblages. *Palaios* 19: 381–395. https://doi.org/bphgmd

Rojas A., Garcia A. & Patarroyo P. 2015. Brachiopods from of the San Bernado Archipelago (Colombian Caribbean), with comments on specific synonymies in *Tichosina* Cooper, 1977. *Zootaxa* 3914 (1): 55–63. https://doi.org/10.11646/ZOOTAXA.3914.1.3

Rojas A., Garcia A., Hernández-Ávila I., Patarroyo P. & Kowalewski M. 2022. Occurrence of the brachiopod *Tichosina* in deep-sea coral bottoms of the Caribbean Sea and its paleoenvironmental implications. *Bulletin of the Florida Museum of Natural History* 59 (1): 1–15. https://doi.org/10.58782/flmnh.amjk8879

Romanin M., Crippa G., Ye F., Brand U., Bitner M.A., Gaspard D., Häussermann V. & Laudien J. 2018. A sampling strategy for recent and fossil brachiopods: selecting the optimal shell segment for geochemical analyses. *Rivista Italiana di Paleontologia e Stratigrafia* 124 (2): 343–359. https://doi.org/10.13130/2039-4942/10193

Scotese Ch.R. 2017. *Atlas of Ancient Oceans & Continents: 1.5 Billion Years – Today*. Palaeomap Project Report 112171A.

Selden P.A. (ed.) 2007. *Treatise on Invertebrate Paleontology, Pt H: Brachiopoda Revised 6*: 2321–3226. The Geological Society of America, Boulder, Colorado and the University of Kansas, Lawrence.

Thayer C.W. & Allmon R.A. 1991. Unpalatable thecideid brachiopods from Palau: Ecological and evolutionary implications. *In*: MacKinnon D.I., Lee D.E. & Campbell J.D. (eds) Brachiopods Through Time. *Proceedings of the 2nd International Brachiopod Congress*: 253–260. Balkema Press, Rotterdam.

Thomson J.A. 1918. Australasian Antarctic Expedition, 1911–14, under the leadership of sir Douglas Mawson, D.Sc., B.E., Brachiopoda. *Scientific Reports* Series C 4 (3): 1–76.

Verrill A.E. 1900. Additions to the Tunicata and Molluscoidea from the Bermudas. *Transactions of the Connecticut Academy of Arts and Sciences* 10: 591–592.

Williams A., Carlson S.J., Brunton C.H.C., Holmer L.E. & Popov L.E. 1996. Supra-ordinal classification of the Brachiopoda. *Philosophical Transactions of the Royal Society of London*, *(Series B)* 351: 1171–1193. https://doi.org/10.1098/rstb.1996.0101

Zezina O.N. 1981. Recent deep-sea Brachiopoda from the Western Pacific. *Galathea Report* 15: 7–20.

Zezina O.N. 1987. Brachiopods collected by BENTHEDI cruise in Mozambique Channel. *Bulletin du Muséum national d'Histoire naturelle, Series 4, section A* 3: 551–563. https://doi.org/10.5962/p.287532

Zezina O.N. 1990. Composition and distribution of articulate brachiopods from the underwater rises of the eastern Pacific. *Akademia Nauk SSSR* 124: 264–268.

Zezina O.N. 2000. Russian collections of the deep-sea brachiopods in the Atlantic Ocean. *In*: Kuztnetsov A.P. & Zezina O.N. (eds) *Benthos of the Russian Seas and the Northern Atlantic*: 26–36. Akademia Nauk, Moscow.

Zuschin M. & Mayrhofer S. 2009. Brachiopods from cryptic coral reef habitats in the northern Red Sea. *Facies* 55: 335–344. https://doi.org/10.1007/s10347-009-0189-1

Printed versions of all papers are deposited in the libraries of two of the institutes that are members of the *EJT* consortium: Muséum national d'Histoire naturelle, Paris, France and Royal Museum for Central Africa, Tervuren, Belgium. The other members of the consortium are: Royal Belgian Institute of Natural Sciences, Brussels, Belgium; Meise Botanic Garden, Meise, Belgium; Natural History Museum of Denmark, Copenhagen, Denmark; Naturalis Biodiversity Center, Leiden, the Netherlands; Museo Nacional de Ciencias Naturales-CSIC, Madrid, Spain; Leibniz Institute for the Analysis of Biodiversity Change, Bonn – Hamburg, Germany; National Museum of the Czech Republic, Prague, Czech Republic; The Steinhardt Museum of Natural History, Tel Aviv, Israël.